

EUROPEAN ORGANISATION FOR NUCLEAR RESEARCH (CERN)



JHEP 11 (2016) 110
 DOI: [10.1007/JHEP11\(2016\)110](https://doi.org/10.1007/JHEP11(2016)110)



CERN-EP-2016-183
 30th November 2016

Study of hard double-parton scattering in four-jet events in pp collisions at $\sqrt{s} = 7$ TeV with the ATLAS experiment

The ATLAS Collaboration

Abstract

Inclusive four-jet events produced in proton–proton collisions at a centre-of-mass energy of $\sqrt{s} = 7$ TeV are analysed for the presence of hard double-parton scattering using data corresponding to an integrated luminosity of 37.3 pb^{-1} , collected with the ATLAS detector at the LHC. The contribution of hard double-parton scattering to the production of four-jet events is extracted using an artificial neural network, assuming that hard double-parton scattering can be approximated by an uncorrelated overlaying of dijet events. For events containing at least four jets with transverse momentum $p_T \geq 20$ GeV and pseudorapidity $|\eta| \leq 4.4$, and at least one having $p_T \geq 42.5$ GeV, the contribution of hard double-parton scattering is estimated to be $f_{\text{DPS}} = 0.092^{+0.005}_{-0.011}$ (stat.) $^{+0.033}_{-0.037}$ (syst.). After combining this measurement with those of the inclusive dijet and four-jet cross-sections in the appropriate phase space regions, the effective cross-section, σ_{eff} , was determined to be $\sigma_{\text{eff}} = 14.9^{+1.2}_{-1.0}$ (stat.) $^{+5.1}_{-3.8}$ (syst.) mb. This result is consistent within the quoted uncertainties with previous measurements of σ_{eff} , performed at centre-of-mass energies between 63 GeV and 8 TeV using various final states, and it corresponds to $21^{+7}_{-6}\%$ of the total inelastic cross-section measured at $\sqrt{s} = 7$ TeV. The distributions of the observables sensitive to the contribution of hard double-parton scattering, corrected for detector effects, are also provided.

1. Introduction

Interactions involving more than one pair of incident partons in the same collision have been discussed on theoretical grounds since the introduction of the parton model to the description of particle production in hadron–hadron collisions [1–3]. These first studies were followed by the generalization of the Altarelli–Parisi evolution equations to the case of multi-parton states in Refs. [4, 5] and a discussion of possible correlations in the colour and spin degrees of freedom of the incident partons [6]. In the first phenomenological studies of such effects, the most prominent role was played by processes known as double-parton scattering (DPS), which is the simplest case of multi-parton interactions (MPI), leading to final states such as four leptons, four jets, three jets plus a photon, or a leptonically decaying gauge boson accompanied by two jets [7–15]. These studies have been supplemented by experimental measurements of DPS effects in hadron collisions at different centre-of-mass energies, which now range over two orders of magnitude, from 63 GeV to 8 TeV [16–30], and which have firmly established the existence of this mechanism. The abundance of MPI phenomena at the LHC and their importance for the full picture of hadronic collisions have reignited the phenomenological interest in DPS and have led to a deepening of its theoretical understanding [31–39]. Despite this progress, quantitative measurements of the effect of DPS on distributions of observables sensitive to it are affected by large systematic uncertainties. This is a clear indication of the experimental challenges and of the complexity of the analysis related to such measurements. Therefore, the cross-section of DPS continues to be estimated by ignoring the likely existence of complicated correlation effects. For a process in which a final state $A + B$ is produced at a hadronic centre-of-mass energy \sqrt{s} , the simplified formalism of Refs. [12, 13] yields

$$d\hat{\sigma}_{A+B}^{(\text{DPS})}(s) = \frac{1}{1 + \delta_{AB}} \frac{d\hat{\sigma}_A(s)d\hat{\sigma}_B(s)}{\sigma_{\text{eff}}(s)}. \quad (1)$$

The quantity δ_{AB} is the Kronecker delta used to construct a symmetry factor such that for identical final states with identical phase space, the DPS cross-section is divided by two. The σ_{eff} , usually referred to as the effective cross-section, is a purely phenomenological parameter describing the effective overlap of the spatial distribution of partons in the plane perpendicular to the direction of motion. In hadronic collisions it was typically found to range between 10 and 25 mb [16–30]. In Eq. (1), the various $\hat{\sigma}$ are the parton-level cross-sections, either for the DPS events, indicated by the subscript $A + B$, or for the production of a final state A or B in a single parton scatter (SPS), given by

$$d\hat{\sigma}_A(s) = \frac{1}{2s} \sum_{ij} \int dx_1 dx_2 f_i(x_1, \mu_F) f_j(x_2, \mu_F) d\Phi_A |\mathcal{M}_{ij \rightarrow A}(x_1 x_2 s, \mu_F, \mu_R)|^2. \quad (2)$$

Here the functions $f_i(x, \mu_F)$ are the single parton distribution functions (PDFs) which at leading order parameterize the probability of finding a parton i at a momentum fraction x at a given factorization scale μ_F in the incident hadron; $d\Phi_A$ is the invariant differential phase-space element for the final state A ; \mathcal{M} is the perturbative matrix element for the process $ij \rightarrow A$; and μ_R is the renormalization scale at which the couplings are evaluated. To constrain the phase space to that allowed by the energy of each incoming proton, a simple two-parton PDF is defined as

$$f_{ij}(\mathbf{b}, x_i, x_j, \mu_F) = \Gamma(\mathbf{b}) f_i(x_i, \mu_F) f_j(x_j, \mu_F) \Theta(1 - x_i - x_j), \quad (3)$$

where $\Theta(x)$ is the Heaviside step function, $\Gamma(\mathbf{b})$ the area overlap function, and the x and scale dependence of the PDF are assumed to be independent of the impact parameter \mathbf{b} . Equation (3) reflects the omission of correlations between the partons in the proton. At high energy, Eq. (1) can be derived using Eq. (3) by neglecting the contribution of the step function.

Typically, the main challenge in measurements of DPS is to determine if the A+B final state was produced in an SPS via the $2 \rightarrow 4$ process or in DPS through two independent $2 \rightarrow 2$ interactions. In one of the first studies of DPS in four-jet production at hadron colliders [10] the kinematic configuration in which there is a pairwise balance of the transverse momenta (p_T) of the jets was identified as increasing the contribution of the DPS mechanism relative to the perturbative QCD production of four jets in SPS. The idea is that in typical $2 \rightarrow 2$ scattering processes the two outgoing particles – here the partons identified as jets – are oriented back-to-back in transverse plane such that their net transverse momentum is zero. Corrections to this simple picture include initial- and final-state radiation as well as fragmentation and hadronization. In addition, recoil against the underlying event can modify the four-momentum of the overall final-state particle configuration. In attempting to describe all of these features, Monte Carlo (MC) event generators form an integral part, providing a link between the experimentally observed jets and the simple partonic picture of DPS as two almost independent $2 \rightarrow 2$ scatters.

An analysis of inclusive four-jet events produced in proton–proton collisions at a centre-of-mass energy of $\sqrt{s} = 7$ TeV at the LHC and collected during 2010 with the ATLAS detector is presented here. The topology of the four jets is exploited to construct observables sensitive to the DPS contribution. The DPS contribution to the four-jet final state is estimated and combined with the measured inclusive dijet and four-jet cross-sections in the appropriate phase space regions to determine σ_{eff} . The normalized differential four-jet cross-sections as a function of DPS-sensitive observables are measured and presented here as well.

2. Analysis strategy

To extract σ_{eff} in the four-jet final state, Eq. (1) is rearranged as follows. The differential cross-sections in Eq. (1) are rewritten for the four-jet and dijet final states and integrated over the phase space defined by the selection requirements of the dijet phase space regions A and B. This yields the following expression for the DPS cross-section in the four-jet final state:

$$\sigma_{4j}^{\text{DPS}} = \frac{1}{1 + \delta_{\text{AB}}} \frac{\sigma_{2j}^{\text{A}} \sigma_{2j}^{\text{B}}}{\sigma_{\text{eff}}}, \quad (4)$$

where σ_{2j}^{A} and σ_{2j}^{B} are the cross-sections for dijet events in the phase space regions labelled A and B respectively. The assumed dependence of the cross-sections and σ_{eff} on s is omitted for simplicity. The DPS cross-section may be expressed as

$$\sigma_{4j}^{\text{DPS}} = f_{\text{DPS}} \cdot \sigma_{4j}, \quad (5)$$

where σ_{4j} is the inclusive cross-section for four-jet events in the phase-space region $A \oplus B$, including all four-jet final states, namely both the SPS and DPS topologies, and where f_{DPS} represents the fraction of DPS events in these four-jet final states. The expression for σ_{eff} then becomes,

$$\sigma_{\text{eff}} = \frac{1}{1 + \delta_{\text{AB}}} \frac{1}{f_{\text{DPS}}} \frac{\sigma_{2j}^{\text{A}} \sigma_{2j}^{\text{B}}}{\sigma_{4j}}. \quad (6)$$

To extract σ_{eff} , it is therefore necessary to measure three cross-sections, σ_{2j}^{A} , σ_{2j}^{B} and σ_{4j} , and estimate f_{DPS} .

The four-jet and dijet final states are defined inclusively [40, 41] such that at least four jets or two jets respectively are required in the event, while no restrictions are applied to additional jets. When measuring the cross-section of n -jet events, the leading (highest- p_T) n jets in the event are considered. The general expression for the measured four-jet and dijet cross-sections may be written as

$$\sigma_{nj} = \frac{N_{nj}}{C_{nj}\mathcal{L}_{nj}}, \quad (7)$$

where the subscript nj denotes either dijet (2j) or four-jet (4j) topologies. For each nj channel, N_{nj} is the number of observed events, C_{nj} is the correction for detector effects, particularly due to the jet energy scale and resolution, and \mathcal{L}_{nj} is the corresponding proton–proton integrated luminosity.

The DPS model contributes in two ways to the production of events with at least four jets, leading to two separate event classifications. In one contribution, the secondary scatter produces two of the four leading jets in the event; such events are classified as complete-DPS (cDPS). In the second contribution of DPS to four-jet production, three of the four leading jets are produced in the hardest scatter, and the fourth jet is produced in the secondary scatter; such events are classified as semi-DPS (sDPS). The DPS fraction is therefore rewritten as $f_{\text{DPS}} = f_{\text{cDPS}} + f_{\text{sDPS}}$, and f_{cDPS} and f_{sDPS} are both determined from data. The dijet cross-sections in Eq. (6) do not require any modification since they are all inclusive cross-sections, i.e., the three-jet cross-section accounting for the production of an sDPS event is already included in the dijet cross-sections.

Denoting the observed cross-section at the detector level by

$$\mathcal{S}_{nj} = \frac{N_{nj}}{\mathcal{L}_{nj}}, \quad (8)$$

and the ratio of the corrections for detector effects by

$$\alpha_{2j}^{4j} = \frac{C_{4j}}{C_{2j}^A C_{2j}^B}, \quad (9)$$

yields the expression from which σ_{eff} is determined,

$$\sigma_{\text{eff}} = \frac{1}{1 + \delta_{AB}} \frac{\alpha_{2j}^{4j}}{f_{\text{cDPS}} + f_{\text{sDPS}}} \frac{\mathcal{S}_{2j}^A \mathcal{S}_{2j}^B}{\mathcal{S}_{4j}}. \quad (10)$$

The main challenge of the measurement is the extraction of $f_{\text{DPS}} = f_{\text{cDPS}} + f_{\text{sDPS}}$ from optimally selected measured observables. An artificial neural network (NN) is used for the classification of events [42], using as input various observables sensitive to the contribution of DPS. The differential distributions of these observables are also presented here.

3. The ATLAS detector

The ATLAS detector is described in detail in Ref. [43]. In this analysis, the tracking detectors are used to define candidate collision events by constructing vertices from tracks, and the calorimeters are used to reconstruct jets.

The inner detector used for tracking and particle identification has complete azimuthal coverage and spans the pseudorapidity region $|\eta| < 2.5$.¹ It consists of layers of silicon pixel detectors, silicon microstrip detectors, and transition-radiation tracking detectors, surrounded by a solenoid magnet that provides a uniform axial field of 2 T.

The electromagnetic calorimetry is provided by the liquid argon (LAr) calorimeters that are split into three regions: the barrel ($|\eta| < 1.475$) and the endcap ($1.375 < |\eta| < 3.2$) regions which consist LAr/Pb calorimeter modules, and the forward (FCal: $3.1 < |\eta| < 4.9$) region which utilizes LAr/Cu modules. The hadronic calorimeter is divided into four distinct regions: the barrel ($|\eta| < 0.8$), the extended barrel ($0.8 < |\eta| < 1.7$), both of which are scintillator/steel sampling calorimeters, the hadronic endcap ($1.5 < |\eta| < 3.2$), which has LAr/Cu calorimeter modules, and the hadronic FCal (same η -range as for the EM-FCal) which uses LAr/W modules. The calorimeter covers the range $|\eta| < 4.9$.

The trigger system for the ATLAS detector consists of a hardware-based level-1 trigger (L1) and the software-based high-level trigger (HLT) [44]. Jets are first identified at L1 using a sliding-window algorithm from coarse granularity calorimeter towers. This is refined using jets reconstructed from calorimeter cells in the HLT. Three different triggers are used to select events for this measurement: the minimum-bias trigger scintillators, the central jet trigger ($|\eta| < 3.2$) and the forward jet trigger ($3.1 < |\eta| < 4.9$). The jet triggers require at least one jet in the event.

4. Monte Carlo simulation

Multi-jet events were generated using fixed-order QCD matrix elements ($2 \rightarrow n$, with $n = 2, 3, 4, 5, 6$) with ALPGEN 2.14 [45] utilizing the CTEQ6L1 PDF set [46], interfaced to JIMMY [47] and HERWIG 6.520 [48]. The events were generated using the AUET2 [49] set of parameters (tune), optimized to describe underlying-event distributions obtained from a subsample of the 2010, 7 TeV ATLAS data as well as from the Tevatron and LEP experiments. The MLM [50] matching scale, which divides the parton emission phase space into regions modelled either by the perturbative matrix-element calculation or by the shower resummation, was set to 15 GeV. The implication of this choice is that partons with $p_T > 15$ GeV in the final state originate from matrix elements, and not from the parton shower. Event-record information was used to extract a sample of SPS candidate events from the sample generated with the ALPGEN + HERWIG + JIMMY MC combination (AHJ). A sample of candidate DPS events was also extracted from AHJ in order to study the topology of such events and validate the measurement methodology.

An additional AHJ sample was available that differed only in its use of the earlier AUET1 [51] tune. Because this sample contained three times as many events, it was used to derive the corrections for detector effects in all differential distributions in the data.

Tree-level matrix elements with up to five outgoing partons were used to generate a sample of multi-jet events without multi-parton interactions using SHERPA 1.4.2 [52, 53] with the CT10 PDF set [54] and the default SHERPA tune. The CKKW [55, 56] matching scale, similarly to the MLM one, was set to 15

¹ ATLAS uses a right-handed coordinate system with its origin at the nominal interaction point (IP) in the centre of the detector and the z -axis along the beam pipe. The x -axis points from the IP to the centre of the LHC ring, and the y -axis points upward. Cylindrical coordinates (r, ϕ) are used in the transverse plane, ϕ being the azimuthal angle around the beam pipe, referred to the x -axis. The pseudorapidity is defined in terms of the polar angle θ with respect to the beamline as $\eta = -\ln \tan(\theta/2)$. When dealing with massive jets and particles, the rapidity $y = \frac{1}{2} \ln \left(\frac{E+p_z}{E-p_z} \right)$ is used, where E is the jet energy and p_z is the z -component of the jet momentum.

GeV. This SPS sample was compared to the SPS sample extracted from the AHJ sample for validation purposes.

In addition, a sample of multi-jet events was generated with PYTHIA 6.425 [57] using a $2 \rightarrow 2$ matrix element at leading order with additional radiation modelled in the leading-logarithmic approximation by p_T -ordered parton showers. The sample was generated utilizing the modified leading-order PDF set MRST LO* [58] with the AMBT1 [59] tune.

To account for the effects of multiple proton–proton interactions in the LHC (pile-up), the multi-jet events were overlaid with inelastic soft QCD events generated with PYTHIA 6.423 using the MRST LO* PDF set with the AMBT1 tune. All the events were processed through the ATLAS detector simulation framework [60], which is based on GEANT4 [61]. They were then reconstructed and analysed by the same program chain used for the data.

5. Cross-section measurements

5.1. Data set and event selection

The measurement presented here is based on the full ATLAS 2010 data sample from proton–proton collisions at $\sqrt{s} = 7$ TeV. The trigger conditions evolved during the year with changing thresholds and prescales. A full description of the trigger strategy, developed and used for the measurement of the dijet cross-section using 2010 data, is given in Ref. [62]. For the events in the samples used in this study, the trigger was fully efficient. In total, the data used correspond to a luminosity of 37.3 pb^{-1} , with a systematic uncertainty of 3.5% [63]. This data set was chosen because it has a low number of proton–proton interactions per bunch crossing, averaging to approximately 0.4. It was therefore possible to collect multi-jet events with low p_T thresholds and to efficiently select events with exactly one reconstructed vertex (single-vertex events), thereby removing any contribution from pile-up collisions to the four-jet final-state topologies.

To reject events initiated by cosmic-ray muons and other non-collision backgrounds, events were required to have at least one reconstructed primary vertex, defined as a vertex that is consistent with the beam spot and is associated with at least five tracks with transverse momentum $p_T^{\text{track}} > 150 \text{ MeV}$. The efficiency for collision events to pass these requirements was over 99%, while the contribution from fake vertices was negligible [62, 64].

Jets were identified using the anti- k_t jet algorithm [65], implemented in the FASTJET [66] package, with radius parameter $R = 0.6$. The inputs to jet reconstruction are the energies in three-dimensional topological clusters [67, 68] built from calorimeter cells, calibrated at the electromagnetic (EM) scale.² A jet energy calibration was subsequently applied at the jet level, relating the jet energy measured with the ATLAS calorimeter to the true energy of the stable particles entering the detector. A full description of the jet energy calibration is given in Ref. [64]. For the MC samples, particle jets were built from particles with a lifetime longer than 30 ps in the Monte Carlo event record, excluding muons and neutrinos.

² The electromagnetic scale is the basic calorimeter signal scale to which the ATLAS calorimeters are calibrated. It was established using test-beam measurements for electrons and muons to give the correct response for the energy deposited by electromagnetic showers, while it does not correct for the lower response to hadrons.

For the purpose of measuring σ_{eff} in the four-jet final state, three samples of events were selected, two dijet samples and one four-jet sample. The former two samples have at least two, and the latter at least four, jets in the final state, where each jet was required to have $p_T \geq 20$ GeV and $|\eta| \leq 4.4$. In each event, jets were sorted in decreasing order of their transverse momenta. The transverse momentum of the i^{th} jet is denoted by p_T^i and the jet with the highest p_T (p_T^1) is referred to as the leading jet. To ensure 100% trigger efficiency, the leading jet in four-jet events was required to have $p_T^1 \geq 42.5$ GeV.

The selection requirements for the dijet samples were dictated by those used to select four-jet events. In one class of dijet events, the requirement on the transverse momentum of the leading jet must be equivalent to the requirement on the leading jet in four-jet events, $p_T^1 \geq 42.5$ GeV. The other type of dijet event corresponds to the sub-leading pair of jets in the four-jet event, with a requirement of $p_T \geq 20$ GeV. In the following, the cross-section for dijets selected with $p_T^1 \geq 20$ GeV is denoted by σ_{2j}^A and the cross-section for dijets with $p_T^1 \geq 42.5$ GeV is denoted by σ_{2j}^B .

To summarize, the measurement was performed using the dijet A sample and its two subsamples (dijet B and four-jet), selected using the following requirements:

$$\begin{aligned} \text{Dijet A: } & N_{\text{jet}} \geq 2, \quad p_T^1 \geq 20 \text{ GeV}, \quad p_T^2 \geq 20 \text{ GeV}, \quad |\eta_{1,2}| \leq 4.4, \\ \text{Dijet B: } & N_{\text{jet}} \geq 2, \quad p_T^1 \geq 42.5 \text{ GeV}, \quad p_T^2 \geq 20 \text{ GeV}, \quad |\eta_{1,2}| \leq 4.4, \\ \text{Four-jet: } & N_{\text{jet}} \geq 4, \quad p_T^1 \geq 42.5 \text{ GeV}, \quad p_T^{2,3,4} \geq 20 \text{ GeV}, \quad |\eta_{1,2,3,4}| \leq 4.4, \end{aligned} \quad (11)$$

where N_{jet} denotes the number of reconstructed jets. All of the selected events were corrected for jet reconstruction and trigger inefficiencies, the corrections ranging from 2%–4% for low- p_T jets to less than 1% for jets with $p_T \geq 60$ GeV. The observed distributions of the p_T and y of the four leading jets in the events are shown in [Figures 1\(a\)](#) and [1\(b\)](#) respectively.

5.2. Correction for detector effects

The correction for detector effects was estimated separately for each class of events using the PYTHIA6 MC sample. The same restrictions on the phase space of reconstructed jets, defined in [Eq. \(11\)](#), were applied to particle jets. The correction is given by

$$C_{nj}^{\text{A,B}} = \frac{N_{nj}^{\text{A,B reco}}}{N_{nj}^{\text{A,B particle}}}, \quad (12)$$

where $N_{nj}^{\text{A,B reco}}$ ($N_{nj}^{\text{A,B particle}}$) is the number of n -jet events passing the A-or-B selection requirements using reconstructed (particle) jets.

This correction is sensitive to the migration of events into and out of the phase space of the measurement. Due to the very steep jet- p_T spectrum in dijet and four-jet events, it is crucial to have good agreement between the jet p_T spectra in data and in MC simulation close to the selection threshold before calculating the correction. Therefore, the jet p_T threshold was lowered to 10 GeV and the fiducial $|\eta|$ range was increased to 4.5 for both the reconstructed and particle jets, and the MC events were reweighted such that the jet p_T - y distributions reproduced those measured in data. The value of α_{2j}^{4j} (see [Eq. \(9\)](#)), as determined from the reweighted MC events, is

$$\alpha_{2j}^{4j} = 0.93 \pm 0.01 \text{ (stat.)}, \quad (13)$$

where the uncertainty is statistical. The systematic uncertainties are discussed in [Section 7](#).

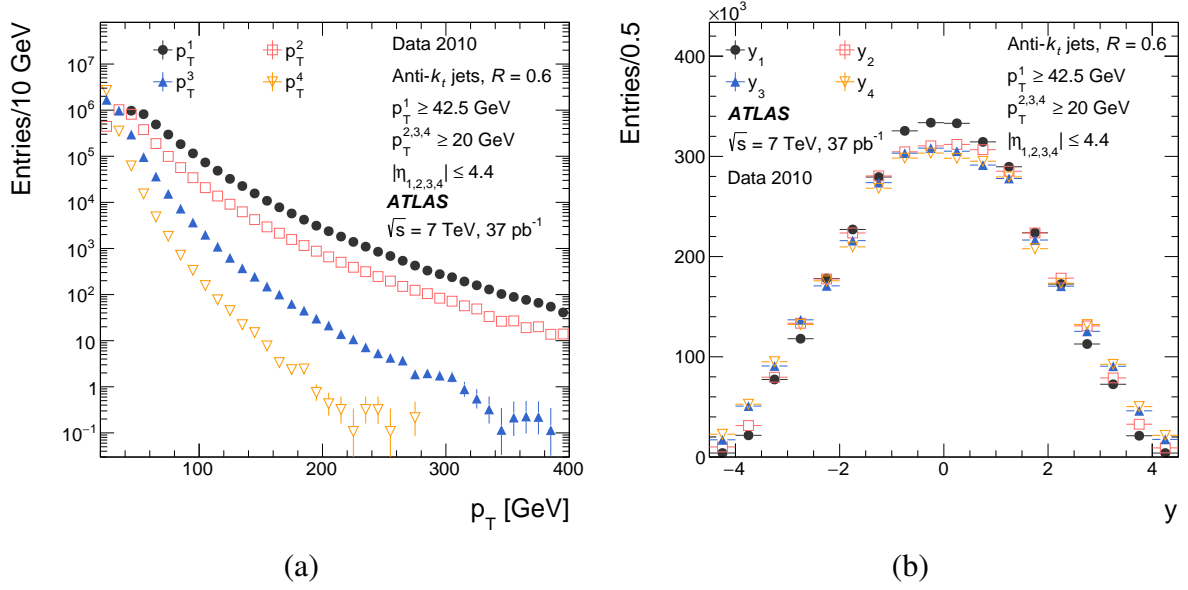


Figure 1: Distributions of the (a) transverse momentum, p_T , and (b) rapidity, y , of the four highest- p_T jets, denoted by $p_T^{1,2,3,4}$ and $y_{1,2,3,4}$, in four-jet events in data selected in the phase space as defined in the legend.

6. Determination of the fraction of DPS events

The main challenge in the measurement of σ_{eff} is to estimate the DPS contribution to the four-jet data sample. It is impossible to extract cDPS and sDPS candidate events on an event-by-event basis. Therefore, the usual approach adopted is to fit the distributions of variables sensitive to cDPS and sDPS in the data to a combination of templates for the expected SPS, cDPS and sDPS contributions. The template for the SPS contribution is extracted from the AHJ MC sample, while the cDPS and sDPS templates are obtained by overlaying two events from the data. In addition to assuming that the two interactions producing the four-jet final state in a DPS event are kinematically decoupled, the analysis relies on the assumption that the SPS template from AHJ properly describes the expected topology of four-jet production in a single interaction. The latter assumption is supported by the observation of good agreement between various distributions in the SPS samples in AHJ and in SHERPA. To exploit the full spectrum of variables sensitive to the various contributions and their correlations, the classification was performed with an artificial neural network.

6.1. Template samples

Differences were observed when comparing the p_T and y distributions in data with those in AHJ. Therefore, before extracting template samples, the events in the four-jet AHJ sample selected with the requirements detailed in Eq. (11) are reweighted such that they reproduce the distributions in data.

In events generated in AHJ, the outgoing partons can be assigned to the primary interaction from the ALPGEN generator or to a secondary interaction, generated by JIMMY, based on the MC generator's event record. The former are referred to as primary-scatter partons and the latter as secondary-scatter partons.

The p_T of secondary-scatter partons was required to be $p_T \geq 15$ GeV in order to match the minimum p_T of primary-scatter partons set by the MLM matching scale in AHJ. Once the outgoing partons were classified, the jets in the event were matched to outgoing partons and the event was classified as an SPS, cDPS or sDPS event.

The matching of jets to partons is done in the ϕ - y plane by calculating the angular distance, $\Delta R_{\text{parton-jet}}$, between the jet and the outgoing parton as

$$\Delta R_{\text{parton-jet}} = \sqrt{(y_{\text{parton}} - y_{\text{jet}})^2 + (\phi_{\text{parton}} - \phi_{\text{jet}})^2}. \quad (14)$$

For 99% of the primary-scatter partons, the parton can be matched to a jet within $\Delta R_{\text{parton-jet}} \leq 1.0$, which was therefore used as a requirement for the matching of jets and partons. Jets were first matched to primary-scatter partons and the remaining jets were matched to secondary-scatter partons.

Events in which none of the leading four jets match a secondary-scatter parton were assigned to the SPS sample. This method of obtaining an SPS sample is preferred over turning off the MPI module in the generator since it retains all of the soft MPI and underlying activity in the selected SPS events. Events were classified as cDPS events if two of the four leading jets match primary-scatter partons and the other two match secondary-scatter partons. Events in which three of the leading jets match primary-scatter partons and the fourth jet matches a secondary-scatter parton were classified as sDPS events.

Four-jet DPS events were modelled by overlaying two different events. To reduce any dependence of the measurement on the modelling of jet production, this construction used events from data rather than MC simulation. Complete-DPS events were built using dijet events from the A and B samples selected from data (see Eq. (11)). To build sDPS events, two other samples were selected with the following requirements:

$$\begin{aligned} \text{One-jet: } & N_{\text{jet}} \geq 1, \quad p_T^1 \geq 20 \text{ GeV}, \quad |\eta_1| \leq 4.4, \\ \text{Three-jet: } & N_{\text{jet}} \geq 3, \quad p_T^1 \geq 42.5 \text{ GeV}, \quad p_T^{2,3} \geq 20 \text{ GeV}, \quad |\eta_{1,2,3}| \leq 4.4. \end{aligned} \quad (15)$$

The overlay was performed at the reconstructed jet level. When constructing cDPS and sDPS events the following conditions were imposed for a given pair of events to be overlaid:

- none of the four jets contains the axis of one of the other jets, i.e., $\Delta R_{\text{jet-jet}} > 0.6$;
- the vertices of the two overlaid events are no more than 10 mm apart in the z direction;
- when building cDPS events, each of the overlaid events contributes two jets to the four leading jets in the constructed event;
- when building sDPS events, one of the overlaid events contributes three jets to the four leading jets in the constructed event and the other contributes one jet.

The first condition ensures that none of the jets would be merged if the four-jet event had been reconstructed as a real event; the second condition avoids possible kinematic bias due to events where two jet pairs originate from far-away vertices; the last two conditions enforce the appropriate composition of the four leading jets in the constructed event.

As is discussed in Section 6.4, the topology of cDPS and sDPS events constructed by overlaying two events is compared to the topology of cDPS and sDPS events extracted from the AHJ sample respectively.

6.2. Kinematic characteristics of event classes

In cDPS, double dijet production should result in pairwise p_T -balanced jets with a distance $|\phi_1 - \phi_2| \approx \pi$ between the jets in each pair. In addition, the azimuthal angle between the two planes of interactions is expected to have a uniform random distribution. In SPS, the pairwise p_T balancing of jets is not as likely; therefore the topology of the four jets is expected to be different for cDPS and SPS.

The topology of three of the jets in sDPS events would resemble the topology of the jets in SPS interactions. The fourth jet initiated by the primary interaction in an SPS is expected to be closer, in the ϕ - y plane, to the other three jets originating from that interaction. In an sDPS event, the jet produced in the secondary interaction would be emitted in a random direction relative to the other three jets.

In constructing possible differentiating variables, three guiding principles were followed:

1. use pairwise relations that have the potential to differentiate between SPS and cDPS topologies;
2. include angular relations between all jets in light of the expected topology of sDPS events;
3. attempt to construct variables least sensitive to systematic uncertainties.

The first two guidelines encapsulate the different characteristics of SPS and DPS events. The third guideline led to the usage of ratios of p_T in order to avoid large dependencies on the jet energy scale (JES) uncertainty. Various studies, including the use of a principal component analysis [69], led to the following list of candidate variables for distinguishing event topologies:

$$\Delta_{ij}^{p_T} = \frac{|\vec{p}_T^i + \vec{p}_T^j|}{p_T^i + p_T^j}; \quad \Delta\phi_{ij} = |\phi_i - \phi_j|; \quad \Delta y_{ij} = |y_i - y_j|; \quad (16)$$

$$|\phi_{1+2} - \phi_{3+4}|; \quad |\phi_{1+3} - \phi_{2+4}|; \quad |\phi_{1+4} - \phi_{2+3}|;$$

where p_T^i , \vec{p}_T^i , y_i and ϕ_i stand for the scalar and vectorial transverse momentum, the rapidity and the azimuthal angle of jet i respectively, with $i = 1, 2, 3, 4$. The variables with the subscript ij are calculated for all possible jet combinations. The term ϕ_{i+j} denotes the azimuthal angle of the four-vector obtained by the sum of jets i and j .

In the following, the pairing notation $\{\langle i, j \rangle \langle k, l \rangle\}$ is used to describe a cDPS event in which jets i and j originate from one interaction and jets k and l originate from the other. In around 85% of cDPS events, the two leading jets originate from one interaction and jets 3 and 4 originate from the other.

Normalized distributions of the $\Delta_{12}^{p_T}$ and $\Delta_{34}^{p_T}$ variables in the three samples (SPS, cDPS and sDPS) are shown in Figures 2(a) and 2(b). In the cDPS sample, the $\Delta_{12}^{p_T}$ and $\Delta_{34}^{p_T}$ distributions peak at low values, indicating that both the leading and the sub-leading jet pairs are balanced in p_T . The small peak around unity is due to events in which the appropriate pairing of the jets is $\{\langle 1, 3 \rangle \langle 2, 4 \rangle\}$ or $\{\langle 1, 4 \rangle \langle 2, 3 \rangle\}$. In the SPS and sDPS samples, the leading jet-pair exhibits a wider peak at higher values of $\Delta_{12}^{p_T}$ compared to that in the cDPS sample. This indicates that the two leading jets are not well balanced in p_T since a significant fraction of the hard-scatter momentum is carried by additional jets.

The $\Delta\phi_{34}$ distributions in the three samples are shown in Figure 2(c). The p_T balance between the jets seen in the $\Delta_{34}^{p_T}$ distribution in the cDPS sample is reflected in the $\Delta\phi_{34}$ distribution. The $\Delta\phi_{34}$ distribution is almost uniform for the SPS and sDPS samples. The correlation between the distributions of the $\Delta_{34}^{p_T}$

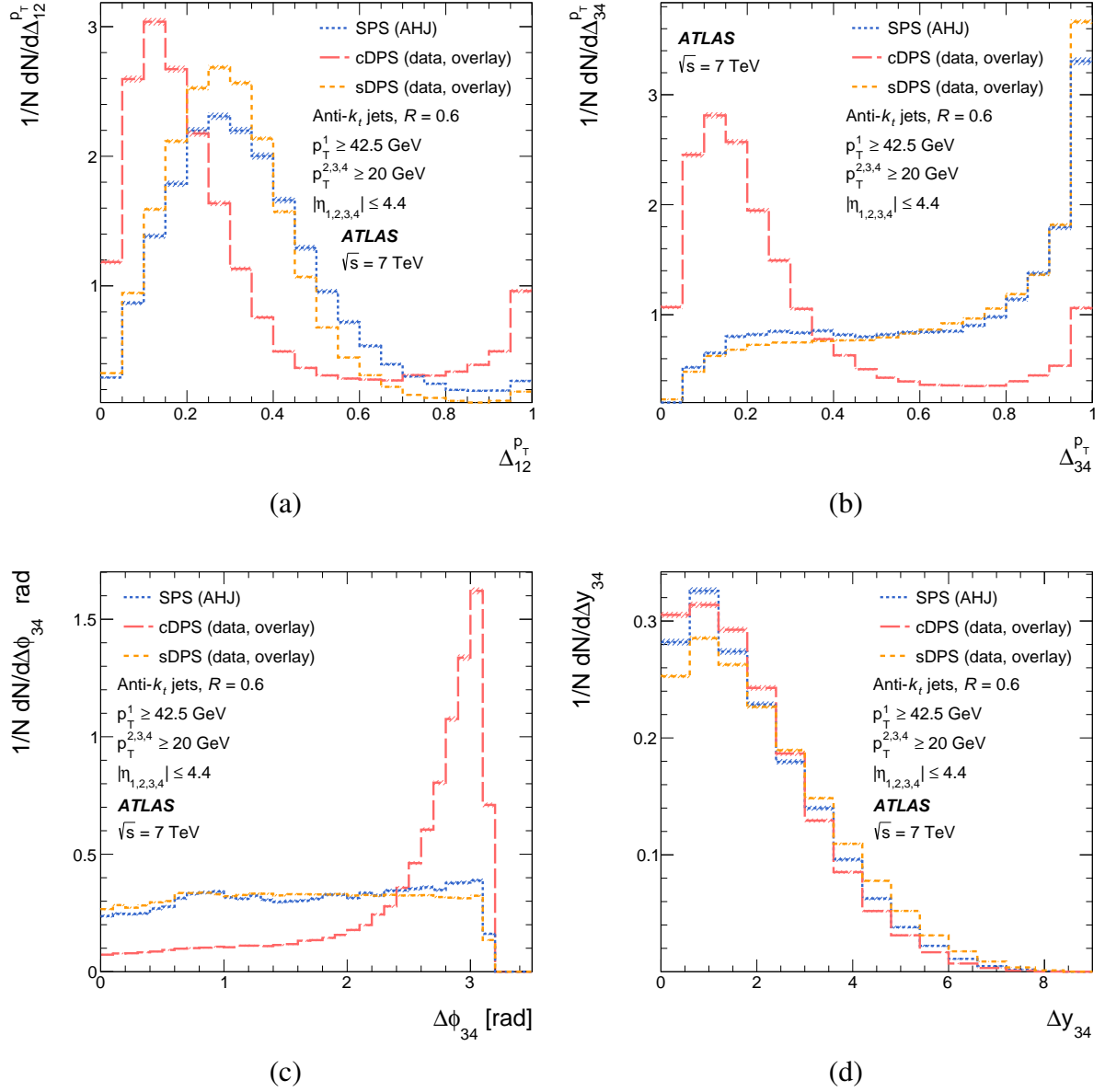


Figure 2: Normalized distributions of the variables, (a) $\Delta_{12}^{p_T}$, (b) $\Delta_{34}^{p_T}$, (c) $\Delta\phi_{34}$ and (d) Δy_{34} , defined in Eq. (16), for the SPS, cDPS and sDPS samples as indicated in the legend. The hatched areas, where visible, represent the statistical uncertainties for each sample.

and $\Delta\phi_{34}$ variables can be readily understood through the following approximation: $p_T^3 \approx p_T^4 \approx p_T$. The expression for $\Delta_{34}^{p_T}$ then becomes

$$\Delta_{34}^{p_T} = \frac{|\vec{p}_T^3 + \vec{p}_T^4|}{p_T^3 + p_T^4} \approx \frac{\sqrt{2p_T + 2p_T \cos(\Delta\phi_{34})}}{2p_T} = \frac{\sqrt{1 + \cos(\Delta\phi_{34})}}{\sqrt{2}}. \quad (17)$$

The peak around unity observed in the $\Delta_{34}^{p_T}$ distributions in the SPS and sDPS samples is thus a direct consequence of the Jacobian of the relation between $\Delta_{34}^{p_T}$ and $\Delta\phi_{34}$.

The set of variables quantifying the distance between jets in rapidity, Δy_{ij} , is particularly important for the sDPS topology. The colour flow is different in SPS leading to the four-jet final state and results in smaller angles between the sub-leading jets. Hence, on average, smaller distances between non-leading jets are expected in the SPS sample compared to the sDPS sample. This is observed in the comparison of the Δy_{34} distributions shown in Figure 2(d), where the distribution in the sDPS sample is slightly wider than in the other two samples.

The study of the various distributions in the three samples is summed up as follows:

- Strong correlations between all variables are observed. The $\Delta_{ij}^{p_T}$ and $\Delta\phi_{ij}$ variables are correlated in a non-linear way, while geometrical constraints correlate the Δy_{ij} and $\Delta\phi_{ij}$ variables. Transverse momentum conservation correlates the $\phi_{i+j} - \phi_{k+l}$ variables with the $\Delta_{ij}^{p_T}$ and $\Delta\phi_{ij}$ variables.
- None of the variables displays a clear separation between all three samples. The variables in which a large difference is observed between the SPS and cDPS distributions, e.g., $\Delta_{34}^{p_T}$, do not provide any differentiating power between SPS and sDPS.
- All variables are important – in cDPS events, where the pairing of the jets is different from $\{(1, 2)(3, 4)\}$, variables relating the other possible pairs, e.g., $\Delta\phi_{13}$, may indicate which is the correct pairing.

These conclusions led to the decision to use a multivariate technique in the form of an NN to perform event classification.

6.3. Extraction of the fraction of DPS events using an artificial neural network

For the purpose of training the NN, events from each sample were divided into two statistically independent subsamples, the training sample and the test sample. The former was used to train the NN and the latter to test the robustness of the result. To avoid bias during training, the events in the SPS, cDPS and sDPS training samples were reweighted such that each sample contributed a third of the total sum of weights. In all subsequent figures, only the test samples are shown.

The NN used is a feed-forward multilayer perceptron with two hidden layers, implemented in the ROOT analysis framework [70]. The input layer has 21 neurons, corresponding to the variables defined in Eq. (16), and the first and second hidden layers have 42 and 12 neurons respectively. These choices represent the product of a study conducted to optimize the performance of the NN and balance the complexity of the network with the computation time of the training. The output of the NN consists of three variables, which are interpreted as the probability for an event to be more like SPS (ξ_{SPS}), cDPS (ξ_{cDPS}) or sDPS (ξ_{sDPS}). During training, each event is marked as belonging to one of the samples; e.g., an event from the cDPS sample is marked as

$$\xi_{\text{SPS}} = 0, \quad \xi_{\text{cDPS}} = 1, \quad \xi_{\text{sDPS}} = 0. \quad (18)$$

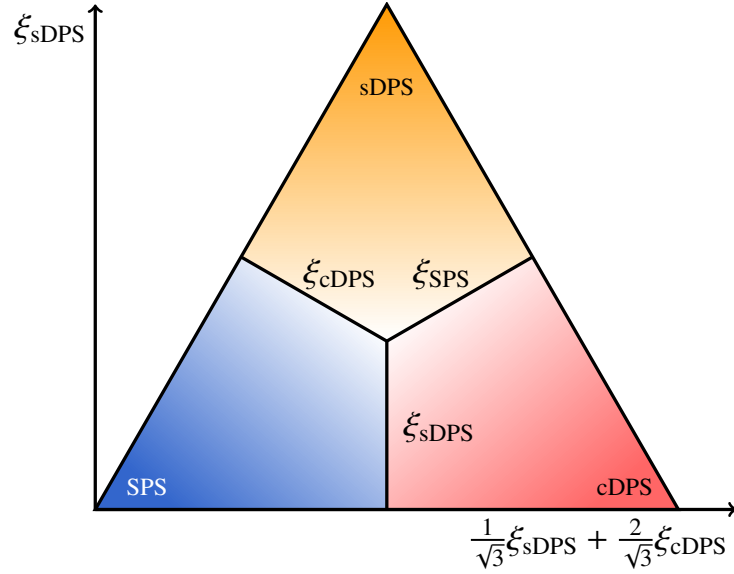


Figure 3: Illustration of the ternary plot constructed from three NN outputs, ξ_{SPS} , ξ_{cDPS} , and ξ_{sDPS} , with the constraint, $\xi_{\text{SPS}} + \xi_{\text{cDPS}} + \xi_{\text{sDPS}} = 1$. The vertical and horizontal axes are defined in the figure. The coloured areas illustrate the classes of events expected to populate the corresponding vertices.

For each event, the three outputs are plotted as a single point inside an equilateral triangle (ternary plot) using the constraint $\xi_{\text{SPS}} + \xi_{\text{cDPS}} + \xi_{\text{sDPS}} = 1$. A point in the triangle expresses the three probabilities as three distances from each of the sides of the triangle. The vertices would therefore be populated by events with high probability to belong to a single sample. Figure 3 shows an illustration of the ternary plot, where the horizontal axis corresponds to $\frac{1}{\sqrt{3}}\xi_{\text{sDPS}} + \frac{2}{\sqrt{3}}\xi_{\text{cDPS}}$ and the vertical axis to the value of ξ_{sDPS} . The coloured areas illustrate where each of the three classes of events is expected to populate the ternary plot.

Figures 4(a), 4(b) and 4(c) show the NN output distribution for the test samples in the ternary plot, presenting the separation power of the NN. The SPS-type events are mostly found in the bottom left corner in Figure 4(a). However, a ridge of SPS events extending towards the sDPS corner is observed as well. A contribution from SPS events is also visible in the bottom right corner. The clearest peak is seen for events from the cDPS sample in the bottom right corner in Figure 4(b). A visible cluster of sDPS events is seen in Figure 4(c) concentrated around $\xi_{\text{sDPS}} \sim 0.75$ and there is a tail of events along the side connecting the SPS and sDPS corners. The NN output distribution in the data, shown in Figure 4(d), is visually consistent with a superposition of the three components, SPS, cDPS and sDPS.

Based on these observations, it is clear that event classification on an event-by-event basis is not possible. However, the differences between the SPS, cDPS and sDPS distributions suggest that an estimation of the different contributions can be performed. To estimate the cDPS and sDPS fractions in four-jet events, the ternary distribution in data (\mathcal{D}) is fitted to a weighted sum of the ternary distributions in the SPS (\mathcal{M}_{SPS}), cDPS ($\mathcal{M}_{\text{cDPS}}$) and sDPS ($\mathcal{M}_{\text{sDPS}}$) samples, each normalized to the measured four-jet cross-section in data, with the fractions as free parameters. The optimal fractions were obtained using a fit of the form,

$$\mathcal{D} = (1 - f_{\text{cDPS}} - f_{\text{sDPS}})\mathcal{M}_{\text{SPS}} + f_{\text{cDPS}}\mathcal{M}_{\text{cDPS}} + f_{\text{sDPS}}\mathcal{M}_{\text{sDPS}}, \quad (19)$$

where a χ^2 minimization was performed, as implemented in the MINUIT [71] package in ROOT, taking into account the statistical uncertainties of all the samples in each bin. The results of the fit are presented in Section 8, after the methodology validation and discussion of systematic uncertainties.

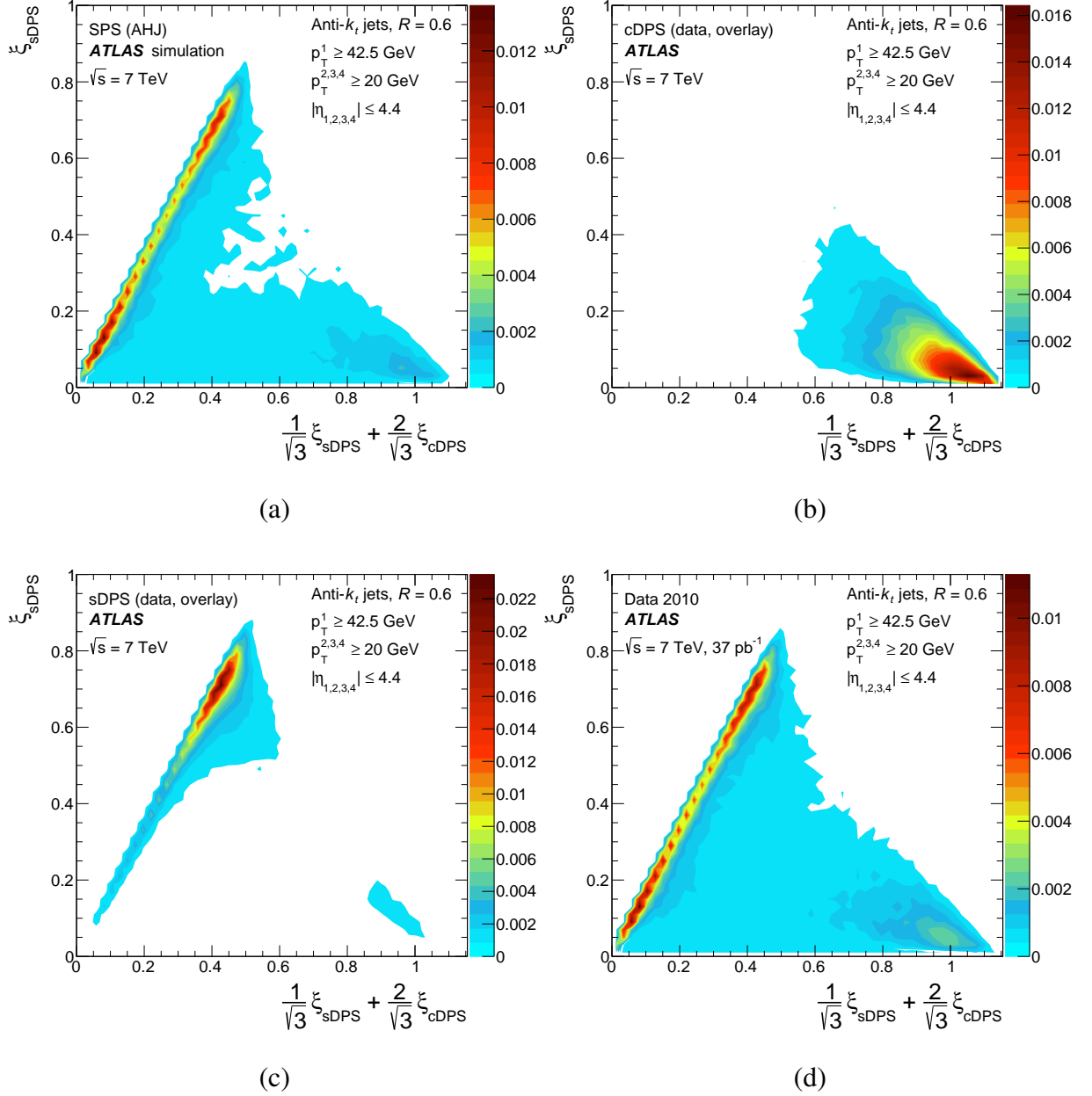


Figure 4: Normalized distributions of the NN outputs, mapped to a ternary plot as described in the text, in the (a) SPS, (b) cDPS, (c) sDPS test samples and (d) in the data.

6.4. Methodology validation

A sizeable discrepancy was found in the $\Delta_{34}^{p_T}$ and $\Delta\phi_{34}$ distributions between the data and AHJ (See [Section 9](#) for details), suggesting that there are more sub-leading jets (jets 3 and 4) that are back-to-back in AHJ than in the data. In order to test that the discrepancies are not from mis-modelling of SPS in AHJ, the $\Delta_{34}^{p_T}$ and $\Delta\phi_{34}$ distributions in the SPS sample extracted from AHJ were compared to the distributions in the SPS sample generated in SHERPA. Good agreement between the shapes of the distributions was observed for both variables. This and further studies indicate that the excess of events with jets 3 and 4 in the back-to-back topology is due to an excess of DPS events in the AHJ sample compared to the data.

In order to verify that the topologies of cDPS and sDPS events can be reproduced by overlaying two events, the overlay samples are compared to the cDPS and sDPS samples extracted from AHJ. An extensive comparison between the distributions of the variables used as input to the NN in the overlay samples and in AHJ was performed and good agreement was observed. This can be summarized by comparing the NN output distributions. The NN is applied to the cDPS and sDPS samples extracted from AHJ and the output distributions are compared to the output distributions in the corresponding samples constructed by overlaying events selected from data. Normalized distributions of the projection of the full ternary plot on the horizontal axis are shown in [Figures 5\(a\)](#) and [5\(b\)](#) for the cDPS and sDPS samples respectively. Good agreement is observed between the distributions. Based on these results, it is concluded that the topology of the four jets in the overlaid events is comparable to that of the four leading jets in DPS events extracted from AHJ. The added advantage of using overlaid events from data to construct the DPS samples is that the jets are at the same JES as the jets in four-jet events in data, leading to a smaller systematic uncertainty in the final result.

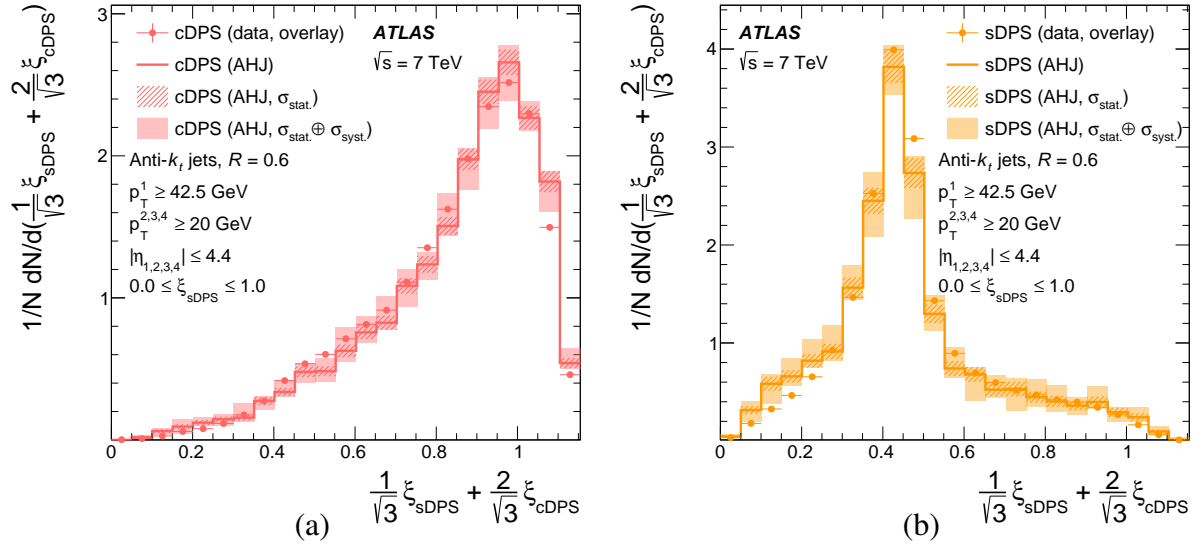


Figure 5: Comparison between the normalized distributions of the NN outputs $\frac{1}{\sqrt{3}}\xi_{sDPS} + \frac{2}{\sqrt{3}}\xi_{cDPS}$, integrated over all ξ_{sDPS} values $0.0 \leq \xi_{sDPS} \leq 1.0$, in DPS events extracted from AHJ and in the DPS samples constructed by overlaying events from data, for (a) cDPS events and (b) sDPS events. In the AHJ distributions, statistical uncertainties are shown as the hatched area and the shaded area represents the sum in quadrature of the statistical and systematic uncertainties.

As an additional validation step, the NN is applied to the inclusive AHJ sample and the resulting distribution is fitted with the NN output distributions of the SPS, cDPS and sDPS samples. The fraction obtained from the fit, $f_{\text{DPS}}^{(\text{MC})}$, is compared to the fraction at parton level, $f_{\text{DPS}}^{(\text{P})}$, extracted from the event record,

$$f_{\text{DPS}}^{(\text{MC})} = 0.129 \pm 0.007 \text{ (stat.)}, \quad f_{\text{DPS}}^{(\text{P})} = 0.142 \pm 0.001 \text{ (stat.)}. \quad (20)$$

Fair agreement is observed between the value obtained from the fit and that at parton level. The larger statistical uncertainty in $f_{\text{DPS}}^{(\text{MC})}$ compared to $f_{\text{DPS}}^{(\text{P})}$ reflects the loss of statistical power due to the use of a template fit to estimate the former.

7. Systematic uncertainties

For jets with $20 \leq p_{\text{T}} < 30$ GeV, the fractional JES uncertainty is about 4.5% in the central region of the detector, rising to about 10% in the forward region [64]. The overall impact of the JES on the distributions, f_{DPS} and α_{2j}^{4j} was estimated by shifting the jet energy upwards and downwards in the MC samples by the JES uncertainty and repeating the analysis. Similarly, the overall impact of the jet energy and angular resolution was determined by varying the jet energy and angular resolution in the MC samples by the corresponding resolution uncertainty [72].

The systematic uncertainties in the measured cross-sections due to the integrated luminosity measurement uncertainty ($\pm 3.5\%$), the jet reconstruction efficiency uncertainty ($\pm 2\%$) and the uncertainty as a result of selecting single-vertex events ($\pm 0.5\%$) were propagated to the uncertainty in σ_{eff} .

The statistical uncertainty in the AHJ sample was translated to a systematic uncertainty in f_{DPS} by varying the reweighting function used to reweight AHJ and repeating the analysis.

The statistical uncertainty in α_{2j}^{4j} ($\sim 1\%$) was propagated as a systematic uncertainty in σ_{eff} . The systematic uncertainty in α_{2j}^{4j} arising from model-dependence ($\pm 2\%$) was determined from deriving α_{2j}^{4j} using SHERPA.

The stability of the value of σ_{eff} relative to the various parameter values used in the measurement was studied. Parameters such as $p_{\text{T}}^{\text{parton}}$ and $\Delta R_{\text{jet-jet}}$ were varied and the requirement $\Delta R_{\text{parton-jet}} \leq 0.6$ was applied, leading to a relative change in σ_{eff} of the order of a few percent. Since the observed relative changes are small compared to the statistical uncertainty in σ_{eff} , no systematic uncertainty was assigned due to these parameters.

The relative systematic uncertainties in f_{DPS} , α_{2j}^{4j} and σ_{eff} are summarized in Table 1. The dominant systematic uncertainty on f_{DPS} originates from the JES variation. A variation in the JES results in a modification of the NN output distribution for the SPS template used in the fit, which directly impacts the value of f_{DPS} .

8. Determination of σ_{eff}

To determine f_{DPS} and σ_{eff} and their statistical uncertainties taking into account all of the correlations, many replica fits were performed by random sampling from the NN output distributions. The systematic

Source of systematic uncertainty	Δf_{DPS}	$\Delta \alpha_{2j}^{4j}$	$\Delta \sigma_{\text{eff}}$
Luminosity			$\pm 3.5 \%$
Model dependence for detector corrections		$\pm 2 \%$	$\pm 2 \%$
Reweightings of AHJ	$\pm 6 \%$		$\pm 6 \%$
Jet reconstruction efficiency			$\pm 0.1 \%$
Single-vertex events selection			$\pm 0.1 \%$
Jet energy and angular resolution	$\pm 15 \%$	$\pm 3 \%$	$\pm 15 \%$
JES uncertainty	$^{+32}_{-37} \%$	$\pm 12 \%$	$^{+31}_{-19} \%$
Total systematic uncertainty	$^{+36}_{-40} \%$	$\pm 13 \%$	$^{+35}_{-25} \%$

Table 1: Summary of the relative systematic uncertainties in f_{DPS} , α_{2j}^{4j} and σ_{eff} .

uncertainties were obtained by propagating the expected variations into this analysis, and the resulting shifts were added in quadrature. The result for f_{DPS} is

$$f_{\text{DPS}} = 0.092^{+0.005}_{-0.011} (\text{stat.})^{+0.033}_{-0.037} (\text{syst.}), \quad (21)$$

where the contribution of f_{sDPS} to f_{DPS} was found to be about 40%. The fraction of DPS estimated in data is $65^{+23}_{-27} \%$ of the fraction in AHJ as extracted from the event record (see Eq. (20)). Taking into account the systematic uncertainties in the calculation of the goodness-of-fit χ^2 , a value for χ^2/N_{DF} of $112/84 = 1.3$ is obtained, where N_{DF} is the number of degrees of freedom in the fit.

In order to visualize the results of the fit, the ternary distribution is divided into five slices,

- $0.0 \leq \xi_{\text{sDPS}} < 0.1$,
- $0.1 \leq \xi_{\text{sDPS}} < 0.3$,
- $0.3 \leq \xi_{\text{sDPS}} < 0.5$,
- $0.5 \leq \xi_{\text{sDPS}} < 0.7$,
- $0.7 \leq \xi_{\text{sDPS}} \leq 1.0$.

A comparison of the fit distributions with the distributions in data in the five slices of the ternary plot is shown in Figure 6. Considering the systematic uncertainties, the most significant difference between the data and the fit is seen for the two left-most bins in the range $0.0 \leq \xi_{\text{sDPS}} < 0.1$ (Figure 6(a)) of the ternary plot. These bins are dominated by the SPS contribution. Thus, a discrepancy between the data and the fit result in these bins is expected to have a negligible effect on the measurement of the DPS rate. A discrepancy between the data and the fit result is also observed in the three rightmost bins in Figure 6(a). These bins have about a 30% contribution from cDPS. To test the effect of this discrepancy on the description of observables in data, the distributions of the various variables in data were compared to a combination of the distributions in the SPS, cDPS and sDPS samples, normalizing the latter three distributions to their respective fractions in the data as obtained in the fit. This comparison for the $\Delta_{34}^{p_T}$ and $\Delta\phi_{34}$ variables is shown in Figure 7, where a good description of the data is observed. The same level of agreement is seen for all the variables.

Before calculating σ_{eff} , the symmetry factor in Eq. (6) has to be adjusted because there is an overlap in the cross-sections σ_{2j}^A and σ_{2j}^B when the leading jet in sample A has $p_T \geq 42.5$ GeV (see Eq. (11)). The

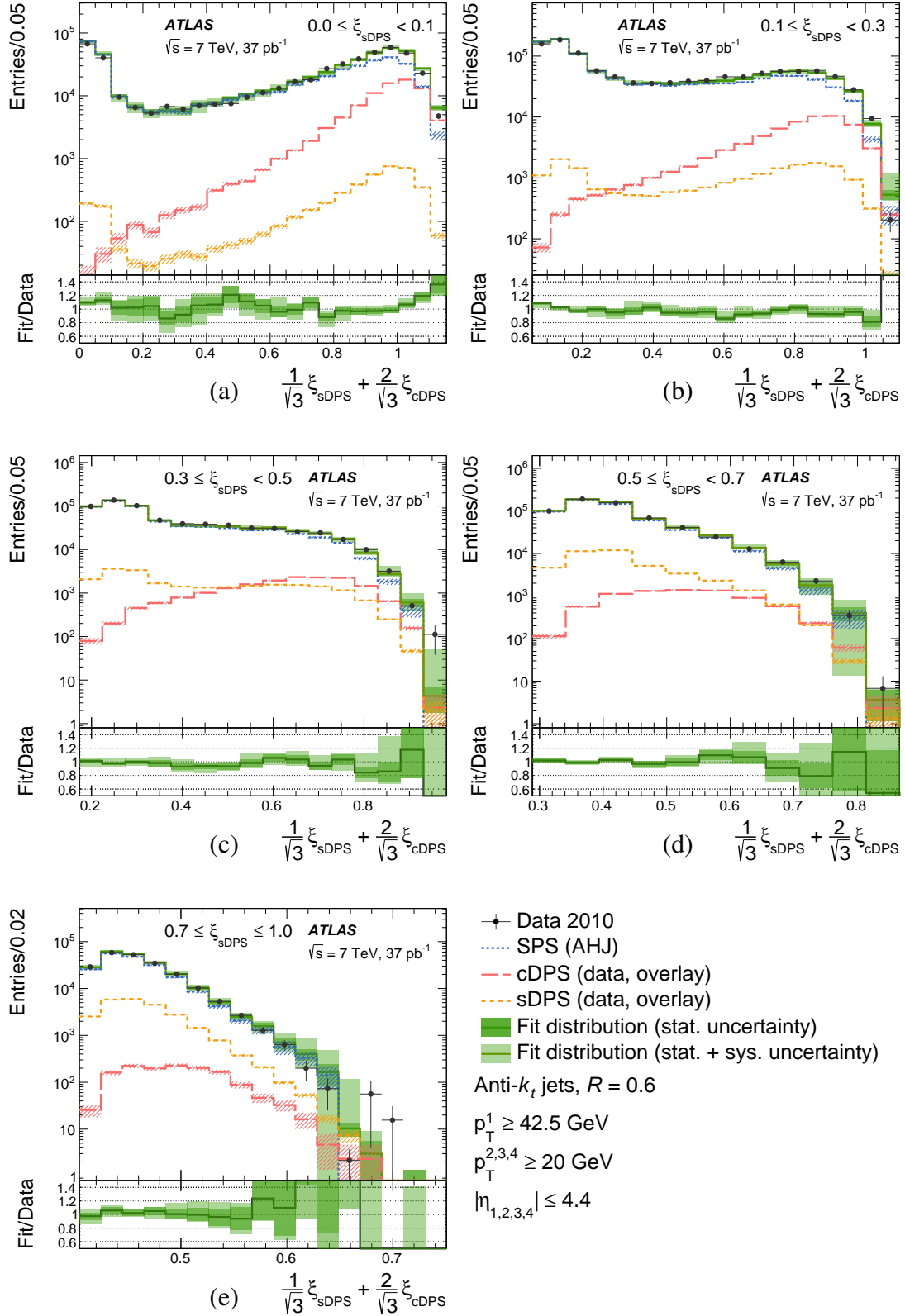


Figure 6: Distributions of the NN outputs, $\frac{1}{\sqrt{3}}\xi_{\text{sDPS}} + \frac{2}{\sqrt{3}}\xi_{\text{cDPS}}$, in the ξ_{sDPS} ranges indicated in the panels, for four-jet events in data, selected in the phase space defined in the legend, compared to the result of fitting a combination of the SPS, cDPS and sDPS contributions, the sum of which is shown as the solid line. In the fit distribution, statistical uncertainties are shown as the dark shaded area and the light shaded area represents the sum in quadrature of the statistical and systematic uncertainties. The ratio of the fit distribution to the data is shown in the bottom panels.

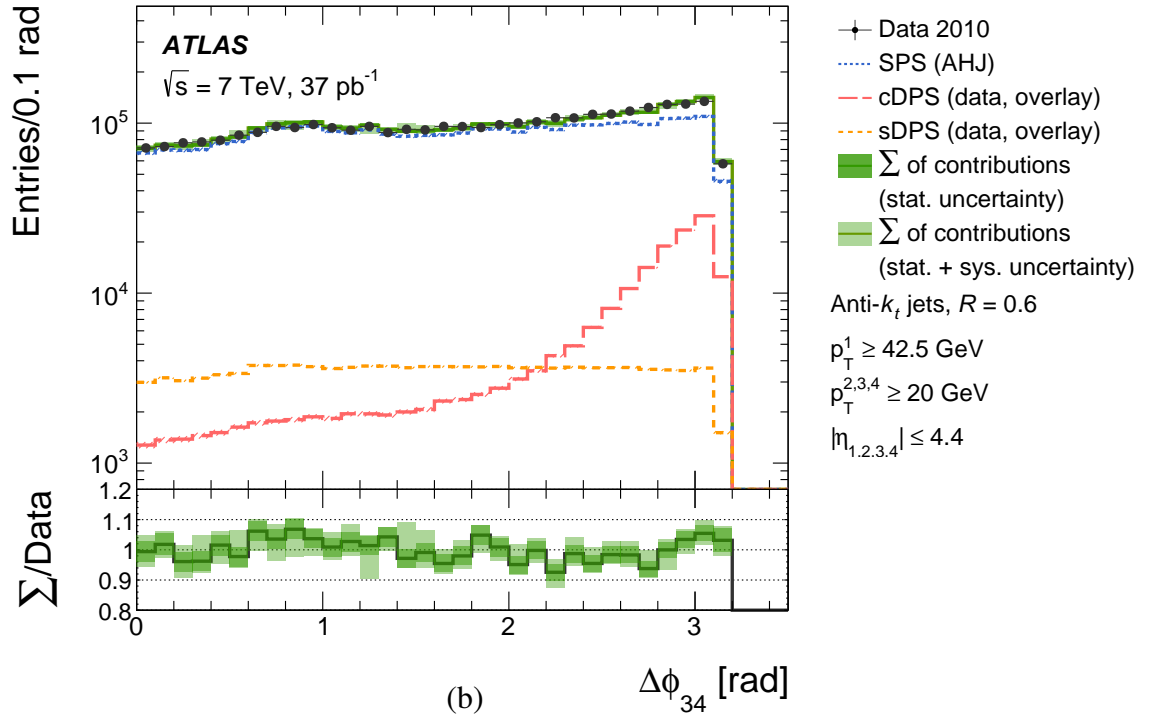
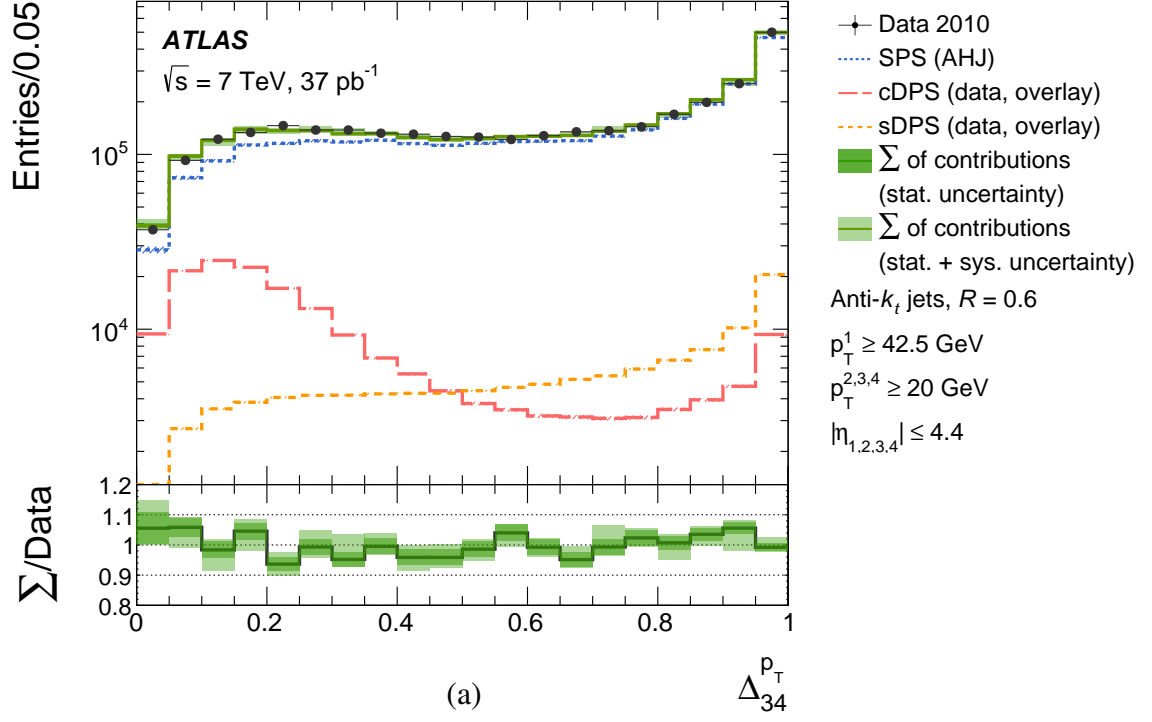


Figure 7: Comparison between the distributions of the variables (a) Δp_{T34}^{PT} and (b) $\Delta\phi_{34}$, defined in Eq. (16), in four-jet events in data and the sum of the SPS, cDPS and sDPS contributions, as indicated in the legend. The sum of the contributions is normalized to the cross-section measured in data and the various contributions are normalized to their respective fractions obtained from the fit. In the sum of contributions, statistical uncertainties are shown as the dark shaded area and the light shaded area represents the sum in quadrature of the statistical and systematic uncertainties. The ratio of the sum of contributions to the data is shown in the bottom panels.

adjusted symmetry factor is

$$\frac{1}{1 + \delta_{AB}} \longrightarrow 1 - \frac{1}{2} \frac{\sigma_{2j}^B}{\sigma_{2j}^A} = 0.9353 \pm 0.0003 \text{ (stat.)}, \quad (22)$$

as determined from the measured dijet cross-sections. This factor was also determined using PYTHIA6 and good agreement was observed between the two values. The relative difference in the value of σ_{eff} obtained by using the symmetry factors extracted from the data and from PYTHIA6 was of the order of 0.2%, a negligible difference compared to the statistical uncertainty of σ_{eff} .

An additional correction of +4% is applied to the measured DPS cross-section due to the probability of jets from the secondary interaction overlapping with jets from the primary interaction. In this configuration, the anti- k_t algorithm merges the two overlapping jets into one, and hence the event cannot pass the four-jet requirement. The value of this correction was determined from the fraction of phase space occupied by a jet. It was also determined directly in AHJ and good agreement between the two values was observed.

Finally, the measurements of the dijet and four-jet cross-sections can be used to calculate the effective cross-section, yielding

$$\sigma_{\text{eff}} = 14.9^{+1.2}_{-1.0} \text{ (stat.) }^{+5.1}_{-3.8} \text{ (syst.) mb}. \quad (23)$$

This value is consistent within the quoted uncertainties with previous measurements, performed by the ATLAS collaboration and by other experiments [16–30], all of which are summarized in Figure 8. Figure 9 shows σ_{eff} as a function of \sqrt{s} , where the AFS result and some of the LHCb results are omitted for clarity. Within the large uncertainties, the measurements are consistent with no \sqrt{s} dependence of σ_{eff} . The σ_{eff} value obtained is $21^{+7}_{-6}\%$ of the inelastic cross-section, σ_{inel} , measured by ATLAS at $\sqrt{s} = 7$ TeV [73].

9. Normalized differential cross-sections

To allow the results of this study to be used in future comparisons with MPI models, the distributions of the variables used as input to the NN were corrected for detector effects. The corrections were derived using an iterative unfolding, producing an unfolding matrix for each observable, relating the particle-level and reconstructed-level quantities. These matrices were derived using samples of four-jet events selected from the AHJ and PYTHIA6 samples by imposing the cuts detailed in Eq. (11) on particle jets. The AHJ sample generated with the AUET1 tune was used to derive the unfolding matrix. The distributions were unfolded with the Bayesian unfolding algorithm, implemented in the RooUnfold package [74], using two iterations.

The unfolding matrices derived from AHJ were taken as the nominal matrices and the differences observed when using the matrices derived from PYTHIA6 were used as an additional systematic uncertainty, typically of the order of a few percent in each bin. The total systematic uncertainty of the differential distributions in data was obtained by summing in quadrature the uncertainty due to MC modelling in a given bin with the systematic uncertainties in this bin due to the JES and jet energy and angular resolution uncertainties, while preserving correlations between bins. Figure 10 shows the normalized differential cross-section distribution in data for the $\Delta_{34}^{p_T}$ and $\Delta\phi_{34}$ variables compared to the particle-level distributions in the AHJ samples generated with the AUET1 and AUET2 tunes. The particle-level distributions

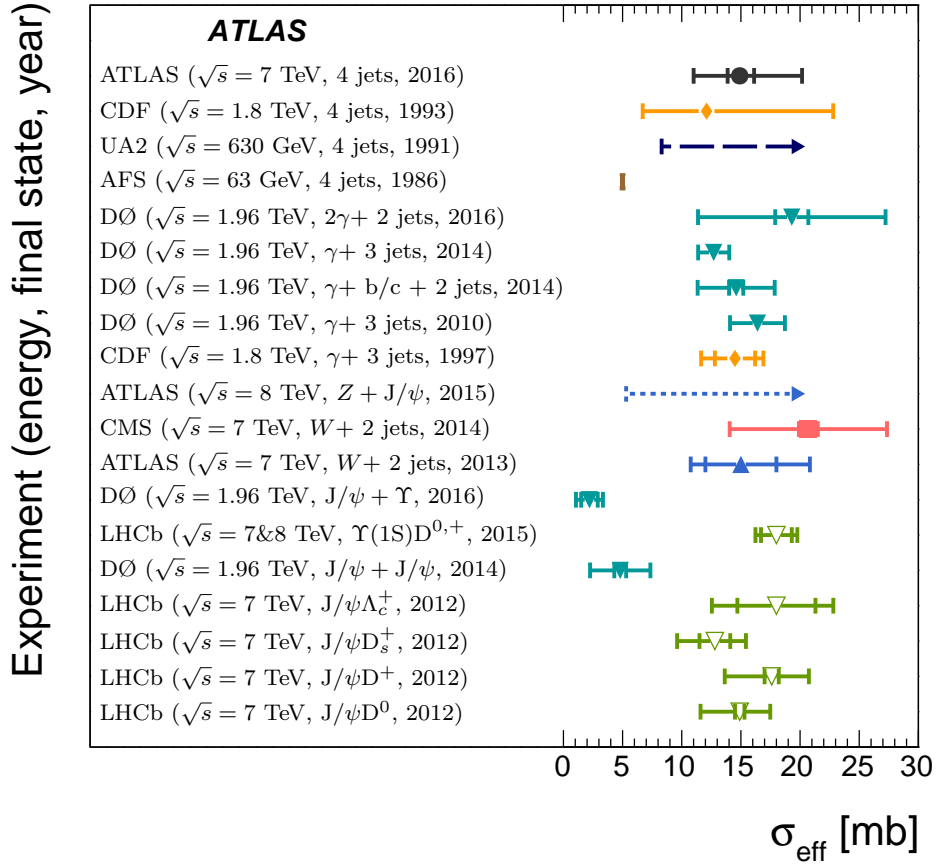


Figure 8: The effective cross-section, σ_{eff} , determined in various final states and in different experiments [16–30]. The inner error bars (where visible) correspond to the statistical uncertainties and the outer error bars represent the sum in quadrature of the statistical and systematic uncertainties. Dashed arrows indicate lower limits and the vertical line represents the AFS measurement published without uncertainties.

in the AUET2 AHJ sample overestimate the normalized differential cross-section distributions in data in the regions $\Delta\phi_{34}^{\text{PT}} \leq 0.15$ and $\Delta\phi_{34} \geq 2.8$, demonstrating the excess of the DPS contribution in this sample compared to the data. On the other hand, the DPS contribution in the data is underestimated by the prediction obtained with the AUET1 tune. These comparisons demonstrate the power of these distributions to constrain MPI models and tunes. In [Appendix A](#), the normalized differential cross-sections in data for the remaining variables are compared to the particle-level distributions in the AHJ samples generated using the AUET1 and AUET2 tunes.

10. Summary and conclusions

A measurement of the rate of hard double-parton scattering in four-jet events was performed using a sample of data collected with the ATLAS experiment at the LHC in 2010, with an average of approximately 0.4 proton–proton interactions per bunch crossing, corresponding to an integrated luminosity of $37.3 \pm 1.3 \text{ pb}^{-1}$. Three different samples were selected, all consisting of single-vertex events from proton–proton collisions at a centre-of-mass energy of $\sqrt{s} = 7 \text{ TeV}$. Four-jet events were defined as

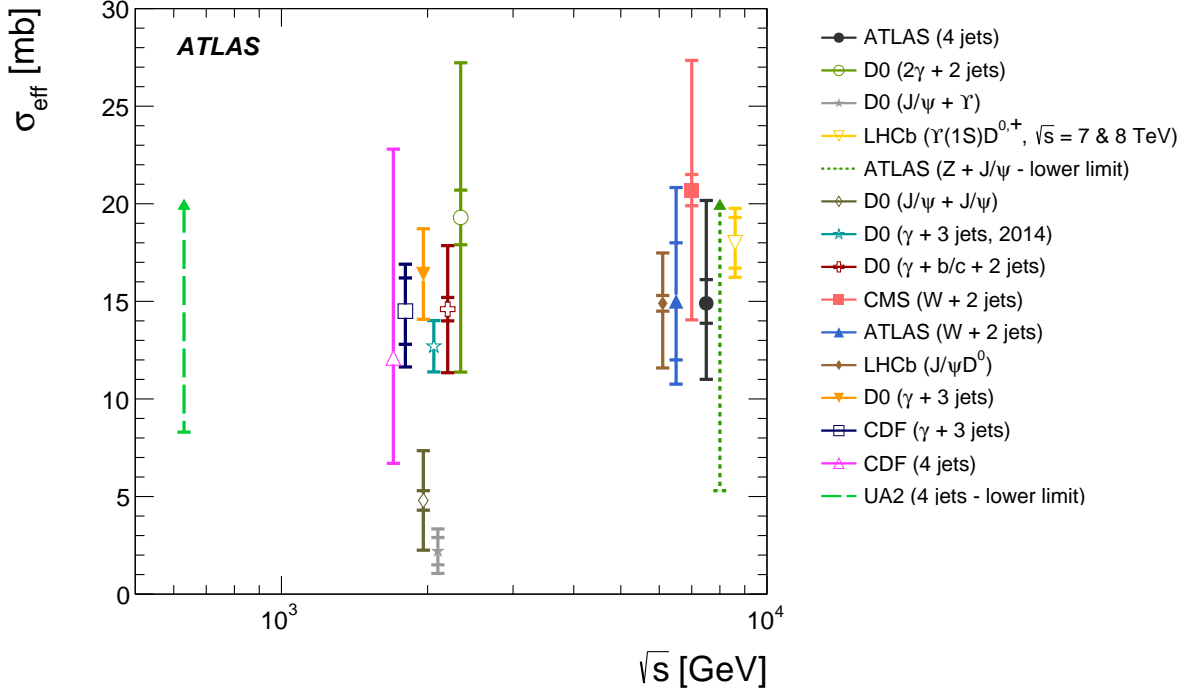


Figure 9: The effective cross-section, σ_{eff} , as a function of the centre-of-mass energy, \sqrt{s} , for a representative set of measurements [17–30]. The inner error bars (where visible) correspond to the statistical uncertainties and the outer error bars represent the sum in quadrature of the statistical and systematic uncertainties. Dashed arrows indicate lower limits. For clarity, measurements at identical centre-of-mass energies are slightly offset in \sqrt{s} .

those containing at least four reconstructed jets with $p_T \geq 20$ GeV and $|\eta| \leq 4.4$, and at least one jet having $p_T \geq 42.5$ GeV. Two additional dijet samples were selected with the requirement of having at least two jets with $p_T \geq 20$ GeV and $|\eta| \leq 4.4$. One of the dijet samples was further constrained such that it contained at least one jet with $p_T \geq 42.5$ GeV.

The contribution of hard double-parton scattering to the production of four-jet events was extracted using an artificial neural network. The four-jet topology originating from hard double-parton scattering was represented by a random combination of events selected in data. The fraction of events corresponding to the contribution made by hard double-parton scattering in four-jet events was determined to be,

$$f_{\text{DPS}} = 0.092^{+0.005}_{-0.011} \text{ (stat.) }^{+0.033}_{-0.037} \text{ (syst.)}. \quad (24)$$

After combining this result with measurements of the dijet and four-jet cross-sections in the appropriate phase space regions, the effective cross-section was determined to be

$$\sigma_{\text{eff}} = 14.9^{+1.2}_{-1.0} \text{ (stat.) }^{+5.1}_{-3.8} \text{ (syst.) mb}.$$

This value is $21^{+7}_{-6}\%$ of the measured value of σ_{inel} at $\sqrt{s} = 7$ TeV and is consistent with previous measurements performed at various centre-of-mass energies and in various final states. It is compatible with a model in which σ_{eff} is a universal parameter that does not depend on the process or phase space. To facilitate future studies of the dynamics of multi-parton interactions, distributions of observables sensitive to the presence of hard double-parton scattering are also presented.

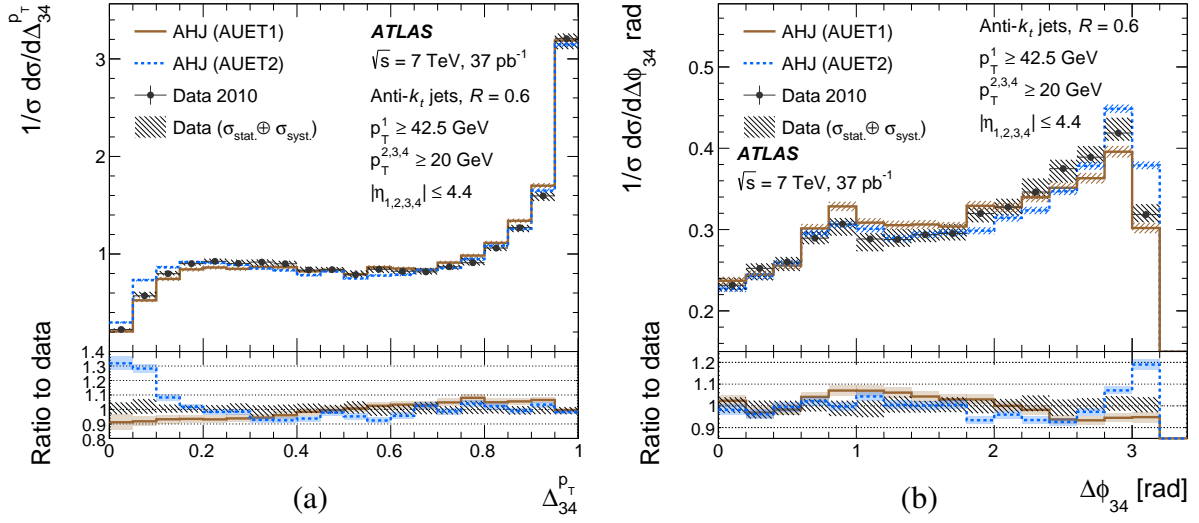


Figure 10: Distributions of the variables (a) Δp_T^{34} and (b) $\Delta \phi_{34}$, defined in Eq. (16), in data after unfolding to particle level, compared to the MC prediction from AHJ at the particle level, generated using the AUET1 and AUET2 tunes, as indicated in the legend. The hatched area represents the sum in quadrature of the statistical and systematic uncertainties in the normalized differential cross-sections and all histograms are normalized to unity. The ratio of the particle-level distribution to the normalized differential cross-section is shown in the bottom panels, where the shaded areas represent statistical uncertainties.

Acknowledgements

We thank CERN for the very successful operation of the LHC, as well as the support staff from our institutions without whom ATLAS could not be operated efficiently.

We acknowledge the support of ANPCyT, Argentina; YerPhI, Armenia; ARC, Australia; BMWFW and FWF, Austria; ANAS, Azerbaijan; SSTC, Belarus; CNPq and FAPESP, Brazil; NSERC, NRC and CFI, Canada; CERN; CONICYT, Chile; CAS, MOST and NSFC, China; COLCIENCIAS, Colombia; MSMT CR, MPO CR and VSC CR, Czech Republic; DNRf and DNSRC, Denmark; IN2P3-CNRS, CEA-DSM/IRFU, France; GNSF, Georgia; BMBF, HGF, and MPG, Germany; GSRT, Greece; RGC, Hong Kong SAR, China; ISF, I-CORE and Benoziyo Center, Israel; INFN, Italy; MEXT and JSPS, Japan; CNRST, Morocco; FOM and NWO, Netherlands; RCN, Norway; MNiSW and NCN, Poland; FCT, Portugal; MNE/IFA, Romania; MES of Russia and NRC KI, Russian Federation; JINR; MESTD, Serbia; MSSR, Slovakia; ARRS and MIZŠ, Slovenia; DST/NRF, South Africa; MINECO, Spain; SRC and Wallenberg Foundation, Sweden; SERI, SNSF and Cantons of Bern and Geneva, Switzerland; MOST, Taiwan; TAEK, Turkey; STFC, United Kingdom; DOE and NSF, United States of America. In addition, individual groups and members have received support from BCKDF, the Canada Council, CANARIE, CRC, Compute Canada, FQRNT, and the Ontario Innovation Trust, Canada; EPLANET, ERC, FP7, Horizon 2020 and Marie Skłodowska-Curie Actions, European Union; Investissements d’Avenir Labex and Idex, ANR, Région Auvergne and Fondation Partager le Savoir, France; DFG and AvH Foundation, Germany; Herakleitos, Thales and Aristeia programmes co-financed by EU-ESF and the Greek NSRF; BSF,

GIF and Minerva, Israel; BRF, Norway; Generalitat de Catalunya, Generalitat Valenciana, Spain; the Royal Society and Leverhulme Trust, United Kingdom.

The crucial computing support from all WLCG partners is acknowledged gratefully, in particular from CERN, the ATLAS Tier-1 facilities at TRIUMF (Canada), NDGF (Denmark, Norway, Sweden), CC-IN2P3 (France), KIT/GridKA (Germany), INFN-CNAF (Italy), NL-T1 (Netherlands), PIC (Spain), ASGC (Taiwan), RAL (UK) and BNL (USA), the Tier-2 facilities worldwide and large non-WLCG resource providers. Major contributors of computing resources are listed in Ref. [75].

Appendix

A. Normalized differential cross-sections

Figures 11–15 show the normalized differential cross-sections in data for all the observables used as input to the NN, compared to the particle-level distributions in the AHJ samples generated using the AUET1 and AUET2 tunes. The hatched areas in the distributions represent the total uncertainty of the normalized differential cross-section, obtained by adding in quadrature the statistical and systematic uncertainties.

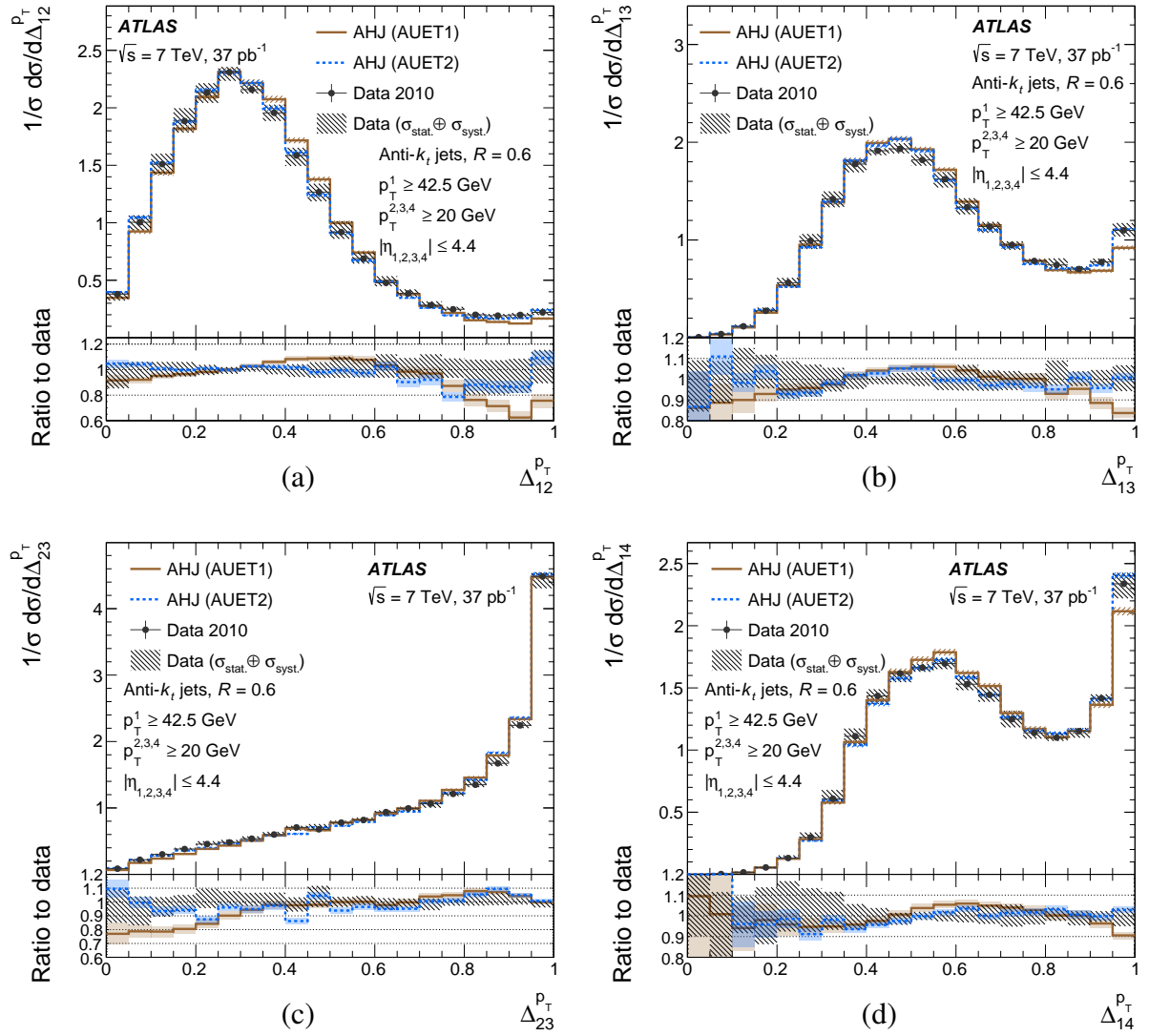


Figure 11: Distributions of the variables (a) $\Delta_{12}^{p_T}$, (b) $\Delta_{13}^{p_T}$, (c) $\Delta_{23}^{p_T}$ and (d) $\Delta_{14}^{p_T}$, defined in Eq. (16), in data after unfolding to particle level, compared to the MC prediction from AHJ at the particle level, generated using the AUET1 and AUET2 tunes, as indicated in the legend. The hatched areas represent the sum in quadrature of the statistical and systematic uncertainties in the normalized differential cross-sections and all histograms are normalized to unity. The ratio of the particle-level distribution to the normalized differential cross-section is shown in the bottom panels, where the shaded areas represent statistical uncertainties.

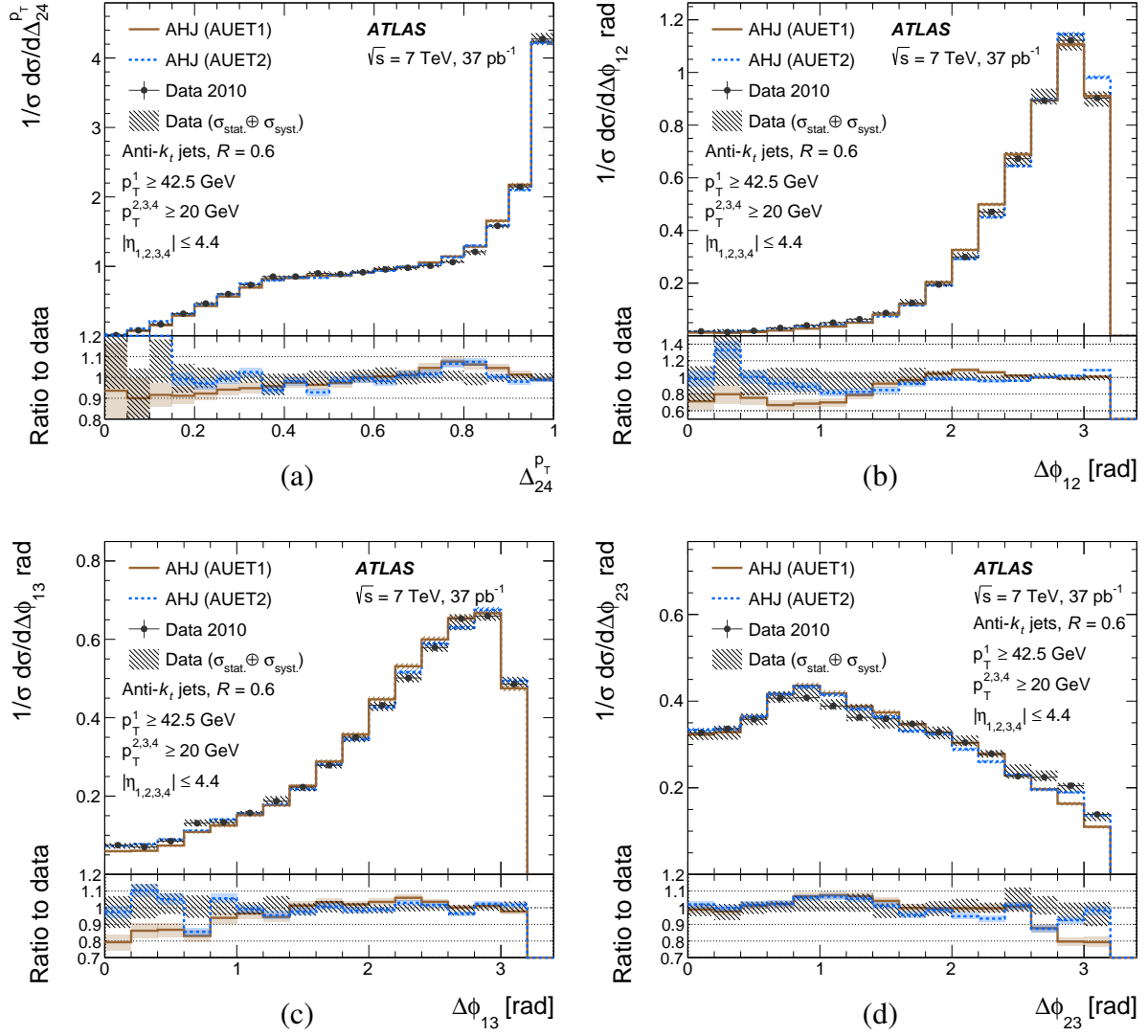


Figure 12: Distributions of the variables (a) $\Delta_{24}^{p_T}$, (b) $\Delta\phi_{12}$, (c) $\Delta\phi_{13}$ and (d) $\Delta\phi_{23}$, defined in Eq. (16), in data after unfolding to particle level, compared to the MC prediction from AHJ at the particle level, generated using the AUET1 and AUET2 tunes, as indicated in the legend. The hatched areas represent the sum in quadrature of the statistical and systematic uncertainties in the normalized differential cross-sections and all histograms are normalized to unity. The ratio of the particle-level distribution to the normalized differential cross-section is shown in the bottom panels, where the shaded areas represent statistical uncertainties.

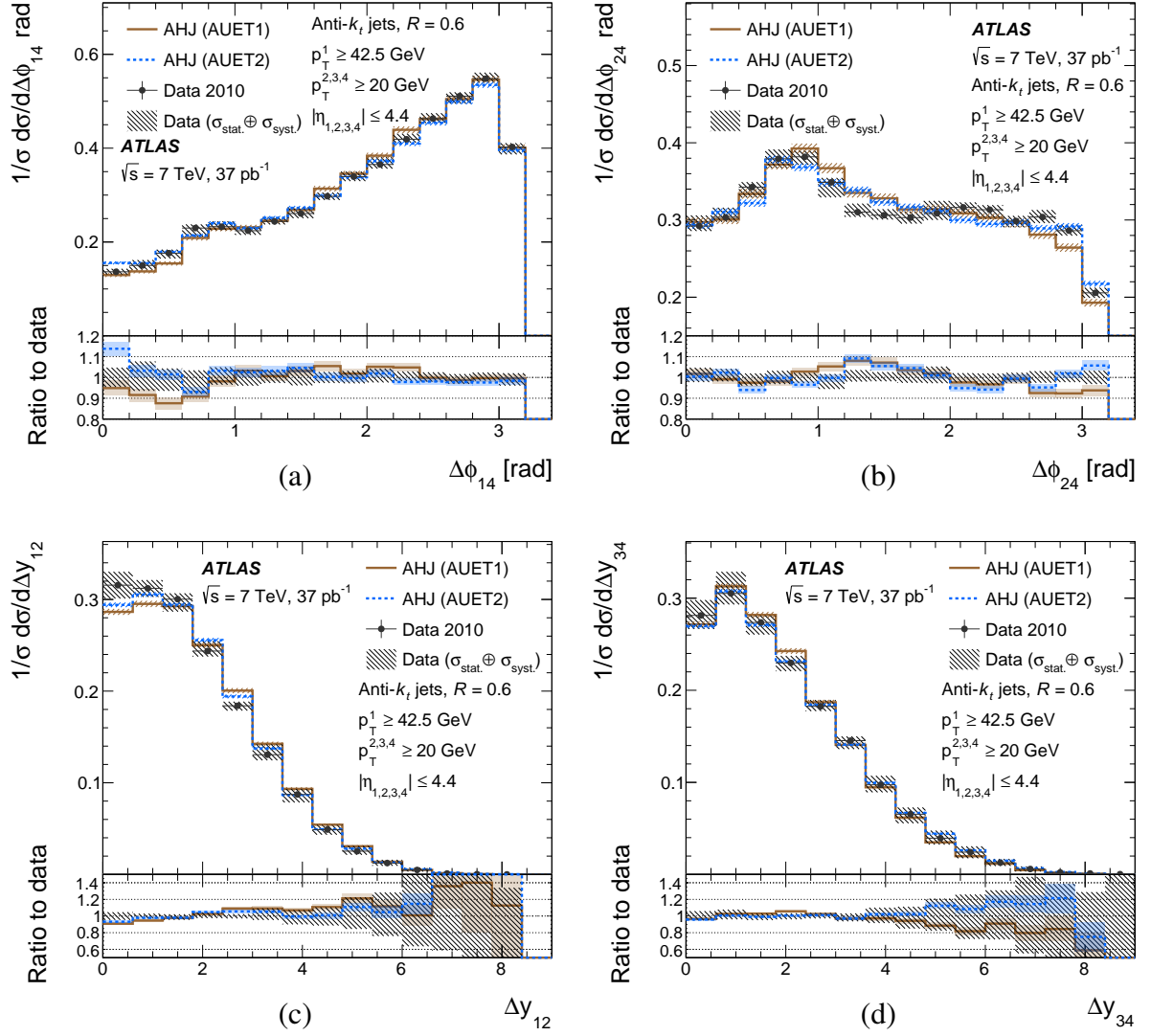


Figure 13: Distributions of the variables (a) $\Delta\phi_{14}$, (b) $\Delta\phi_{24}$, (c) Δy_{12} and (d) Δy_{34} , defined in Eq. (16), in data after unfolding to particle level, compared to the MC prediction from AHJ at the particle level, generated using the AUET1 and AUET2 tunes, as indicated in the legend. The hatched areas represent the sum in quadrature of the statistical and systematic uncertainties in the normalized differential cross-sections and all histograms are normalized to unity. The ratio of the particle-level distribution to the normalized differential cross-section is shown in the bottom panels, where the shaded areas represent statistical uncertainties.

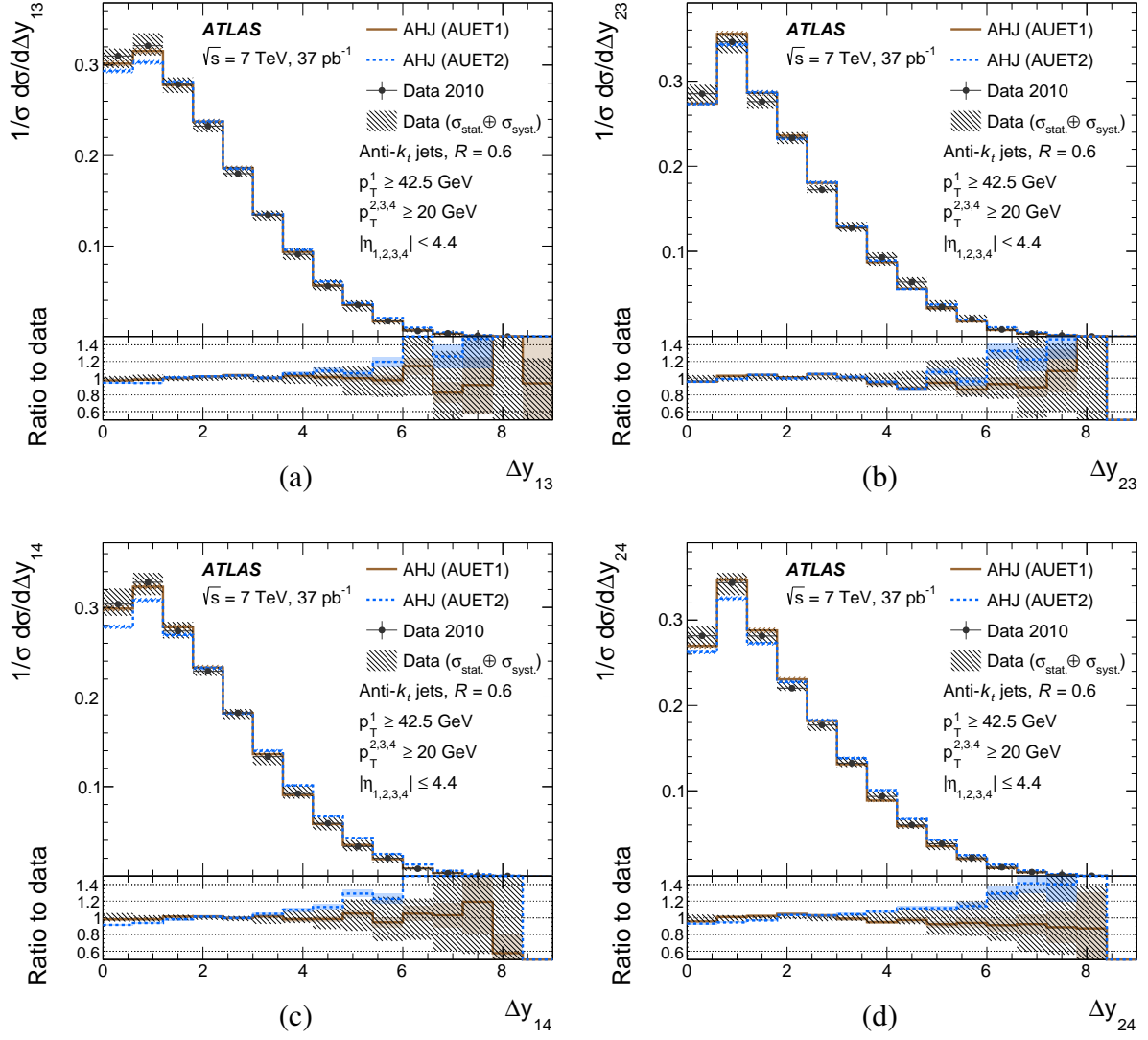


Figure 14: Distributions of the variables (a) Δy_{13} , (b) Δy_{23} , (c) Δy_{14} and (d) Δy_{24} defined in Eq. (16), in data after unfolding to particle level, compared to the MC prediction from AHJ at the particle level, generated using the AUET1 and AUET2 tunes, as indicated in the legend. The hatched areas represent the sum in quadrature of the statistical and systematic uncertainties in the normalized differential cross-sections and all histograms are normalized to unity. The ratio of the particle-level distribution to the normalized differential cross-section is shown in the bottom panels, where the shaded areas represent statistical uncertainties.

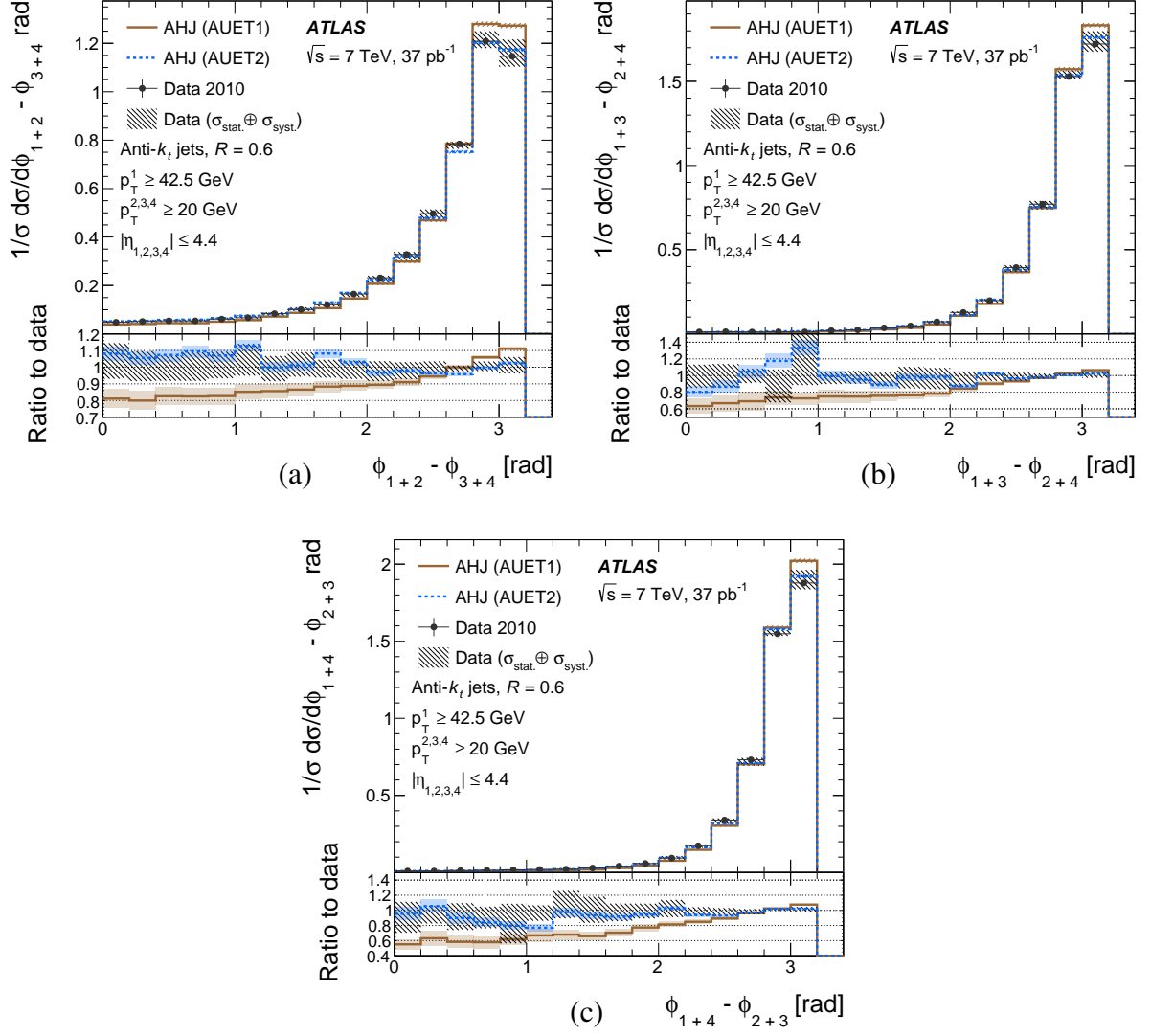


Figure 15: Distributions of the variables (a) $\phi_{1+2} - \phi_{3+4}$, (b) $\phi_{1+3} - \phi_{2+4}$ and (c) $\phi_{1+4} - \phi_{2+3}$, defined in Eq. (16), in data after unfolding to particle level, compared to the MC prediction from AHJ at the particle level, generated using the AUET1 and AUET2 tunes, as indicated in the legend. The hatched areas represent the sum in quadrature of the statistical and systematic uncertainties in the normalized differential cross-sections and all histograms are normalized to unity. The ratio of the differential distribution to the particle-level distributions is shown in the bottom panels, where the shaded areas represent statistical uncertainties.

References

- [1] P. V. Landshoff and J. C. Polkinghorne, *Calorimeter triggers for hard collisions*, [Phys. Rev. D **18** \(1978\) 3344](#).
- [2] F. Takagi, *Multiple Production of Quark Jets off Nuclei*, [Phys. Rev. Lett. **43** \(1979\) 1296](#).
- [3] C. Goebel, D. M. Scott, and F. Halzen, *Double Drell-Yan annihilations in hadron collisions: Novel tests of the constituent picture*, [Phys. Rev. D **22** \(1980\) 2789](#).
- [4] R. Kirschner, *Generalized Lipatov-Altarelli-Parisi equations and jet calculus rules*, [Phys. Lett. B **84** \(1979\) 266](#).
- [5] V. P. Shelest, A. M. Snigirev, and G. M. Zinovev, *The Multiparton Distribution Equations in QCD*, [Phys. Lett. B **113** \(1982\) 325](#).
- [6] M. Mekhfi, *Correlations in Color and Spin in Multiparton Processes*, [Phys. Rev. D **32** \(1985\) 2380](#).
- [7] N. Paver and D. Treleani, *Multi - Quark Scattering and Large p_T Jet Production in Hadronic Collisions*, [Nuovo Cim. A **70** \(1982\) 215](#).
- [8] N. Paver and D. Treleani, *Multiple Parton Interactions and Multi - Jet Events at Collider and Tevatron Energies*, [Phys. Lett. B **146** \(1984\) 252](#).
- [9] M. Mekhfi, *Multiparton Processes: An Application To Double Drell-Yan*, [Phys. Rev. D **32** \(1985\) 2371](#).
- [10] B. Humpert, *Are There Multi - Quark Interactions?*, [Phys. Lett. B **131** \(1983\) 461](#).
- [11] B. Humpert, *The production of gauge boson pairs by p anti- p colliders*, [Phys. Lett. B **135** \(1984\) 179](#).
- [12] B. Humpert and R. Odorico, *Multiparton scattering and QCD radiation as sources of four jet events*, [Phys. Lett. B **154** \(1985\) 211](#).
- [13] L. Ametller, N. Paver, and D. Treleani, *Possible signature of multiple parton interactions in collider four jet events*, [Phys. Lett. B **169** \(1986\) 289](#).
- [14] F. Halzen, P. Hoyer, and W. J. Stirling, *Evidence for Multiple Parton Interactions From the Observation of Multi - Muon Events in Drell-Yan Experiments*, [Phys. Lett. B **188** \(1987\) 375](#).
- [15] R. M. Godbole, S. Gupta, and J. Lindfors, *Double Parton Scattering Contribution To $W + \text{Jets}$* , [Z. Phys. C **47** \(1990\) 69](#).
- [16] T. Akesson et al., *Double Parton Scattering in pp Collisions at $\sqrt{s} = 63 \text{ GeV}$* , [Z. Phys. C **34** \(1987\) 163](#).
- [17] J. Alitti et al., *A study of multi-jet events at the CERN pp collider and a search for double parton scattering*, [Phys. Lett. B **268** \(1991\) 145](#).
- [18] F. Abe et al., *Study of four-jet events and evidence for double parton interactions in $p\bar{p}$ collisions at $\sqrt{s} = 1.8 \text{ TeV}$* , [Phys. Rev. D **47** \(1993\) 4857](#).
- [19] F. Abe et al., *Measurement of double parton scattering in $p\bar{p}$ collisions at $\sqrt{s} = 1.8 \text{ TeV}$* , [Phys. Rev. Lett. **79** \(1997\) 584](#).

- [20] F. Abe et al., *Double parton scattering in $\bar{p}p$ collisions at $\sqrt{s} = 1.8\text{TeV}$* , [Phys. Rev. D **56** \(1997\) 3811](#).
- [21] V. Abazov et al., *Double parton interactions in photon+3 jet events in $p\bar{p}$ collisions $\sqrt{s} = 1.96\text{TeV}$* , [Phys. Rev. D **81** \(2010\) 052012](#).
- [22] R. Aaij et al., *Observation of double charm production involving open charm in pp collisions at $\sqrt{s} = 7\text{TeV}$* , [JHEP **1206** \(2012\) 141](#), [Addendum: [JHEP **1403** \(2014\) 108](#)].
- [23] ATLAS Collaboration, *Measurement of hard double-parton interactions in $W(\rightarrow l\nu) + 2\text{ jet}$ events at $\sqrt{s}=7\text{TeV}$ with the ATLAS detector*, [New J. Phys. **15** \(2013\) 033038](#).
- [24] CMS Collaboration, *Study of double parton scattering using $W + 2\text{-jet}$ events in proton-proton collisions at $\sqrt{s} = 7\text{TeV}$* , [JHEP **1403** \(2014\) 032](#).
- [25] V. M. Abazov et al., *Double parton interactions in photon + 3 jet and photon + b/c jet + 2 jet events in $ppbar$ collisions at $\sqrt{s}=1.96\text{TeV}$* , [Phys. Rev. D **89** \(2014\) 072006](#).
- [26] V. M. Abazov et al., *Observation and studies of double J/ψ production at the Tevatron*, [Phys. Rev. D **90** \(2014\) 111101](#).
- [27] ATLAS Collaboration, *Observation and measurements of the production of prompt and non-prompt J/ψ mesons in association with a Z boson in pp collisions at $\sqrt{s} = 8\text{TeV}$ with the ATLAS detector*, [Eur. Phys. J. C **75** \(2015\) 229](#).
- [28] R. Aaij et al., *Production of associated Υ and open charm hadrons in pp collisions at $\sqrt{s} = 7$ and 8TeV via double parton scattering*, [JHEP **1607** \(2016\) 052](#).
- [29] V. M. Abazov et al., *Evidence for simultaneous production of J/ψ and Υ mesons*, [Phys. Rev. Lett. **116** \(2016\) 082002](#).
- [30] V. M. Abazov et al., *Study of double parton interactions in diphoton + dijet events in $p\bar{p}$ collisions at $\sqrt{s} = 1.96\text{TeV}$* , [Phys. Rev. D **93** \(2016\) 052008](#).
- [31] B. Blok, Y. Dokshitzer, L. Frankfurt, and M. Strikman, *The Four jet production at LHC and Tevatron in QCD*, [Phys. Rev. D **83** \(2011\) 071501](#).
- [32] J. R. Gaunt and W. J. Stirling, *Double Parton Scattering Singularity in One-Loop Integrals*, [JHEP **1106** \(2011\) 048](#).
- [33] B. Blok, Y. Dokshitzer, L. Frankfurt, and M. Strikman, *$pQCD$ physics of multiparton interactions*, [Eur. Phys. J. C **72** \(2012\) 1963](#).
- [34] M. Diehl, D. Ostermeier, and A. Schafer, *Elements of a theory for multiparton interactions in QCD*, [JHEP **1203** \(2012\) 089](#).
- [35] T. Kasemets and M. Diehl, *Angular correlations in the double Drell-Yan process*, [JHEP **1301** \(2013\) 121](#).
- [36] B. Blok, Yu. Dokshitzer, L. Frankfurt, and M. Strikman, *Perturbative QCD correlations in multi-parton collisions*, [Eur. Phys. J. C **74** \(2014\) 2926](#).
- [37] M. Diehl, T. Kasemets, and S. Keane, *Correlations in double parton distributions: effects of evolution*, [JHEP **1405** \(2014\) 118](#).
- [38] J. R. Gaunt, *Glauber Gluons and Multiple Parton Interactions*, [JHEP **1407** \(2014\) 110](#).

- [39] J. R. Gaunt, R. Maciula, and A. Szczurek, *Conventional versus single-ladder-splitting contributions to double parton scattering production of two quarkonia, two Higgs bosons and $c\bar{c}c\bar{c}$* , *Phys. Rev. D* **90** (2014) 054017.
- [40] D. Treleani, *Double parton scattering, diffraction and effective cross section*, *Phys. Rev. D* **76** (2007) 076006.
- [41] M. Bahr, M. Myska, M. H. Seymour, and A. Siodmok, *Extracting $\sigma_{\text{effective}}$ from the CDF $\gamma+3\text{jets}$ measurement*, *JHEP* **1303** (2013) 129.
- [42] D. Michie, D. J. Spiegelhalter, and C. C. Taylor, *Machine Learning, Neural and Statistical Classification*. Ellis Horwood, New York, NY, 1994.
- [43] ATLAS Collaboration, *The ATLAS Experiment at the CERN Large Hadron Collider*, *JINST* **3** (2008) S08003.
- [44] ATLAS Collaboration, *Performance of the ATLAS Trigger System in 2010*, *Eur. Phys. J. C* **72** (2012) 1849.
- [45] M. L. Mangano, M. Moretti, F. Piccinini, R. Pittau, and A. D. Polosa, *ALPGEN, a generator for hard multiparton processes in hadronic collisions*, *JHEP* **0307** (2003) 001.
- [46] J. Pumplin et al., *New generation of parton distributions with uncertainties from global QCD analysis*, *JHEP* **0207** (2002) 012.
- [47] J. Butterworth, J. R. Forshaw, and M. Seymour, *Multiparton interactions in photoproduction at HERA*, *Z. Phys. C* **72** (1996) 637.
- [48] G. Corcella et al., *HERWIG 6.5: an event generator for Hadron Emission Reactions With Interfering Gluons (including supersymmetric processes)*, *JHEP* **0101** (2001) 010.
- [49] ATLAS Collaboration, *New ATLAS event generator tunes to 2010 data*, *ATL-PHYS-PUB-2011-008*, CERN, 2011. <http://cds.cern.ch/record/1345343>.
- [50] M. L. Mangano, M. Moretti, and R. Pittau, *Multijet matrix elements and shower evolution in hadronic collisions: $Wb\bar{b} + n\text{ jets}$ as a case study*, *Nucl. Phys. B* **632** (2002) 343.
- [51] ATLAS Collaboration, *First tuning of HERWIG/JIMMY to ATLAS data*, *ATL-PHYS-PUB-2010-014*, CERN, 2010. <http://cds.cern.ch/record/1303025>.
- [52] F. Krauss, R. Kuhn, and G. Soff, *AMEGIC++ 1.0: A Matrix element generator in C++*, *JHEP* **0202** (2002) 044.
- [53] T. Gleisberg, S. Hoeche, F. Krauss, M. Schonherr, S. Schumann, F. Siegert, and J. Winter, *Event generation with SHERPA 1.1*, *JHEP* **0902** (2009) 007.
- [54] H.-L. Lai et al., *New parton distributions for collider physics*, *Phys. Rev. D* **82** (2010) 074024.
- [55] S. Catani, F. Krauss, R. Kuhn, and B. Webber, *QCD matrix elements + parton showers*, *JHEP* **0111** (2001) 063.
- [56] F. Krauss, *Matrix elements and parton showers in hadronic interactions*, *JHEP* **0208** (2002) 015.
- [57] T. Sjöstrand, S. Mrenna, and P. Z. Skands, *PYTHIA 6.4 Physics and Manual*, *JHEP* **0605** (2006) 026.

- [58] A. Sherstnev and R. Thorne, *Parton Distributions for LO Generators*, *Eur. Phys. J. C* **55** (2008) 553.
- [59] ATLAS Collaboration, *Charged-particle multiplicities in pp interactions measured with the ATLAS detector at the LHC*, *New J. Phys.* **13** (2011) 053033.
- [60] ATLAS Collaboration, *The ATLAS Simulation Infrastructure*, *Eur. Phys. J. C* **70** (2010) 823.
- [61] S. Agostinelli et al., *GEANT4: A Simulation toolkit*, *Nucl. Instrum. Meth. A* **506** (2003) 250.
- [62] ATLAS Collaboration, *Measurement of inclusive jet and dijet production in pp collisions at $\sqrt{s} = 7$ TeV using the ATLAS detector*, *Phys. Rev. D* **86** (2012) 014022.
- [63] ATLAS Collaboration, *Improved luminosity determination in pp collisions at $\sqrt{s} = 7$ TeV using the ATLAS detector at the LHC*, *Eur. Phys. J. C* **73** (2013) 2518.
- [64] ATLAS Collaboration, *Jet energy measurement with the ATLAS detector in proton-proton collisions at $\sqrt{s} = 7$ TeV*, *Eur. Phys. J. C* **73** (2013) 2304.
- [65] M. Cacciari, G. P. Salam, and G. Soyez, *The anti- k_t jet clustering algorithm*, *JHEP* **0804** (2008) 063.
- [66] M. Cacciari and G. P. Salam, *Dispelling the N^3 myth for the k_t jet-finder*, *Phys. Lett. B* **641** (2006) 57.
- [67] C. Cojocaru et al., *Hadronic calibration of the ATLAS liquid argon end-cap calorimeter in the pseudorapidity region $1.6 < |\eta| < 1.8$ in beam tests*, *Nucl. Instrum. Meth. A* **531** (2004) 481.
- [68] W. Lampl et al., *Calorimeter clustering algorithms: description and performance*, ATL-LARG-PUB-2008-002, CERN, April, 2008. <http://cds.cern.ch/record/1099735>.
- [69] I. T. Jolliffe, *Principal Component Analysis*. Springer Series in Statistics. Springer-Verlag, 2 ed., 2002.
- [70] R. Brun and F. Rademakers, *ROOT: An object oriented data analysis framework*, *Nucl. Instrum. Meth. A* **389** (1997) 81.
- [71] F. James and M. Roos, *Minuit: A System for Function Minimization and Analysis of the Parameter Errors and Correlations*, *Comput. Phys. Commun.* **10** (1975) 343.
- [72] ATLAS Collaboration, *Jet energy resolution in proton-proton collisions at $\sqrt{s} = 7$ TeV recorded in 2010 with the ATLAS detector*, *Eur. Phys. J. C* **73** (2013) 2306.
- [73] ATLAS Collaboration, *Measurement of the total cross section from elastic scattering in pp collisions at $\sqrt{s} = 7$ TeV with the ATLAS detector*, *Nucl. Phys. B* **889** (2014) 486.
- [74] T. Adye, *Unfolding algorithms and tests using RooUnfold*, in *Proceedings of the PHYSTAT 2011 Workshop*, CERN. 2011.
- [75] ATLAS Collaboration, *ATLAS Computing Acknowledgements 2016-2017*, ATL-GEN-PUB-2016-002, 2016, <http://cds.cern.ch/record/2202407>.

The ATLAS Collaboration

M. Aaboud^{136d}, G. Aad⁸⁷, B. Abbott¹¹⁴, J. Abdallah⁸, O. Abdinov¹², B. Abeloos¹¹⁸, R. Aben¹⁰⁸, O.S. AbouZeid¹³⁸, N.L. Abraham¹⁵², H. Abramowicz¹⁵⁶, H. Abreu¹⁵⁵, R. Abreu¹¹⁷, Y. Abulaiti^{149a,149b}, B.S. Acharya^{168a,168b,a}, S. Adachi¹⁵⁸, L. Adamczyk^{40a}, D.L. Adams²⁷, J. Adelman¹⁰⁹, S. Adomeit¹⁰¹, T. Adye¹³², A.A. Affolder⁷⁶, T. Agatonovic-Jovin¹⁴, J.A. Aguilar-Saavedra^{127a,127f}, S.P. Ahlen²⁴, F. Ahmadov^{67,b}, G. Aielli^{134a,134b}, H. Akerstedt^{149a,149b}, T.P.A. Åkesson⁸³, A.V. Akimov⁹⁷, G.L. Alberghi^{22a,22b}, J. Albert¹⁷³, S. Albrand⁵⁷, M.J. Alconada Verzini⁷³, M. Aleksa³², I.N. Aleksandrov⁶⁷, C. Alexa^{28b}, G. Alexander¹⁵⁶, T. Alexopoulos¹⁰, M. Alhroob¹¹⁴, B. Ali¹²⁹, M. Aliev^{75a,75b}, G. Alimonti^{93a}, J. Alison³³, S.P. Alkire³⁷, B.M.M. Allbrooke¹⁵², B.W. Allen¹¹⁷, P.P. Allport¹⁹, A. Aloisio^{105a,105b}, A. Alonso³⁸, F. Alonso⁷³, C. Alpigiani¹³⁹, A.A. Alshehri⁵⁵, M. Alstady⁸⁷, B. Alvarez Gonzalez³², D. Álvarez Piqueras¹⁷¹, M.G. Alvigi^{105a,105b}, B.T. Amadio¹⁶, K. Amako⁶⁸, Y. Amaral Coutinho^{26a}, C. Amelung²⁵, D. Amidei⁹¹, S.P. Amor Dos Santos^{127a,127c}, A. Amorim^{127a,127b}, S. Amoroso³², G. Amundsen²⁵, C. Anastopoulos¹⁴², L.S. Ancu⁵¹, N. Andari¹⁹, T. Andeen¹¹, C.F. Anders^{60b}, G. Anders³², J.K. Anders⁷⁶, K.J. Anderson³³, A. Andreazza^{93a,93b}, V. Andrei^{60a}, S. Angelidakis⁹, I. Angelozzi¹⁰⁸, A. Angerami³⁷, F. Anghinolfi³², A.V. Anisenkov^{110,c}, N. Anjos¹³, A. Annovi^{125a,125b}, C. Antel^{60a}, M. Antonelli⁴⁹, A. Antonov^{99,*}, F. Anulli^{133a}, M. Aoki⁶⁸, L. Aperio Bella¹⁹, G. Arabidze⁹², Y. Arai⁶⁸, J.P. Araque^{127a}, A.T.H. Arce⁴⁷, F.A. Arduh⁷³, J-F. Arguin⁹⁶, S. Argyropoulos⁶⁵, M. Arik^{20a}, A.J. Armbruster¹⁴⁶, L.J. Armitage⁷⁸, O. Arnaez³², H. Arnold⁵⁰, M. Arratia³⁰, O. Arslan²³, A. Artamonov⁹⁸, G. Artoni¹²¹, S. Artz⁸⁵, S. Asai¹⁵⁸, N. Asbah⁴⁴, A. Ashkenazi¹⁵⁶, B. Åsman^{149a,149b}, L. Asquith¹⁵², K. Assamagan²⁷, R. Astalos^{147a}, M. Atkinson¹⁷⁰, N.B. Atlay¹⁴⁴, K. Augsten¹²⁹, G. Avolio³², B. Axen¹⁶, M.K. Ayoub¹¹⁸, G. Azuelos^{96,d}, M.A. Baak³², A.E. Baas^{60a}, M.J. Baca¹⁹, H. Bachacou¹³⁷, K. Bachas^{75a,75b}, M. Backes¹²¹, M. Backhaus³², P. Bagiacchi^{133a,133b}, P. Bagnaia^{133a,133b}, Y. Bai^{35a}, J.T. Baines¹³², O.K. Baker¹⁸⁰, E.M. Baldin^{110,c}, P. Balek¹⁷⁶, T. Balestri¹⁵¹, F. Balli¹³⁷, W.K. Balunas¹²³, E. Banas⁴¹, Sw. Banerjee^{177,e}, A.A.E. Bannoura¹⁷⁹, L. Barak³², E.L. Barberio⁹⁰, D. Barberis^{52a,52b}, M. Barbero⁸⁷, T. Barillari¹⁰², M-S Barisits³², T. Barklow¹⁴⁶, N. Barlow³⁰, S.L. Barnes⁸⁶, B.M. Barnett¹³², R.M. Barnett¹⁶, Z. Barnovska-Blenessy⁵⁹, A. Baroncelli^{135a}, G. Barone²⁵, A.J. Barr¹²¹, L. Barranco Navarro¹⁷¹, F. Barreiro⁸⁴, J. Barreiro Guimarães da Costa^{35a}, R. Bartoldus¹⁴⁶, A.E. Barton⁷⁴, P. Bartos^{147a}, A. Basalaev¹²⁴, A. Bassalat^{118,f}, R.L. Bates⁵⁵, S.J. Batista¹⁶², J.R. Batley³⁰, M. Battaglia¹³⁸, M. Bause^{133a,133b}, F. Bauer¹³⁷, H.S. Bawa^{146,g}, J.B. Beacham¹¹², M.D. Beattie⁷⁴, T. Beau⁸², P.H. Beauchemin¹⁶⁶, P. Bechtel²³, H.P. Beck^{18,h}, K. Becker¹²¹, M. Becker⁸⁵, M. Beckingham¹⁷⁴, C. Becot¹¹¹, A.J. Beddall^{20e}, A. Beddall^{20b}, V.A. Bednyakov⁶⁷, M. Bedognetti¹⁰⁸, C.P. Bee¹⁵¹, L.J. Beemster¹⁰⁸, T.A. Beermann³², M. Begel²⁷, J.K. Behr⁴⁴, C. Belanger-Champagne⁸⁹, A.S. Bell⁸⁰, G. Bella¹⁵⁶, L. Bellagamba^{22a}, A. Bellerive³¹, M. Bellomo⁸⁸, K. Belotskiy⁹⁹, O. Beltramello³², N.L. Belyaev⁹⁹, O. Benary^{156,*}, D. Bencheikroun^{136a}, M. Bender¹⁰¹, K. Bendtz^{149a,149b}, N. Benekos¹⁰, Y. Benhammou¹⁵⁶, E. Benhar Noccioli¹⁸⁰, J. Benitez⁶⁵, D.P. Benjamin⁴⁷, J.R. Bensinger²⁵, S. Bentvelsen¹⁰⁸, L. Beresford¹²¹, M. Beretta⁴⁹, D. Berge¹⁰⁸, E. Bergeas Kuutmann¹⁶⁹, N. Berger⁵, J. Beringer¹⁶, S. Berlendis⁵⁷, N.R. Bernard⁸⁸, C. Bernius¹¹¹, F.U. Bernlochner²³, T. Berry⁷⁹, P. Berta¹³⁰, C. Bertella⁸⁵, G. Bertoli^{149a,149b}, F. Bertolucci^{125a,125b}, I.A. Bertram⁷⁴, C. Bertsche⁴⁴, D. Bertsche¹¹⁴, G.J. Besjes³⁸, O. Bessidskaia Bylund^{149a,149b}, M. Bessner⁴⁴, N. Besson¹³⁷, C. Betancourt⁵⁰, A. Bethani⁵⁷, S. Bethke¹⁰², A.J. Bevan⁷⁸, R.M. Bianchi¹²⁶, L. Bianchini²⁵, M. Bianco³², O. Biebel¹⁰¹, D. Biedermann¹⁷, R. Bielski⁸⁶, N.V. Biesuz^{125a,125b}, M. Biglietti^{135a}, J. Bilbao De Mendizabal⁵¹, T.R.V. Billoud⁹⁶, H. Bilokon⁴⁹, M. Bindi⁵⁶, S. Binet¹¹⁸, A. Bingul^{20b}, C. Bini^{133a,133b}, S. Biondi^{22a,22b}, T. Bisanz⁵⁶, D.M. Bjergaard⁴⁷, C.W. Black¹⁵³, J.E. Black¹⁴⁶, K.M. Black²⁴, D. Blackburn¹³⁹, R.E. Blair⁶, J.-B. Blanchard¹³⁷, T. Blazek^{147a}, I. Bloch⁴⁴, C. Blocker²⁵, A. Blue⁵⁵, W. Blum^{85,*},

U. Blumenschein⁵⁶, S. Blunier^{34a}, G.J. Bobbink¹⁰⁸, V.S. Bobrovnikov^{110,c}, S.S. Bocchetta⁸³, A. Bocci⁴⁷, C. Bock¹⁰¹, M. Boehler⁵⁰, D. Boerner¹⁷⁹, J.A. Bogaerts³², D. Bogavac¹⁴, A.G. Bogdanchikov¹¹⁰, C. Bohm^{149a}, V. Boisvert⁷⁹, P. Bokan¹⁴, T. Bold^{40a}, A.S. Boldyrev^{168a,168c}, M. Bomben⁸², M. Bona⁷⁸, M. Boonekamp¹³⁷, A. Borisov¹³¹, G. Borissov⁷⁴, J. Bortfeldt³², D. Bortoletto¹²¹, V. Bortolotto^{62a,62b,62c}, K. Bos¹⁰⁸, D. Boscherini^{22a}, M. Bosman¹³, J.D. Bossio Sola²⁹, J. Boudreau¹²⁶, J. Bouffard², E.V. Bouhova-Thacker⁷⁴, D. Boumediene³⁶, C. Bourdarios¹¹⁸, S.K. Boutle⁵⁵, A. Boveia³², J. Boyd³², I.R. Boyko⁶⁷, J. Bracinik¹⁹, A. Brandt⁸, G. Brandt⁵⁶, O. Brandt^{60a}, U. Bratzler¹⁵⁹, B. Brau⁸⁸, J.E. Brau¹¹⁷, W.D. Breaden Madden⁵⁵, K. Brendlinger¹²³, A.J. Brennan⁹⁰, L. Brenner¹⁰⁸, R. Brenner¹⁶⁹, S. Bressler¹⁷⁶, T.M. Bristow⁴⁸, D. Britton⁵⁵, D. Britzger⁴⁴, F.M. Brochu³⁰, I. Brock²³, R. Brock⁹², G. Brooijmans³⁷, T. Brooks⁷⁹, W.K. Brooks^{34b}, J. Brosamer¹⁶, E. Brost¹⁰⁹, J.H. Broughton¹⁹, P.A. Bruckman de Renstrom⁴¹, D. Bruncko^{147b}, R. Bruneliere⁵⁰, A. Bruni^{22a}, G. Bruni^{22a}, L.S. Bruni¹⁰⁸, B.H. Brunt³⁰, M. Bruschi^{22a}, N. Bruscino²³, P. Bryant³³, L. Bryngemark⁸³, T. Buanes¹⁵, Q. Buat¹⁴⁵, P. Buchholz¹⁴⁴, A.G. Buckley⁵⁵, I.A. Budagov⁶⁷, F. Buehrer⁵⁰, M.K. Bugge¹²⁰, O. Bulekov⁹⁹, D. Bullock⁸, H. Burckhart³², S. Burdin⁷⁶, C.D. Burgard⁵⁰, B. Burghgrave¹⁰⁹, K. Burka⁴¹, S. Burke¹³², I. Burmeister⁴⁵, J.T.P. Burr¹²¹, E. Busato³⁶, D. Büscher⁵⁰, V. Büscher⁸⁵, P. Bussey⁵⁵, J.M. Butler²⁴, C.M. Buttar⁵⁵, J.M. Butterworth⁸⁰, P. Butti¹⁰⁸, W. Buttinger²⁷, A. Buzatu⁵⁵, A.R. Buzykaev^{110,c}, S. Cabrera Urbán¹⁷¹, D. Caforio¹²⁹, V.M. Cairo^{39a,39b}, O. Cakir^{4a}, N. Calace⁵¹, P. Calafiura¹⁶, A. Calandri⁸⁷, G. Calderini⁸², P. Calfayan⁶³, G. Callea^{39a,39b}, L.P. Caloba^{26a}, S. Calvente Lopez⁸⁴, D. Calvet³⁶, S. Calvet³⁶, T.P. Calvet⁸⁷, R. Camacho Toro³³, S. Camarda³², P. Camarri^{134a,134b}, D. Cameron¹²⁰, R. Caminal Armadans¹⁷⁰, C. Camincher⁵⁷, S. Campana³², M. Campanelli⁸⁰, A. Camplani^{93a,93b}, A. Campoverde¹⁴⁴, V. Canale^{105a,105b}, A. Canepa^{164a}, M. Cano Bret¹⁴¹, J. Cantero¹¹⁵, T. Cao⁴², M.D.M. Capeans Garrido³², I. Caprini^{28b}, M. Caprini^{28b}, M. Capua^{39a,39b}, R.M. Carbone³⁷, R. Cardarelli^{134a}, F. Cardillo⁵⁰, I. Carli¹³⁰, T. Carli³², G. Carlino^{105a}, L. Carminati^{93a,93b}, R.M.D. Carney^{149a,149b}, S. Caron¹⁰⁷, E. Carquin^{34b}, G.D. Carrillo-Montoya³², J.R. Carter³⁰, J. Carvalho^{127a,127c}, D. Casadei¹⁹, M.P. Casado^{13,i}, M. Casolino¹³, D.W. Casper¹⁶⁷, E. Castaneda-Miranda^{148a}, R. Castelijns¹⁰⁸, A. Castelli¹⁰⁸, V. Castillo Gimenez¹⁷¹, N.F. Castro^{127a,j}, A. Catinaccio³², J.R. Catmore¹²⁰, A. Cattai³², J. Caudron²³, V. Cavaliere¹⁷⁰, E. Cavallaro¹³, D. Cavalli^{93a}, M. Cavalli-Sforza¹³, V. Cavasinni^{125a,125b}, F. Ceradini^{135a,135b}, L. Cerda Alberich¹⁷¹, A.S. Cerqueira^{26b}, A. Cerri¹⁵², L. Cerrito^{134a,134b}, F. Cerutti¹⁶, M. Cerv³², A. Cervelli¹⁸, S.A. Cetin^{20d}, A. Chafaq^{136a}, D. Chakraborty¹⁰⁹, S.K. Chan⁵⁸, Y.L. Chan^{62a}, P. Chang¹⁷⁰, J.D. Chapman³⁰, D.G. Charlton¹⁹, A. Chatterjee⁵¹, C.C. Chau¹⁶², C.A. Chavez Barajas¹⁵², S. Che¹¹², S. Cheatham^{168a,168c}, A. Chegwidan⁹², S. Chekanov⁶, S.V. Chekulaev^{164a}, G.A. Chelkov^{67,k}, M.A. Chelstowska⁹¹, C. Chen⁶⁶, H. Chen²⁷, K. Chen¹⁵¹, S. Chen^{35b}, S. Chen¹⁵⁸, X. Chen^{35c}, Y. Chen⁶⁹, H.C. Cheng⁹¹, H.J. Cheng^{35a}, Y. Cheng³³, A. Cheplakov⁶⁷, E. Cheremushkina¹³¹, R. Cherkaoui El Moursli^{136e}, V. Chernyatin^{27,*}, E. Cheu⁷, L. Chevalier¹³⁷, V. Chiarella⁴⁹, G. Chiarelli^{125a,125b}, G. Chiodini^{75a}, A.S. Chisholm³², A. Chitan^{28b}, M.V. Chizhov⁶⁷, K. Choi⁶³, A.R. Chomont³⁶, S. Chouridou⁹, B.K.B. Chow¹⁰¹, V. Christodoulou⁸⁰, D. Chromek-Burckhart³², J. Chudoba¹²⁸, A.J. Chuinard⁸⁹, J.J. Chwastowski⁴¹, L. Chytka¹¹⁶, G. Ciapetti^{133a,133b}, A.K. Ciftci^{4a}, D. Cinca⁴⁵, V. Cindro⁷⁷, I.A. Cioara²³, C. Ciocca^{22a,22b}, A. Ciochio¹⁶, F. Ciotto^{105a,105b}, Z.H. Citron¹⁷⁶, M. Citterio^{93a}, M. Ciubancan^{28b}, A. Clark⁵¹, B.L. Clark⁵⁸, M.R. Clark³⁷, P.J. Clark⁴⁸, R.N. Clarke¹⁶, C. Clement^{149a,149b}, Y. Coadou⁸⁷, M. Cobal^{168a,168c}, A. Coccaro⁵¹, J. Cochran⁶⁶, L. Colasurdo¹⁰⁷, B. Cole³⁷, A.P. Colijn¹⁰⁸, J. Collot⁵⁷, T. Colombo¹⁶⁷, G. Compostella¹⁰², P. Conde Muiño^{127a,127b}, E. Coniavitis⁵⁰, S.H. Connell^{148b}, I.A. Connelly⁷⁹, V. Consorti⁵⁰, S. Constantinescu^{28b}, G. Conti³², F. Conventi^{105a,l}, M. Cooke¹⁶, B.D. Cooper⁸⁰, A.M. Cooper-Sarkar¹²¹, K.J.R. Cormier¹⁶², T. Cornelissen¹⁷⁹, M. Corradi^{133a,133b}, F. Corriveau^{89,m}, A. Cortes-Gonzalez³², G. Cortiana¹⁰², G. Costa^{93a}, M.J. Costa¹⁷¹, D. Costanzo¹⁴², G. Cottin³⁰, G. Cowan⁷⁹, B.E. Cox⁸⁶, K. Cranmer¹¹¹, S.J. Crawley⁵⁵, G. Cree³¹, S. Crépe-Renaudin⁵⁷, F. Crescioli⁸², W.A. Cribbs^{149a,149b},

M. Crispin Ortuzar¹²¹, M. Cristinziani²³, V. Croft¹⁰⁷, G. Crosetti^{39a,39b}, A. Cueto⁸⁴,
T. Cuhadar Donszelmann¹⁴², J. Cummings¹⁸⁰, M. Curatolo⁴⁹, J. Cúth⁸⁵, H. Czirr¹⁴⁴, P. Czodrowski³,
G. D'amen^{22a,22b}, S. D'Auria⁵⁵, M. D'Onofrio⁷⁶, M.J. Da Cunha Sargedas De Sousa^{127a,127b},
C. Da Via⁸⁶, W. Dabrowski^{40a}, T. Dado^{147a}, T. Dai⁹¹, O. Dale¹⁵, F. Dallaire⁹⁶, C. Dallapiccola⁸⁸,
M. Dam³⁸, J.R. Dandoy³³, N.P. Dang⁵⁰, A.C. Daniels¹⁹, N.S. Dann⁸⁶, M. Danninger¹⁷²,
M. Dano Hoffmann¹³⁷, V. Dao⁵⁰, G. Darbo^{52a}, S. Darmora⁸, J. Dassoulas³, A. Dattagupta¹¹⁷,
W. Davey²³, C. David¹⁷³, T. Davidek¹³⁰, M. Davies¹⁵⁶, P. Davison⁸⁰, E. Dawe⁹⁰, I. Dawson¹⁴², K. De⁸,
R. de Asmundis^{105a}, A. De Benedetti¹¹⁴, S. De Castro^{22a,22b}, S. De Cecco⁸², N. De Groot¹⁰⁷,
P. de Jong¹⁰⁸, H. De la Torre⁹², F. De Lorenzi⁶⁶, A. De Maria⁵⁶, D. De Pedis^{133a}, A. De Salvo^{133a},
U. De Sanctis¹⁵², A. De Santo¹⁵², J.B. De Vivie De Regie¹¹⁸, W.J. Dearnaley⁷⁴, R. Debbé²⁷,
C. Debenedetti¹³⁸, D.V. Dedovich⁶⁷, N. Dehghanian³, I. Deigaard¹⁰⁸, M. Del Gaudio^{39a,39b},
J. Del Peso⁸⁴, T. Del Prete^{125a,125b}, D. Delgove¹¹⁸, F. Deliot¹³⁷, C.M. Delitzsch⁵¹, A. Dell'Acqua³²,
L. Dell'Asta²⁴, M. Dell'Orso^{125a,125b}, M. Della Pietra^{105a,l}, D. della Volpe⁵¹, M. Delmastro⁵,
P.A. Delsart⁵⁷, D.A. DeMarco¹⁶², S. Demers¹⁸⁰, M. Demichev⁶⁷, A. Demilly⁸², S.P. Denisov¹³¹,
D. Denysiuk¹³⁷, D. Derendarz⁴¹, J.E. Derkaoui^{136d}, F. Derue⁸², P. Dervan⁷⁶, K. Desch²³, C. Deterre⁴⁴,
K. Dette⁴⁵, P.O. Deviveiros³², A. Dewhurst¹³², S. Dhaliwal²⁵, A. Di Ciaccio^{134a,134b}, L. Di Ciaccio⁵,
W.K. Di Clemente¹²³, C. Di Donato^{105a,105b}, A. Di Girolamo³², B. Di Girolamo³², B. Di Micco^{135a,135b},
R. Di Nardo³², A. Di Simone⁵⁰, R. Di Sipio¹⁶², D. Di Valentino³¹, C. Diaconu⁸⁷, M. Diamond¹⁶²,
F.A. Dias⁴⁸, M.A. Diaz^{34a}, E.B. Diehl⁹¹, J. Dietrich¹⁷, S. Díez Cornell⁴⁴, A. Dimitrievska¹⁴,
J. Dingfelder²³, P. Dita^{28b}, S. Dita^{28b}, F. Dittus³², F. Djama⁸⁷, T. Djobava^{53b}, J.I. Djuvsland^{60a},
M.A.B. do Vale^{26c}, D. Dobos³², M. Dobre^{28b}, C. Doglioni⁸³, J. Dolejsi¹³⁰, Z. Dolezal¹³⁰,
M. Donadelli^{26d}, S. Donati^{125a,125b}, P. Dondero^{122a,122b}, J. Donini³⁶, J. Dopke¹³², A. Doria^{105a},
M.T. Dova⁷³, A.T. Doyle⁵⁵, E. Drechsler⁵⁶, M. Dris¹⁰, Y. Du¹⁴⁰, J. Duarte-Campderros¹⁵⁶,
E. Duchovni¹⁷⁶, G. Duckeck¹⁰¹, O.A. Ducu^{96,n}, D. Duda¹⁰⁸, A. Dudarev³², A.Ch. Dudder⁸⁵,
E.M. Duffield¹⁶, L. Duflo¹¹⁸, M. Dührssen³², M. Dumancic¹⁷⁶, M. Dunford^{60a}, H. Duran Yildiz^{4a},
M. Düren⁵⁴, A. Durglishvili^{53b}, D. Duschinger⁴⁶, B. Dutta⁴⁴, M. Dyndal⁴⁴, C. Eckardt⁴⁴, K.M. Ecker¹⁰²,
R.C. Edgar⁹¹, N.C. Edwards⁴⁸, T. Eifert³², G. Eigen¹⁵, K. Einsweiler¹⁶, T. Ekelof¹⁶⁹, M. El Kacimi^{136c},
V. Ellajosyula⁸⁷, M. Ellert¹⁶⁹, S. Elles⁵, F. Ellinghaus¹⁷⁹, A.A. Elliot¹⁷³, N. Ellis³², J. Elmsheuser²⁷,
M. Elsing³², D. Emelianov¹³², Y. Enari¹⁵⁸, O.C. Endner⁸⁵, J.S. Ennis¹⁷⁴, J. Erdmann⁴⁵, A. Ereditato¹⁸,
G. Ernis¹⁷⁹, J. Ernst², M. Ernst²⁷, S. Errede¹⁷⁰, E. Ertel⁸⁵, M. Escalier¹¹⁸, H. Esch⁴⁵, C. Escobar¹²⁶,
B. Esposito⁴⁹, A.I. Etienne¹³⁷, E. Etzion¹⁵⁶, H. Evans⁶³, A. Ezhilov¹²⁴, M. Ezzi^{136e}, F. Fabbri^{22a,22b},
L. Fabbri^{22a,22b}, G. Facini³³, R.M. Fakhruddinov¹³¹, S. Falciano^{133a}, R.J. Falla⁸⁰, J. Faltova³², Y. Fang^{35a},
M. Fanti^{93a,93b}, A. Farbin⁸, A. Farilla^{135a}, C. Farina¹²⁶, E.M. Farina^{122a,122b}, T. Farooque¹³, S. Farrell¹⁶,
S.M. Farrington¹⁷⁴, P. Farthouat³², F. Fassi^{136e}, P. Fassnacht³², D. Fassouliotis⁹, M. Fauci Giannelli⁷⁹,
A. Favareto^{52a,52b}, W.J. Fawcett¹²¹, L. Fayard¹¹⁸, O.L. Fedin^{124,o}, W. Fedorko¹⁷², S. Feigl¹²⁰,
L. Feligioni⁸⁷, C. Feng¹⁴⁰, E.J. Feng³², H. Feng⁹¹, A.B. Fenyuk¹³¹, L. Feremenga⁸,
P. Fernandez Martinez¹⁷¹, S. Fernandez Perez¹³, J. Ferrando⁴⁴, A. Ferrari¹⁶⁹, P. Ferrari¹⁰⁸, R. Ferrari^{122a},
D.E. Ferreira de Lima^{60b}, A. Ferrer¹⁷¹, D. Ferrere⁵¹, C. Ferretti⁹¹, A. Ferretto Parodi^{52a,52b}, F. Fiedler⁸⁵,
A. Filipčič⁷⁷, M. Filipuzzi⁴⁴, F. Filthaut¹⁰⁷, M. Fincke-Keeler¹⁷³, K.D. Finelli¹⁵³,
M.C.N. Fiolhais^{127a,127c}, L. Fiorini¹⁷¹, A. Firan⁴², A. Fischer², C. Fischer¹³, J. Fischer¹⁷⁹, W.C. Fisher⁹²,
N. Flaschel⁴⁴, I. Fleck¹⁴⁴, P. Fleischmann⁹¹, G.T. Fletcher¹⁴², R.R.M. Fletcher¹²³, T. Flick¹⁷⁹,
L.R. Flores Castillo^{62a}, M.J. Flowerdew¹⁰², G.T. Forcolin⁸⁶, A. Formica¹³⁷, A. Forti⁸⁶, A.G. Foster¹⁹,
D. Fournier¹¹⁸, H. Fox⁷⁴, S. Fracchia¹³, P. Francavilla⁸², M. Franchini^{22a,22b}, D. Francis³²,
L. Franconi¹²⁰, M. Franklin⁵⁸, M. Frate¹⁶⁷, M. Fraternali^{122a,122b}, D. Freeborn⁸⁰,
S.M. Fressard-Batraneanu³², F. Friedrich⁴⁶, D. Froidevaux³², J.A. Frost¹²¹, C. Fukunaga¹⁵⁹,
E. Fullana Torregrosa⁸⁵, T. Fusayasu¹⁰³, J. Fuster¹⁷¹, C. Gabaldon⁵⁷, O. Gabizon¹⁵⁵, A. Gabrielli^{22a,22b},
A. Gabrielli¹⁶, G.P. Gach^{40a}, S. Gadatsch³², S. Gadowski⁷⁹, G. Gagliardi^{52a,52b}, L.G. Gagnon⁹⁶,

P. Gagnon⁶³, C. Galea¹⁰⁷, B. Galhardo^{127a,127c}, E.J. Gallas¹²¹, B.J. Gallop¹³², P. Gallus¹²⁹, G. Galster³⁸, K.K. Gan¹¹², S. Ganguly³⁶, J. Gao⁵⁹, Y. Gao⁴⁸, Y.S. Gao^{146,g}, F.M. Garay Walls⁴⁸, C. García¹⁷¹, J.E. García Navarro¹⁷¹, M. Garcia-Sciveres¹⁶, R.W. Gardner³³, N. Garelli¹⁴⁶, V. Garonne¹²⁰, A. Gascon Bravo⁴⁴, K. Gasnikova⁴⁴, C. Gatti⁴⁹, A. Gaudiello^{52a,52b}, G. Gaudio^{122a}, L. Gauthier⁹⁶, I.L. Gavrilenko⁹⁷, C. Gay¹⁷², G. Gaycken²³, E.N. Gazis¹⁰, Z. Gecse¹⁷², C.N.P. Gee¹³², Ch. Geich-Gimbel²³, M. Geisen⁸⁵, M.P. Geisler^{60a}, K. Gellerstedt^{149a,149b}, C. Gemme^{52a}, M.H. Genest⁵⁷, C. Geng^{59,p}, S. Gentile^{133a,133b}, C. Gentsos¹⁵⁷, S. George⁷⁹, D. Gerbaudo¹³, A. Gershon¹⁵⁶, S. Ghasemi¹⁴⁴, M. Ghneimat²³, B. Giacobbe^{22a}, S. Giagu^{133a,133b}, P. Giannetti^{125a,125b}, B. Gibbard²⁷, S.M. Gibson⁷⁹, M. Gignac¹⁷², M. Gilchriese¹⁶, T.P.S. Gillam³⁰, D. Gillberg³¹, G. Gilles¹⁷⁹, D.M. Gingrich^{3,d}, N. Giokaris⁹, M.P. Giordani^{168a,168c}, F.M. Giorgi^{22a}, F.M. Giorgi¹⁷, P.F. Giraud¹³⁷, P. Giromini⁵⁸, D. Giugni^{93a}, F. Giuli¹²¹, C. Giuliani¹⁰², M. Giulini^{60b}, B.K. Gjølsten¹²⁰, S. Gkaitatzis¹⁵⁷, I. Gkialas¹⁵⁷, E.L. Gkougkousis¹¹⁸, L.K. Gladilin¹⁰⁰, C. Glasman⁸⁴, J. Glatzer⁵⁰, P.C.F. Glaysheer⁴⁸, A. Glazov⁴⁴, M. Goblirsch-Kolb²⁵, J. Godlewski⁴¹, S. Goldfarb⁹⁰, T. Golling⁵¹, D. Golubkov¹³¹, A. Gomes^{127a,127b,127d}, R. Gonçalo^{127a}, J. Goncalves Pinto Firmino Da Costa¹³⁷, G. Gonella⁵⁰, L. Gonella¹⁹, A. Gongadze⁶⁷, S. González de la Hoz¹⁷¹, S. Gonzalez-Sevilla⁵¹, L. Goossens³², P.A. Gorbounov⁹⁸, H.A. Gordon²⁷, I. Gorelov¹⁰⁶, B. Gorini³², E. Gorini^{75a,75b}, A. Gorišek⁷⁷, E. Gornicki⁴¹, A.T. Goshaw⁴⁷, C. Gössling⁴⁵, M.I. Gostkin⁶⁷, C.R. Goudet¹¹⁸, D. Goujdami^{136c}, A.G. Goussiou¹³⁹, N. Govender^{148b,q}, E. Gozani¹⁵⁵, L. Graber⁵⁶, I. Grabowska-Bold^{40a}, P.O.J. Gradin⁵⁷, P. Grafström^{22a,22b}, J. Gramling⁵¹, E. Gramstad¹²⁰, S. Grancagnolo¹⁷, V. Gratchev¹²⁴, P.M. Gravila^{28e}, H.M. Gray³², E. Graziani^{135a}, Z.D. Greenwood^{81,r}, C. Grefe²³, K. Gregersen⁸⁰, I.M. Gregor⁴⁴, P. Grenier¹⁴⁶, K. Grevtsov⁵, J. Griffiths⁸, A.A. Grillo¹³⁸, K. Grimm⁷⁴, S. Grinstein^{13,s}, Ph. Gris³⁶, J.-F. Grivaz¹¹⁸, S. Groh⁸⁵, E. Gross¹⁷⁶, J. Grosse-Knetter⁵⁶, G.C. Grossi⁸¹, Z.J. Grout⁸⁰, L. Guan⁹¹, W. Guan¹⁷⁷, J. Guenther⁶⁴, F. Guescini⁵¹, D. Guest¹⁶⁷, O. Gueta¹⁵⁶, B. Gui¹¹², E. Guido^{52a,52b}, T. Guillemin⁵, S. Guindon², U. Gul⁵⁵, C. Gumpert³², J. Guo¹⁴¹, Y. Guo^{59,p}, R. Gupta⁴², S. Gupta¹²¹, G. Gustavino^{133a,133b}, P. Gutierrez¹¹⁴, N.G. Gutierrez Ortiz⁸⁰, C. Gutsche⁴⁶, C. Guyot¹³⁷, C. Gwenlan¹²¹, C.B. Gwilliam⁷⁶, A. Haas¹¹¹, C. Haber¹⁶, H.K. Hadavand⁸, N. Haddad^{136e}, A. Hadeef⁸⁷, S. Hageböck²³, M. Hagihara¹⁶⁵, Z. Hajduk⁴¹, H. Hakobyan^{181,*}, M. Haleem⁴⁴, J. Haley¹¹⁵, G. Halladjian⁹², G.D. Hallewell⁸⁷, K. Hamacher¹⁷⁹, P. Hamal¹¹⁶, K. Hamano¹⁷³, A. Hamilton^{148a}, G.N. Hamity¹⁴², P.G. Hamnett⁴⁴, L. Han⁵⁹, K. Hanagaki^{68,t}, K. Hanawa¹⁵⁸, M. Hance¹³⁸, B. Haney¹²³, P. Hanke^{60a}, R. Hanna¹³⁷, J.B. Hansen³⁸, J.D. Hansen³⁸, M.C. Hansen²³, P.H. Hansen³⁸, K. Hara¹⁶⁵, A.S. Hard¹⁷⁷, T. Harenberg¹⁷⁹, F. Hariri¹¹⁸, S. Harkusha⁹⁴, R.D. Harrington⁴⁸, P.F. Harrison¹⁷⁴, F. Hartjes¹⁰⁸, N.M. Hartmann¹⁰¹, M. Hasegawa⁶⁹, Y. Hasegawa¹⁴³, A. Hasib¹¹⁴, S. Hassani¹³⁷, S. Haug¹⁸, R. Hauser⁹², L. Hauswald⁴⁶, M. Havranek¹²⁸, C.M. Hawkes¹⁹, R.J. Hawkins³², D. Hayakawa¹⁶⁰, D. Hayden⁹², C.P. Hays¹²¹, J.M. Hays⁷⁸, H.S. Hayward⁷⁶, S.J. Haywood¹³², S.J. Head¹⁹, T. Heck⁸⁵, V. Hedberg⁸³, L. Heelan⁸, S. Heim¹²³, T. Heim¹⁶, B. Heinemann¹⁶, J.J. Heinrich¹⁰¹, L. Heinrich¹¹¹, C. Heinz⁵⁴, J. Hejbal¹²⁸, L. Helary³², S. Hellman^{149a,149b}, C. Helsens³², J. Henderson¹²¹, R.C.W. Henderson⁷⁴, Y. Heng¹⁷⁷, S. Henkelmann¹⁷², A.M. Henriques Correia³², S. Henrot-Versille¹¹⁸, G.H. Herbert¹⁷, H. Herde²⁵, V. Herget¹⁷⁸, Y. Hernández Jiménez¹⁷¹, G. Herten⁵⁰, R. Hertenberger¹⁰¹, L. Hervas³², G.G. Hesketh⁸⁰, N.P. Hessey¹⁰⁸, J.W. Hetherly⁴², R. Hickling⁷⁸, E. Higón-Rodríguez¹⁷¹, E. Hill¹⁷³, J.C. Hill³⁰, K.H. Hiller⁴⁴, S.J. Hillier¹⁹, I. Hinchliffe¹⁶, E. Hines¹²³, R.R. Hinman¹⁶, M. Hirose⁵⁰, D. Hirschbuehl¹⁷⁹, J. Hobbs¹⁵¹, N. Hod^{164a}, M.C. Hodgkinson¹⁴², P. Hodgson¹⁴², A. Hoecker³², M.R. Hoefkamp¹⁰⁶, F. Hoenig¹⁰¹, D. Hohn²³, T.R. Holmes¹⁶, M. Homann⁴⁵, T. Honda⁶⁸, T.M. Hong¹²⁶, B.H. Hooberman¹⁷⁰, W.H. Hopkins¹¹⁷, Y. Horii¹⁰⁴, A.J. Horton¹⁴⁵, J.-Y. Hostachy⁵⁷, S. Hou¹⁵⁴, A. Hoummada^{136a}, J. Howarth⁴⁴, J. Hoya⁷³, M. Hrabovsky¹¹⁶, I. Hristova¹⁷, J. Hrivnac¹¹⁸, T. Hryn'ova⁵, A. Hrynevich⁹⁵, C. Hsu^{148c}, P.J. Hsu^{154,u}, S.-C. Hsu¹³⁹, Q. Hu⁵⁹, S. Hu¹⁴¹, Y. Huang⁴⁴, Z. Hubacek¹²⁹, F. Hubaut⁸⁷, F. Huegging²³, T.B. Huffman¹²¹, E.W. Hughes³⁷, G. Hughes⁷⁴, M. Huhtinen³², P. Huo¹⁵¹, N. Huseynov^{67,b}, J. Huston⁹²,

J. Huth⁵⁸, G. Iacobucci⁵¹, G. Iakovidis²⁷, I. Ibragimov¹⁴⁴, L. Iconomidou-Fayard¹¹⁸, E. Ideal¹⁸⁰, Z. Idrissi^{136e}, P. Iengo³², O. Igonkina^{108,v}, T. Iizawa¹⁷⁵, Y. Ikegami⁶⁸, M. Ikeno⁶⁸, Y. Ilchenko^{11,w}, D. Iliadis¹⁵⁷, N. Ilic¹⁴⁶, T. Ince¹⁰², G. Introzzi^{122a,122b}, P. Ioannou^{9,*}, M. Iodice^{135a}, K. Iordanidou³⁷, V. Ippolito⁵⁸, N. Ishijima¹¹⁹, M. Ishino¹⁵⁸, M. Ishitsuka¹⁶⁰, R. Ishmukhametov¹¹², C. Issever¹²¹, S. Istin^{20a}, F. Ito¹⁶⁵, J.M. Iturbe Ponce⁸⁶, R. Iuppa^{163a,163b}, W. Iwanski⁶⁴, H. Iwasaki⁶⁸, J.M. Izen⁴³, V. Izzo^{105a}, S. Jabbar³, B. Jackson¹²³, P. Jackson¹, V. Jain², K.B. Jakobi⁸⁵, K. Jakobs⁵⁰, S. Jakobsen³², T. Jakoubek¹²⁸, D.O. Jamin¹¹⁵, D.K. Jana⁸¹, R. Jansky⁶⁴, J. Janssen²³, M. Janus⁵⁶, G. Jarlskog⁸³, N. Javadov^{67,b}, T. Javůrek⁵⁰, F. Jeanneau¹³⁷, L. Jeanty¹⁶, G.-Y. Jeng¹⁵³, D. Jennens⁹⁰, P. Jenni^{50,x}, C. Jeske¹⁷⁴, S. Jézéquel⁵, H. Ji¹⁷⁷, J. Jia¹⁵¹, H. Jiang⁶⁶, Y. Jiang⁵⁹, Z. Jiang¹⁴⁶, S. Jiggins⁸⁰, J. Jimenez Pena¹⁷¹, S. Jin^{35a}, A. Jinaru^{28b}, O. Jinnouchi¹⁶⁰, H. Jivan^{148c}, P. Johansson¹⁴², K.A. Johns⁷, W.J. Johnson¹³⁹, K. Jon-And^{149a,149b}, G. Jones¹⁷⁴, R.W.L. Jones⁷⁴, S. Jones⁷, T.J. Jones⁷⁶, J. Jongmanns^{60a}, P.M. Jorge^{127a,127b}, J. Jovicevic^{164a}, X. Ju¹⁷⁷, A. Juste Rozas^{13,s}, M.K. Köhler¹⁷⁶, A. Kaczmarska⁴¹, M. Kado¹¹⁸, H. Kagan¹¹², M. Kagan¹⁴⁶, S.J. Kahn⁸⁷, T. Kaji¹⁷⁵, E. Kajomovitz⁴⁷, C.W. Kalderon¹²¹, A. Kaluza⁸⁵, S. Kama⁴², A. Kamenshchikov¹³¹, N. Kanaya¹⁵⁸, S. Kaneti³⁰, L. Kanjir⁷⁷, V.A. Kantserov⁹⁹, J. Kanzaki⁶⁸, B. Kaplan¹¹¹, L.S. Kaplan¹⁷⁷, A. Kapliy³³, D. Kar^{148c}, K. Karakostas¹⁰, A. Karamaoun³, N. Karastathis¹⁰, M.J. Kareem⁵⁶, E. Karentzos¹⁰, M. Karnevskiy⁸⁵, S.N. Karpov⁶⁷, Z.M. Karpova⁶⁷, K. Karthik¹¹¹, V. Kartvelishvili⁷⁴, A.N. Karyukhin¹³¹, K. Kasahara¹⁶⁵, L. Kashif¹⁷⁷, R.D. Kass¹¹², A. Kastanas¹⁵⁰, Y. Kataoka¹⁵⁸, C. Kato¹⁵⁸, A. Katre⁵¹, J. Katzy⁴⁴, K. Kawade¹⁰⁴, K. Kawagoe⁷², T. Kawamoto¹⁵⁸, G. Kawamura⁵⁶, V.F. Kazanin^{110,c}, R. Keeler¹⁷³, R. Kehoe⁴², J.S. Keller⁴⁴, J.J. Kempster⁷⁹, H. Keoshkerian¹⁶², O. Kepka¹²⁸, B.P. Kerševan⁷⁷, S. Kersten¹⁷⁹, R.A. Keyes⁸⁹, M. Khader¹⁷⁰, F. Khalil-zada¹², A. Khanov¹¹⁵, A.G. Kharlamov^{110,c}, T. Kharlamova¹¹⁰, T.J. Khoo⁵¹, V. Khovanskiy⁹⁸, E. Khramov⁶⁷, J. Khubua^{53b,y}, S. Kido⁶⁹, C.R. Kilby⁷⁹, H.Y. Kim⁸, S.H. Kim¹⁶⁵, Y.K. Kim³³, N. Kimura¹⁵⁷, O.M. Kind¹⁷, B.T. King⁷⁶, M. King¹⁷¹, J. Kirk¹³², A.E. Kiryunin¹⁰², T. Kishimoto¹⁵⁸, D. Kisielewska^{40a}, F. Kiss⁵⁰, K. Kiuchi¹⁶⁵, O. Kivernyk¹³⁷, E. Kladiva^{147b}, M.H. Klein³⁷, M. Klein⁷⁶, U. Klein⁷⁶, K. Kleinknecht⁸⁵, P. Klimek¹⁰⁹, A. Klimentov²⁷, R. Klingenberg⁴⁵, J.A. Klinger¹⁴², T. Klioutchnikova³², E.-E. Kluge^{60a}, P. Kluit¹⁰⁸, S. Kluth¹⁰², J. Knapik⁴¹, E. Kneringer⁶⁴, E.B.F.G. Knoop⁸⁷, A. Knue⁵⁵, A. Kobayashi¹⁵⁸, D. Kobayashi¹⁶⁰, T. Kobayashi¹⁵⁸, M. Kobel¹⁴⁶, M. Kocian¹⁴⁶, P. Kodys¹³⁰, N.M. Koehler¹⁰², T. Koffas³¹, E. Koffeman¹⁰⁸, T. Koi¹⁴⁶, H. Kolanoski¹⁷, M. Kolb^{60b}, I. Koletsou⁵, A.A. Komar^{97,*}, Y. Komori¹⁵⁸, T. Kondo⁶⁸, N. Kondrashova⁴⁴, K. Köneke⁵⁰, A.C. König¹⁰⁷, T. Kono^{68,z}, R. Konoplich^{111,aa}, N. Konstantinidis⁸⁰, R. Kopeliansky⁶³, S. Koperny^{40a}, L. Köpke⁸⁵, A.K. Kopp⁵⁰, K. Korcyl⁴¹, K. Kordas¹⁵⁷, A. Korn⁸⁰, A.A. Korol^{110,c}, I. Korolkov¹³, E.V. Korolkova¹⁴², O. Kortner¹⁰², S. Kortner¹⁰², T. Kosek¹³⁰, V.V. Kostyukhin²³, A. Kotwal⁴⁷, A. Koulouris¹⁰, A. Kourkouveli-Charalampidi^{122a,122b}, C. Kourkoumelis⁹, V. Kouskoura²⁷, A.B. Kowalewska⁴¹, R. Kowalewski¹⁷³, T.Z. Kowalski^{40a}, C. Kozakai¹⁵⁸, W. Kozanecki¹³⁷, A.S. Kozhin¹³¹, V.A. Kramarenko¹⁰⁰, G. Kramberger⁷⁷, D. Krasnopevtsev⁹⁹, M.W. Krasny⁸², A. Krasznahorkay³², F. Krauss^{ab}, A. Kravchenko²⁷, M. Kretz^{60c}, J. Kretzschmar⁷⁶, K. Kreutzfeldt⁵⁴, P. Krieger¹⁶², K. Krizka³³, K. Kroeninger⁴⁵, H. Kroha¹⁰², J. Kroll¹²³, J. Kroseberg²³, J. Krstic¹⁴, U. Kruchonak⁶⁷, H. Krüger²³, N. Krumnack⁶⁶, M.C. Kruse⁴⁷, M. Kruskal²⁴, T. Kubota⁹⁰, H. Kucuk⁸⁰, S. Kudah^{4b}, J.T. Kuechler¹⁷⁹, S. Kuehn⁵⁰, A. Kugel^{60c}, F. Kuger¹⁷⁸, A. Kuhl¹³⁸, T. Kuhl⁴⁴, V. Kukhtin⁶⁷, R. Kukla¹³⁷, Y. Kulchitsky⁹⁴, S. Kuleshov^{34b}, M. Kuna^{133a,133b}, T. Kunigo⁷⁰, A. Kupco¹²⁸, H. Kurashige⁶⁹, Y.A. Kurochkin⁹⁴, V. Kus¹²⁸, E.S. Kuwertz¹⁷³, M. Kuze¹⁶⁰, J. Kvita¹¹⁶, T. Kwan¹⁷³, D. Kyriazopoulos¹⁴², A. La Rosa¹⁰², J.L. La Rosa Navarro^{26d}, L. La Rotonda^{39a,39b}, C. Lacasta¹⁷¹, F. Lacava^{133a,133b}, J. Lacey³¹, H. Lacker¹⁷, D. Lacour⁸², V.R. Lacuesta¹⁷¹, E. Ladygin⁶⁷, R. Lafaye⁵, B. Laforge⁸², T. Lagouri¹⁸⁰, S. Lai⁵⁶, S. Lammers⁶³, W. Lampl⁷, E. Lançon¹³⁷, U. Landgraf⁵⁰, M.P.J. Landon⁷⁸, M.C. Lanfermann⁵¹, V.S. Lang^{60a}, J.C. Lange¹³, A.J. Lankford¹⁶⁷, F. Lanni²⁷, K. Lantzsche²³, A. Lanza^{122a}, S. Laplace⁸², C. Lapoire³², J.F. Laporte¹³⁷, T. Lari^{93a},

F. Lasagni Manghi^{22a,22b}, M. Lassnig³², P. Laurelli⁴⁹, W. Lavrijsen¹⁶, A.T. Law¹³⁸, P. Laycock⁷⁶, T. Lazovich⁵⁸, M. Lazzaroni^{93a,93b}, B. Le⁹⁰, O. Le Dortz⁸², E. Le Guirriec⁸⁷, E.P. Le Quilleuc¹³⁷, M. LeBlanc¹⁷³, T. LeCompte⁶, F. Ledroit-Guillon⁵⁷, C.A. Lee²⁷, S.C. Lee¹⁵⁴, L. Lee¹, B. Lefebvre⁸⁹, G. Lefebvre⁸², M. Lefebvre¹⁷³, F. Legger¹⁰¹, C. Leggett¹⁶, A. Lehan⁷⁶, G. Lehmann Miotto³², X. Lei⁷, W.A. Leight³¹, A.G. Leister¹⁸⁰, M.A.L. Leite^{26d}, R. Leitner¹³⁰, D. Lellouch¹⁷⁶, B. Lemmer⁵⁶, K.J.C. Leney⁸⁰, T. Lenz²³, B. Lenzi³², R. Leone⁷, S. Leone^{125a,125b}, C. Leonidopoulos⁴⁸, S. Leontsinis¹⁰, G. Lerner¹⁵², C. Leroy⁹⁶, A.A.J. Lesage¹³⁷, C.G. Lester³⁰, M. Levchenko¹²⁴, J. Levêque⁵, D. Levin⁹¹, L.J. Levinson¹⁷⁶, M. Levy¹⁹, D. Lewis⁷⁸, A.M. Leyko²³, M. Leyton⁴³, B. Li^{59,p}, C. Li⁵⁹, H. Li¹⁵¹, H.L. Li³³, L. Li⁴⁷, L. Li¹⁴¹, Q. Li^{35a}, S. Li⁴⁷, X. Li⁸⁶, Y. Li¹⁴⁴, Z. Liang^{35a}, B. Liberti^{134a}, A. Liblong¹⁶², P. Lichard³², K. Lie¹⁷⁰, J. Liebal²³, W. Liebig¹⁵, A. Limosani¹⁵³, S.C. Lin^{154,ac}, T.H. Lin⁸⁵, B.E. Lindquist¹⁵¹, A.E. Lioni⁵¹, E. Lipeles¹²³, A. Lipniacka¹⁵, M. Lisovyi^{60b}, T.M. Liss¹⁷⁰, A. Lister¹⁷², A.M. Litke¹³⁸, B. Liu^{154,ad}, D. Liu¹⁵⁴, H. Liu⁹¹, H. Liu²⁷, J. Liu⁸⁷, J.B. Liu⁵⁹, K. Liu⁸⁷, L. Liu¹⁷⁰, M. Liu⁴⁷, M. Liu⁵⁹, Y.L. Liu⁵⁹, Y. Liu⁵⁹, M. Livan^{122a,122b}, A. Lleres⁵⁷, J. Llorente Merino^{35a}, S.L. Lloyd⁷⁸, F. Lo Sterzo¹⁵⁴, E.M. Lobodzinska⁴⁴, P. Loch⁷, F.K. Loebinger⁸⁶, K.M. Loew²⁵, A. Loginov^{180,*}, T. Lohse¹⁷, K. Lohwasser⁴⁴, M. Lokajicek¹²⁸, B.A. Long²⁴, J.D. Long¹⁷⁰, R.E. Long⁷⁴, L. Longo^{75a,75b}, K.A. Looper¹¹², J.A. López^{34b}, D. Lopez Mateos⁵⁸, B. Lopez Paredes¹⁴², I. Lopez Paz¹³, A. Lopez Solis⁸², J. Lorenz¹⁰¹, N. Lorenzo Martinez⁶³, M. Losada²¹, P.J. Lösel¹⁰¹, X. Lou^{35a}, A. Lounis¹¹⁸, J. Love⁶, P.A. Love⁷⁴, H. Lu^{62a}, N. Lu⁹¹, H.J. Lubatti¹³⁹, C. Luci^{133a,133b}, A. Lucotte⁵⁷, C. Luedtke⁵⁰, F. Luehring⁶³, W. Lukas⁶⁴, L. Luminari^{133a}, O. Lundberg^{149a,149b}, B. Lund-Jensen¹⁵⁰, P.M. Luzzi⁸², D. Lynn²⁷, R. Lysak¹²⁸, E. Lytken⁸³, V. Lyubushkin⁶⁷, H. Ma²⁷, L.L. Ma¹⁴⁰, Y. Ma¹⁴⁰, G. Maccarrone⁴⁹, A. Macchiolo¹⁰², C.M. Macdonald¹⁴², B. Maček⁷⁷, J. Machado Miguens^{123,127b}, D. Madaffari⁸⁷, R. Madar³⁶, H.J. Maddocks¹⁶⁹, W.F. Mader⁴⁶, A. Madsen⁴⁴, J. Maeda⁶⁹, S. Maeland¹⁵, T. Maeno²⁷, A. Maevskiy¹⁰⁰, E. Magradze⁵⁶, J. Mahlstedt¹⁰⁸, C. Maiani¹¹⁸, C. Maidantchik^{26a}, A.A. Maier¹⁰², T. Maier¹⁰¹, A. Maio^{127a,127b,127d}, S. Majewski¹¹⁷, Y. Makida⁶⁸, N. Makovec¹¹⁸, B. Malaescu⁸², Pa. Malecki⁴¹, V.P. Maleev¹²⁴, F. Malek⁵⁷, U. Mallik⁶⁵, D. Malon⁶, C. Malone¹⁴⁶, C. Malone³⁰, S. Maltezos¹⁰, S. Malyukov³², J. Mamuzic¹⁷¹, G. Mancini⁴⁹, L. Mandelli^{93a}, I. Mandić⁷⁷, J. Maneira^{127a,127b}, L. Manhaes de Andrade Filho^{26b}, J. Manjarres Ramos^{164b}, A. Mann¹⁰¹, A. Manousos³², B. Mansoulie¹³⁷, J.D. Mansour^{35a}, R. Mantifel⁸⁹, M. Mantoani⁵⁶, S. Manzoni^{93a,93b}, L. Mapelli³², G. Marceca²⁹, L. March⁵¹, G. Marchiori⁸², M. Marcisovsky¹²⁸, M. Marjanovic¹⁴, D.E. Marley⁹¹, F. Marroquim^{26a}, S.P. Marsden⁸⁶, Z. Marshall¹⁶, S. Marti-Garcia¹⁷¹, B. Martin⁹², T.A. Martin¹⁷⁴, V.J. Martin⁴⁸, B. Martin dit Latour¹⁵, M. Martinez^{13,s}, V.I. Martinez Outschoorn¹⁷⁰, S. Martin-Haugh¹³², V.S. Martoiu^{28b}, A.C. Martyniuk⁸⁰, A. Marzin³², L. Masetti⁸⁵, T. Mashimo¹⁵⁸, R. Mashinistov⁹⁷, J. Masik⁸⁶, A.L. Maslennikov^{110,c}, I. Massa^{22a,22b}, L. Massa^{22a,22b}, P. Mastrandrea⁵, A. Mastroberardino^{39a,39b}, T. Masubuchi¹⁵⁸, P. Mättig¹⁷⁹, J. Mattmann⁸⁵, J. Maurer^{28b}, S.J. Maxfield⁷⁶, D.A. Maximov^{110,c}, R. Mazini¹⁵⁴, I. Maznas¹⁵⁷, S.M. Mazza^{93a,93b}, N.C. Mc Fadden¹⁰⁶, G. Mc Goldrick¹⁶², S.P. Mc Kee⁹¹, A. McCarn⁹¹, R.L. McCarthy¹⁵¹, T.G. McCarthy¹⁰², L.I. McClymont⁸⁰, E.F. McDonald⁹⁰, J.A. Mcfayden⁸⁰, G. Mchedlidze⁵⁶, S.J. McMahon¹³², R.A. McPherson^{173,m}, M. Medinnis⁴⁴, S. Meehan¹³⁹, S. Mehlhase¹⁰¹, A. Mehta⁷⁶, K. Meier^{60a}, C. Meineck¹⁰¹, B. Meirose⁴³, D. Melini¹⁷¹, B.R. Mellado Garcia^{148c}, M. Melo^{147a}, F. Meloni¹⁸, A. Mengarelli^{22a,22b}, S. Menke¹⁰², E. Meoni¹⁶⁶, S. Mergelmeyer¹⁷, P. Mermod⁵¹, L. Merola^{105a,105b}, C. Meroni^{93a}, F.S. Merritt³³, A. Messina^{133a,133b}, J. Metcalfe⁶, A.S. Mete¹⁶⁷, C. Meyer⁸⁵, C. Meyer¹²³, J-P. Meyer¹³⁷, J. Meyer¹⁰⁸, H. Meyer Zu Theenhausen^{60a}, F. Miano¹⁵², R.P. Middleton¹³², S. Miglioranza^{52a,52b}, L. Mijović⁴⁸, G. Mikenberg¹⁷⁶, M. Mikestikova¹²⁸, M. Mikuž⁷⁷, M. Milesi⁹⁰, A. Milic⁶⁴, D.W. Miller³³, C. Mills⁴⁸, A. Milov¹⁷⁶, D.A. Milstead^{149a,149b}, A.A. Minaenko¹³¹, Y. Minami¹⁵⁸, I.A. Minashvili⁶⁷, A.I. Mincer¹¹¹, B. Mindur^{40a}, M. Mineev⁶⁷, Y. Minegishi¹⁵⁸, Y. Ming¹⁷⁷, L.M. Mir¹³, K.P. Mistry¹²³, T. Mitani¹⁷⁵, J. Mitrevski¹⁰¹, V.A. Mitsou¹⁷¹, A. Miucci¹⁸, P.S. Miyagawa¹⁴², J.U. Mjörnmark⁸³, M. Mlynarikova¹³⁰,

T. Moa^{149a,149b}, K. Mochizuki⁹⁶, S. Mohapatra³⁷, S. Molander^{149a,149b}, R. Moles-Valls²³, R. Monden⁷⁰, M.C. Mondragon⁹², K. Mönig⁴⁴, J. Monk³⁸, E. Monnier⁸⁷, A. Montalbano¹⁵¹, J. Montejo Berlingen³², F. Monticelli⁷³, S. Monzani^{93a,93b}, R.W. Moore³, N. Morange¹¹⁸, D. Moreno²¹, M. Moreno Llacer⁵⁶, P. Morettini^{52a}, S. Morgenstern³², D. Mori¹⁴⁵, T. Mori¹⁵⁸, M. Morii⁵⁸, M. Morinaga¹⁵⁸, V. Morisbak¹²⁰, S. Moritz⁸⁵, A.K. Morley¹⁵³, G. Mornacchi³², J.D. Morris⁷⁸, S.S. Mortensen³⁸, L. Morvaj¹⁵¹, M. Mosidze^{53b}, J. Moss^{146,ae}, K. Motohashi¹⁶⁰, R. Mount¹⁴⁶, E. Mountricha²⁷, E.J.W. Moyse⁸⁸, S. Muanza⁸⁷, R.D. Mudd¹⁹, F. Mueller¹⁰², J. Mueller¹²⁶, R.S.P. Mueller¹⁰¹, T. Mueller³⁰, D. Muenstermann⁷⁴, P. Mullen⁵⁵, G.A. Mullier¹⁸, F.J. Munoz Sanchez⁸⁶, J.A. Murillo Quijada¹⁹, W.J. Murray^{174,132}, H. Musheghyan⁵⁶, M. Muškinja⁷⁷, A.G. Myagkov^{131,af}, M. Myska¹²⁹, B.P. Nachman¹⁴⁶, O. Nackenhorst⁵¹, K. Nagai¹²¹, R. Nagai^{68,z}, K. Nagano⁶⁸, Y. Nagasaka⁶¹, K. Nagata¹⁶⁵, M. Nagel⁵⁰, E. Nagy⁸⁷, A.M. Nairz³², Y. Nakahama¹⁰⁴, K. Nakamura⁶⁸, T. Nakamura¹⁵⁸, I. Nakano¹¹³, R.F. Naranjo Garcia⁴⁴, R. Narayan¹¹, D.I. Narrias Villar^{60a}, I. Naryshkin¹²⁴, T. Naumann⁴⁴, G. Navarro²¹, R. Nayyar⁷, H.A. Neal⁹¹, P.Yu. Nechaeva⁹⁷, T.J. Neep⁸⁶, A. Negri^{122a,122b}, M. Negrini^{22a}, S. Nektarijevic¹⁰⁷, C. Nellist¹¹⁸, A. Nelson¹⁶⁷, S. Nemecek¹²⁸, P. Nemethy¹¹¹, A.A. Nepomuceno^{26a}, M. Nessi^{32,ag}, M.S. Neubauer¹⁷⁰, M. Neumann¹⁷⁹, R.M. Neves¹¹¹, P. Nevski²⁷, P.R. Newman¹⁹, D.H. Nguyen⁶, T. Nguyen Manh⁹⁶, R.B. Nickerson¹²¹, R. Nicolaidou¹³⁷, J. Nielsen¹³⁸, A. Nikiforov¹⁷, V. Nikolaenko^{131,af}, I. Nikolic-Audit⁸², K. Nikolopoulos¹⁹, J.K. Nilsen¹²⁰, P. Nilsson²⁷, Y. Ninomiya¹⁵⁸, A. Nisati^{133a}, R. Nisius¹⁰², T. Nobe¹⁵⁸, M. Nomachi¹¹⁹, I. Nomidis³¹, T. Nooney⁷⁸, S. Norberg¹¹⁴, M. Nordberg³², N. Norjoharuddeen¹²¹, O. Novgorodova⁴⁶, S. Nowak¹⁰², M. Nozaki⁶⁸, L. Nozka¹¹⁶, K. Ntekas¹⁶⁷, E. Nurse⁸⁰, F. Nuti⁹⁰, F. O'grady⁷, D.C. O'Neil¹⁴⁵, A.A. O'Rourke⁴⁴, V. O'Shea⁵⁵, F.G. Oakham^{31,d}, H. Oberlack¹⁰², T. Obermann²³, J. Ocariz⁸², A. Ochi⁶⁹, I. Ochoa³⁷, J.P. Ochoa-Ricoux^{34a}, S. Oda⁷², S. Odaka⁶⁸, H. Ogren⁶³, A. Oh⁸⁶, S.H. Oh⁴⁷, C.C. Ohm¹⁶, H. Ohman¹⁶⁹, H. Oide^{52a,52b}, H. Okawa¹⁶⁵, Y. Okumura¹⁵⁸, T. Okuyama⁶⁸, A. Olariu^{28b}, L.F. Oleiro Seabra^{127a}, S.A. Olivares Pino⁴⁸, D. Oliveira Damazio²⁷, A. Olszewski⁴¹, J. Olszowska⁴¹, A. Onofre^{127a,127e}, K. Onogi¹⁰⁴, P.U.E. Onyisi^{11,w}, M.J. Oreglia³³, Y. Oren¹⁵⁶, D. Orestano^{135a,135b}, N. Orlando^{62b}, R.S. Orr¹⁶², B. Osculati^{52a,52b,*}, R. Ospanov⁸⁶, G. Otero y Garzon²⁹, H. Otono⁷², M. Ouchrif^{136d}, F. Ould-Saada¹²⁰, A. Ouraou¹³⁷, K.P. Oussoren¹⁰⁸, Q. Ouyang^{35a}, M. Owen⁵⁵, R.E. Owen¹⁹, V.E. Ozcan^{20a}, N. Ozturk⁸, K. Pachal¹⁴⁵, A. Pacheco Pages¹³, L. Pacheco Rodriguez¹³⁷, C. Padilla Aranda¹³, M. Pagáčová⁵⁰, S. Pagan Griso¹⁶, M. Paganini¹⁸⁰, F. Paige²⁷, P. Pais⁸⁸, K. Pajchel¹²⁰, G. Palacino^{164b}, S. Palazzo^{39a,39b}, S. Palestini³², M. Palka^{40b}, D. Pallin³⁶, E.St. Panagiotopoulou¹⁰, C.E. Pandini⁸², J.G. Panduro Vazquez⁷⁹, P. Pani^{149a,149b}, S. Panitkin²⁷, D. Pantea^{28b}, L. Paolozzi⁵¹, Th.D. Papadopoulou¹⁰, K. Papageorgiou¹⁵⁷, A. Paramonov⁶, D. Paredes Hernandez¹⁸⁰, A.J. Parker⁷⁴, M.A. Parker³⁰, K.A. Parker¹⁴², F. Parodi^{52a,52b}, J.A. Parsons³⁷, U. Parzefall⁵⁰, V.R. Pascuzzi¹⁶², E. Pasqualucci^{133a}, S. Passaggio^{52a}, Fr. Pastore⁷⁹, G. Pásztor^{31,ah}, S. Patariaia¹⁷⁹, J.R. Pater⁸⁶, T. Pauly³², J. Pearce¹⁷³, B. Pearson¹¹⁴, L.E. Pedersen³⁸, M. Pedersen¹²⁰, S. Pedraza Lopez¹⁷¹, R. Pedro^{127a,127b}, S.V. Peleganchuk^{110,c}, O. Penc¹²⁸, C. Peng^{35a}, H. Peng⁵⁹, J. Penwell⁶³, B.S. Peralva^{26b}, M.M. Perego¹³⁷, D.V. Perepelitsa²⁷, E. Perez Codina^{164a}, L. Perini^{93a,93b}, H. Pernegger³², S. Perrella^{105a,105b}, R. Peschke⁴⁴, V.D. Peshekhonov⁶⁷, K. Peters⁴⁴, R.F.Y. Peters⁸⁶, B.A. Petersen³², T.C. Petersen³⁸, E. Petit⁵⁷, A. Petridis¹, C. Petridou¹⁵⁷, P. Petroff¹¹⁸, E. Petrolo^{133a}, M. Petrov¹²¹, F. Petrucci^{135a,135b}, N.E. Pettersson⁸⁸, A. Peyaud¹³⁷, R. Pezoa^{34b}, P.W. Phillips¹³², G. Piacquadio^{146,ai}, E. Pianori¹⁷⁴, A. Picazio⁸⁸, E. Piccaro⁷⁸, M. Piccinini^{22a,22b}, M.A. Pickering¹²¹, R. Piegaia²⁹, J.E. Pilcher³³, A.D. Pilkington⁸⁶, A.W.J. Pin⁸⁶, M. Pinamonti^{168a,168c,aj}, J.L. Pinfold³, A. Pingel³⁸, S. Pires⁸², H. Pirumov⁴⁴, M. Pitt¹⁷⁶, L. Plazak^{147a}, M.-A. Pleier²⁷, V. Pleskot⁸⁵, E. Plotnikova⁶⁷, P. Plucinski⁹², D. Pluth⁶⁶, R. Poettgen^{149a,149b}, L. Poggioli¹¹⁸, D. Pohl²³, G. Polesello^{122a}, A. Poley⁴⁴, A. Policicchio^{39a,39b}, R. Polifka¹⁶², A. Polini^{22a}, C.S. Pollard⁵⁵, V. Polychronakos²⁷, K. Pommès³², L. Pontecorvo^{133a}, B.G. Pope⁹², G.A. Popeneciu^{28c}, A. Poppleton³², S. Pospisil¹²⁹, K. Potamianos¹⁶, I.N. Potrap⁶⁷, C.J. Potter³⁰, C.T. Potter¹¹⁷, G. Poulard³², J. Poveda³²,

V. Pozdnyakov⁶⁷, M.E. Pozo Astigarraga³², P. Pralavorio⁸⁷, A. Pranko¹⁶, S. Prell⁶⁶, D. Price⁸⁶, L.E. Price⁶, M. Primavera^{75a}, S. Prince⁸⁹, K. Prokofiev^{62c}, F. Prokoshin^{34b}, S. Protopopescu²⁷, J. Proudfoot⁶, M. Przybycien^{40a}, D. Puddu^{135a,135b}, M. Purohit^{27,ak}, P. Puzo¹¹⁸, J. Qian⁹¹, G. Qin⁵⁵, Y. Qin⁸⁶, A. Quadt⁵⁶, W.B. Quayle^{168a,168b}, M. Queitsch-Maitland⁸⁶, D. Quilty⁵⁵, S. Raddum¹²⁰, V. Radeka²⁷, V. Radescu¹²¹, S.K. Radhakrishnan¹⁵¹, P. Radloff¹¹⁷, P. Rados⁹⁰, F. Ragusa^{93a,93b}, G. Rahal¹⁸², J.A. Raine⁸⁶, S. Rajagopalan²⁷, M. Rammensee³², C. Rangel-Smith¹⁶⁹, M.G. Ratti^{93a,93b}, D.M. Rauch⁴⁴, F. Rauscher¹⁰¹, S. Rave⁸⁵, T. Ravenscroft⁵⁵, I. Ravinovich¹⁷⁶, M. Raymond³², A.L. Read¹²⁰, N.P. Readioff⁷⁶, M. Reale^{75a,75b}, D.M. Rebuzzi^{122a,122b}, A. Redelbach¹⁷⁸, G. Redlinger²⁷, R. Reece¹³⁸, R.G. Reed^{148c}, K. Reeves⁴³, L. Rehnisch¹⁷, J. Reichert¹²³, A. Reiss⁸⁵, C. Rembser³², H. Ren^{35a}, M. Rescigno^{133a}, S. Resconi^{93a}, O.L. Rezanova^{110,c}, P. Reznicek¹³⁰, R. Rezvani⁹⁶, R. Richter¹⁰², S. Richter⁸⁰, E. Richter-Was^{40b}, O. Ricken²³, M. Ridel⁸², P. Rieck¹⁷, C.J. Riegel¹⁷⁹, J. Rieger⁵⁶, O. Rifki¹¹⁴, M. Rijssenbeek¹⁵¹, A. Rimoldi^{122a,122b}, M. Rimoldi¹⁸, L. Rinaldi^{22a}, B. Ristic⁵¹, E. Ritsch³², I. Riu¹³, F. Rizatdinova¹¹⁵, E. Rizvi⁷⁸, C. Rizzi¹³, S.H. Robertson^{89,m}, A. Robichaud-Veronneau⁸⁹, D. Robinson³⁰, J.E.M. Robinson⁴⁴, A. Robson⁵⁵, C. Roda^{125a,125b}, Y. Rodina^{87,al}, A. Rodriguez Perez¹³, D. Rodriguez Rodriguez¹⁷¹, S. Roe³², C.S. Rogan⁵⁸, O. Røhne¹²⁰, J. Roloff⁵⁸, A. Romaniouk⁹⁹, M. Romano^{22a,22b}, S.M. Romano Saez³⁶, E. Romero Adam¹⁷¹, N. Rompotis¹³⁹, M. Ronzani⁵⁰, L. Roos⁸², E. Ros¹⁷¹, S. Rosati^{133a}, K. Rosbach⁵⁰, P. Rose¹³⁸, N.-A. Rosien⁵⁶, V. Rossetti^{149a,149b}, E. Rossi^{105a,105b}, L.P. Rossi^{52a}, J.H.N. Rosten³⁰, R. Rosten¹³⁹, M. Rotaru^{28b}, I. Roth¹⁷⁶, J. Rothberg¹³⁹, D. Rousseau¹¹⁸, A. Rozanov⁸⁷, Y. Rozen¹⁵⁵, X. Ruan^{148c}, F. Rubbo¹⁴⁶, M.S. Rudolph¹⁶², F. Rühr⁵⁰, A. Ruiz-Martinez³¹, Z. Rurikova⁵⁰, N.A. Rusakovich⁶⁷, A. Ruschke¹⁰¹, H.L. Russell¹³⁹, J.P. Rutherford⁷, N. Ruthmann³², Y.F. Ryabov¹²⁴, M. Rybar¹⁷⁰, G. Rybkin¹¹⁸, S. Ryu⁶, A. Ryzhov¹³¹, G.F. Rzehorz⁵⁶, A.F. Saavedra¹⁵³, G. Sabato¹⁰⁸, S. Sacerdoti²⁹, H.F.-W. Sadrozinski¹³⁸, R. Sadykov⁶⁷, F. Safai Tehrani^{133a}, P. Saha¹⁰⁹, M. Sahinsoy^{60a}, M. Saimpert¹³⁷, T. Saito¹⁵⁸, H. Sakamoto¹⁵⁸, Y. Sakurai¹⁷⁵, G. Salamanna^{135a,135b}, A. Salamon^{134a,134b}, J.E. Salazar Loyola^{34b}, D. Salek¹⁰⁸, P.H. Sales De Bruin¹³⁹, D. Salihagic¹⁰², A. Salnikov¹⁴⁶, J. Salt¹⁷¹, D. Salvatore^{39a,39b}, F. Salvatore¹⁵², A. Salvucci^{62a,62b,62c}, A. Salzburger³², D. Sammel⁵⁰, D. Sampsonidis¹⁵⁷, A. Sanchez^{105a,105b}, J. Sánchez¹⁷¹, V. Sanchez Martinez¹⁷¹, H. Sandaker¹²⁰, R.L. Sandbach⁷⁸, M. Sandhoff¹⁷⁹, C. Sandoval²¹, D.P.C. Sankey¹³², M. Sannino^{52a,52b}, A. Sansoni⁴⁹, C. Santoni³⁶, R. Santonico^{134a,134b}, H. Santos^{127a}, I. Santoyo Castillo¹⁵², K. Sapp¹²⁶, A. Saprnov⁶⁷, J.G. Saraiva^{127a,127d}, B. Sarrazin²³, O. Sasaki⁶⁸, K. Sato¹⁶⁵, E. Sauvan⁵, G. Savage⁷⁹, P. Savard^{162,d}, N. Savic¹⁰², C. Sawyer¹³², L. Sawyer^{81,r}, J. Saxon³³, C. Sbarra^{22a}, A. Sbrizzi^{22a,22b}, T. Scanlon⁸⁰, D.A. Scannicchio¹⁶⁷, M. Scarcella¹⁵³, V. Scarfone^{39a,39b}, J. Schaarschmidt¹⁷⁶, P. Schacht¹⁰², B.M. Schachtner¹⁰¹, D. Schaefer³², L. Schaefer¹²³, R. Schaefer⁴⁴, J. Schaeffer⁸⁵, S. Schaepe²³, S. Schaetzel^{60b}, U. Schäfer⁸⁵, A.C. Schaffer¹¹⁸, D. Schaile¹⁰¹, R.D. Schamberger¹⁵¹, V. Scharf^{60a}, V.A. Schegelsky¹²⁴, D. Scheirich¹³⁰, M. Schernau¹⁶⁷, C. Schiavi^{52a,52b}, S. Schier¹³⁸, C. Schillo⁵⁰, M. Schioppa^{39a,39b}, S. Schlenker³², K.R. Schmidt-Sommerfeld¹⁰², K. Schmieden³², C. Schmitt⁸⁵, S. Schmitt⁴⁴, S. Schmitz⁸⁵, B. Schneider^{164a}, U. Schnoor⁵⁰, L. Schoeffel¹³⁷, A. Schoening^{60b}, B.D. Schoenrock⁹², E. Schopf²³, M. Schott⁸⁵, J.F.P. Schouwenberg¹⁰⁷, J. Schovancova⁸, S. Schramm⁵¹, M. Schreyer¹⁷⁸, N. Schuh⁸⁵, A. Schulte⁸⁵, M.J. Schultens²³, H.-C. Schultz-Coulon^{60a}, H. Schulz¹⁷, M. Schumacher⁵⁰, B.A. Schumm¹³⁸, Ph. Schune¹³⁷, A. Schwartzman¹⁴⁶, T.A. Schwarz⁹¹, H. Schweiger⁸⁶, Ph. Schwemling¹³⁷, R. Schwienhorst⁹², J. Schwindling¹³⁷, T. Schwindt²³, G. Sciolla²⁵, F. Scuri^{125a,125b}, F. Scutti⁹⁰, J. Searcy⁹¹, P. Seema²³, S.C. Seidel¹⁰⁶, A. Seiden¹³⁸, F. Seifert¹²⁹, J.M. Seixas^{26a}, G. Sekhniaidze^{105a}, K. Sekhon⁹¹, S.J. Sekula⁴², D.M. Seliverstov^{124,*}, N. Semprini-Cesari^{22a,22b}, C. Serfon¹²⁰, L. Serin¹¹⁸, L. Serkin^{168a,168b}, M. Sessa^{135a,135b}, R. Seuster¹⁷³, H. Severini¹¹⁴, T. Sfiligoi⁷⁷, F. Sforza³², A. Sfyrila⁵¹, E. Shabalina⁵⁶, N.W. Shaikh^{149a,149b}, L.Y. Shan^{35a}, R. Shang¹⁷⁰, J.T. Shank²⁴, M. Shapiro¹⁶, P.B. Shatalov⁹⁸, K. Shaw^{168a,168b}, S.M. Shaw⁸⁶, A. Shcherbakova^{149a,149b}, C.Y. Shehu¹⁵², P. Sherwood⁸⁰, L. Shi^{154,am}, S. Shimizu⁶⁹, C.O. Shimmin¹⁶⁷,

M. Shimojima¹⁰³, S. Shirabe⁷², M. Shiyakova^{67,an}, A. Shmeleva⁹⁷, D. Shoaleh Saadi⁹⁶, M.J. Shochet³³, S. Shojaii^{93a,93b}, D.R. Shope¹¹⁴, S. Shrestha¹¹², E. Shulga⁹⁹, M.A. Shupe⁷, P. Sicho¹²⁸, A.M. Sickles¹⁷⁰, P.E. Sidebo¹⁵⁰, E. Sideras Haddad^{148c}, O. Sidiropoulou¹⁷⁸, D. Sidorov¹¹⁵, A. Sidoti^{22a,22b}, F. Siegert⁴⁶, Dj. Sijacki¹⁴, J. Silva^{127a,127d}, S.B. Silverstein^{149a}, V. Simak¹²⁹, Lj. Simic¹⁴, S. Simion¹¹⁸, E. Simioni⁸⁵, B. Simmons⁸⁰, D. Simon³⁶, M. Simon⁸⁵, P. Sinervo¹⁶², N.B. Sinev¹¹⁷, M. Sioli^{22a,22b}, G. Siragusa¹⁷⁸, S.Yu. Sivoklov¹⁰⁰, J. Sjölin^{149a,149b}, M.B. Skinner⁷⁴, H.P. Skottowe⁵⁸, P. Skubic¹¹⁴, M. Slater¹⁹, T. Slavicek¹²⁹, M. Slawinska¹⁰⁸, K. Sliwa¹⁶⁶, R. Slovak¹³⁰, V. Smakhtin¹⁷⁶, B.H. Smart⁵, L. Smestad¹⁵, J. Smiesko^{147a}, S.Yu. Smirnov⁹⁹, Y. Smirnov⁹⁹, L.N. Smirnova^{100,ao}, O. Smirnova⁸³, M.N.K. Smith³⁷, R.W. Smith³⁷, M. Smizanska⁷⁴, K. Smolek¹²⁹, A.A. Snesarev⁹⁷, I.M. Snyder¹¹⁷, S. Snyder²⁷, R. Sobie^{173,m}, F. Socher⁴⁶, A. Soffer¹⁵⁶, D.A. Soh¹⁵⁴, G. Sokhrannyi⁷⁷, C.A. Solans Sanchez³², M. Solar¹²⁹, E.Yu. Soldatov⁹⁹, U. Soldevila¹⁷¹, A.A. Solodkov¹³¹, A. Soloshenko⁶⁷, O.V. Solovyanov¹³¹, V. Solovye¹²⁴, P. Sommer⁵⁰, H. Son¹⁶⁶, H.Y. Song^{59,ap}, A. Sood¹⁶, A. Sopczak¹²⁹, V. Sopko¹²⁹, V. Sorin¹³, D. Sosa^{60b}, C.L. Sotiropoulou^{125a,125b}, R. Soualah^{168a,168c}, A.M. Soukharev^{110,c}, D. South⁴⁴, B.C. Sowden⁷⁹, S. Spagnolo^{75a,75b}, M. Spalla^{125a,125b}, M. Spangenberg¹⁷⁴, F. Spanò⁷⁹, D. Sperlich¹⁷, F. Spettel¹⁰², R. Spighi^{22a}, G. Spigo³², L.A. Spiller⁹⁰, M. Spousta¹³⁰, R.D. St. Denis^{55,*}, A. Stabile^{93a}, R. Stamen^{60a}, S. Stamm¹⁷, E. Stanecka⁴¹, R.W. Stanek⁶, C. Stanescu^{135a}, M. Stanescu-Bellu⁴⁴, M.M. Stanitzki⁴⁴, S. Stapnes¹²⁰, E.A. Starchenko¹³¹, G.H. Stark³³, J. Stark⁵⁷, P. Staroba¹²⁸, P. Starovoitov^{60a}, S. Stärz³², R. Staszewski⁴¹, P. Steinberg²⁷, B. Stelzer¹⁴⁵, H.J. Stelzer³², O. Stelzer-Chilton^{164a}, H. Stenzel⁵⁴, G.A. Stewart⁵⁵, J.A. Stillings²³, M.C. Stockton⁸⁹, M. Stoebe⁸⁹, G. Stoicea^{28b}, P. Stolte⁵⁶, S. Stonjek¹⁰², A.R. Stradling⁸, A. Straessner⁴⁶, M.E. Stramaglia¹⁸, J. Strandberg¹⁵⁰, S. Strandberg^{149a,149b}, A. Strandlie¹²⁰, M. Strauss¹¹⁴, P. Strizenec^{147b}, R. Ströhmer¹⁷⁸, D.M. Strom¹¹⁷, R. Stroynowski⁴², A. Strubig¹⁰⁷, S.A. Stucci²⁷, B. Stugu¹⁵, N.A. Styles⁴⁴, D. Su¹⁴⁶, J. Su¹²⁶, S. Suchek^{60a}, Y. Sugaya¹¹⁹, M. Suk¹²⁹, V.V. Sulin⁹⁷, S. Sultansoy^{4c}, T. Sumida⁷⁰, S. Sun⁵⁸, X. Sun^{35a}, J.E. Sundermann⁵⁰, K. Suruliz¹⁵², G. Susinno^{39a,39b}, M.R. Sutton¹⁵², S. Suzuki⁶⁸, M. Svatos¹²⁸, M. Swiatlowski³³, I. Sykora^{147a}, T. Sykora¹³⁰, D. Ta⁵⁰, C. Taccini^{135a,135b}, K. Tackmann⁴⁴, J. Taenzer¹⁶², A. Taffard¹⁶⁷, R. Tahirout^{164a}, N. Taiblum¹⁵⁶, H. Takai²⁷, R. Takashima⁷¹, T. Takeshita¹⁴³, Y. Takubo⁶⁸, M. Talby⁸⁷, A.A. Talyshev^{110,c}, K.G. Tan⁹⁰, J. Tanaka¹⁵⁸, M. Tanaka¹⁶⁰, R. Tanaka¹¹⁸, S. Tanaka⁶⁸, R. Tanioka⁶⁹, B.B. Tannenwald¹¹², S. Tapia Araya^{34b}, S. Tapprogge⁸⁵, S. Tarem¹⁵⁵, G.F. Tartarelli^{93a}, P. Tas¹³⁰, M. Tasevsky¹²⁸, T. Tashiro⁷⁰, E. Tassi^{39a,39b}, A. Tavares Delgado^{127a,127b}, Y. Tayalati^{136e}, A.C. Taylor¹⁰⁶, G.N. Taylor⁹⁰, P.T.E. Taylor⁹⁰, W. Taylor^{164b}, F.A. Teischinger³², P. Teixeira-Dias⁷⁹, K.K. Temming⁵⁰, D. Temple¹⁴⁵, H. Ten Kate³², P.K. Teng¹⁵⁴, J.J. Teoh¹¹⁹, F. Tepel¹⁷⁹, S. Terada⁶⁸, K. Terashi¹⁵⁸, J. Terron⁸⁴, S. Terzo¹³, M. Testa⁴⁹, R.J. Teuscher^{162,m}, T. Theveneaux-Pelzer⁸⁷, J.P. Thomas¹⁹, J. Thomas-Wilsker⁷⁹, P.D. Thompson¹⁹, A.S. Thompson⁵⁵, L.A. Thomsen¹⁸⁰, E. Thomson¹²³, M.J. Tibbetts¹⁶, R.E. Ticse Torres⁸⁷, V.O. Tikhomirov^{97,aq}, Yu.A. Tikhonov^{110,c}, S. Timoshenko⁹⁹, P. Tipton¹⁸⁰, S. Tisserant⁸⁷, K. Todome¹⁶⁰, T. Todorov^{5,*}, S. Todorova-Nova¹³⁰, J. Tojo⁷², S. Tokár^{147a}, K. Tokushuku⁶⁸, E. Tolley⁵⁸, L. Tomlinson⁸⁶, M. Tomoto¹⁰⁴, L. Tompkins^{146,ar}, K. Toms¹⁰⁶, B. Tong⁵⁸, P. Tornambe⁵⁰, E. Torrence¹¹⁷, H. Torres¹⁴⁵, E. Torró Pastor¹³⁹, J. Toth^{87,as}, F. Touchard⁸⁷, D.R. Tovey¹⁴², T. Trefzger¹⁷⁸, A. Tricoli²⁷, I.M. Trigger^{164a}, S. Trincas-Duvoid⁸², M.F. Tripiana¹³, W. Trischuk¹⁶², B. Trocme⁵⁷, A. Trofymov⁴⁴, C. Troncon^{93a}, M. Trotter-McDonald¹⁶, M. Trovatelli¹⁷³, L. Truong^{168a,168c}, M. Trzebinski⁴¹, A. Trzupek⁴¹, J.C-L. Tseng¹²¹, P.V. Tsiarashka⁹⁴, G. Tsipolitis¹⁰, N. Tsirintanis⁹, S. Tsiskaridze¹³, V. Tsiskaridze⁵⁰, E.G. Tskhadadze^{53a}, K.M. Tsui^{62a}, I.I. Tsukerman⁹⁸, V. Tsulaia¹⁶, S. Tsuno⁶⁸, D. Tsybychev¹⁵¹, Y. Tu^{62b}, A. Tudorache^{28b}, V. Tudorache^{28b}, A.N. Tuna⁵⁸, S.A. Tupputi^{22a,22b}, S. Turchikhin⁶⁷, D. Turecek¹²⁹, D. Turgeman¹⁷⁶, R. Turra^{93a,93b}, P.M. Tuts³⁷, M. Tyndel¹³², G. Ucchielli^{22a,22b}, I. Ueda¹⁵⁸, M. Ughetto^{149a,149b}, F. Ukegawa¹⁶⁵, G. Unal³², A. Undrus²⁷, G. Unel¹⁶⁷, F.C. Ungaro⁹⁰, Y. Unno⁶⁸, C. Unverdorben¹⁰¹, J. Urban^{147b}, P. Urquijo⁹⁰, P. Urrejola⁸⁵, G. Usai⁸, J. Usui⁶⁸, L. Vacavant⁸⁷, V. Vacek¹²⁹, B. Vachon⁸⁹, C. Valderanis¹⁰¹, E. Valdes Santurio^{149a,149b},

N. Valencic¹⁰⁸, S. Valentinetti^{22a,22b}, A. Valero¹⁷¹, L. Valery¹³, S. Valkar¹³⁰, J.A. Valls Ferrer¹⁷¹, W. Van Den Wollenberg¹⁰⁸, P.C. Van Der Deijl¹⁰⁸, H. van der Graaf¹⁰⁸, N. van Eldik¹⁵⁵, P. van Gemmeren⁶, J. Van Nieuwkoop¹⁴⁵, I. van Vulpen¹⁰⁸, M.C. van Woerden¹⁰⁸, M. Vanadia^{133a,133b}, W. Vandelli³², R. Vanguri¹²³, A. Vaniachine¹⁶¹, P. Vankov¹⁰⁸, G. Vardanyan¹⁸¹, R. Vari^{133a}, E.W. Varnes⁷, T. Varol⁴², D. Varouchas⁸², A. Vartapetian⁸, K.E. Varvell¹⁵³, J.G. Vasquez¹⁸⁰, G.A. Vasquez^{34b}, F. Vazeille³⁶, T. Vazquez Schroeder⁸⁹, J. Veatch⁵⁶, V. Veeraraghavan⁷, L.M. Veloce¹⁶², F. Veloso^{127a,127c}, S. Veneziano^{133a}, A. Ventura^{75a,75b}, M. Venturi¹⁷³, N. Venturi¹⁶², A. Venturini²⁵, V. Vercesi^{122a}, M. Verducci^{133a,133b}, W. Verkerke¹⁰⁸, J.C. Vermeulen¹⁰⁸, A. Vest^{46,at}, M.C. Vetterli^{145,d}, O. Viazlo⁸³, I. Vichou^{170,*}, T. Vickey¹⁴², O.E. Vickey Boeriu¹⁴², G.H.A. Viehhauser¹²¹, S. Viel¹⁶, L. Vigani¹²¹, M. Villa^{22a,22b}, M. Villaplana Perez^{93a,93b}, E. Vilucchi⁴⁹, M.G. Vinciter³¹, V.B. Vinogradov⁶⁷, C. Vittori^{22a,22b}, I. Vivarelli¹⁵², S. Vlachos¹⁰, M. Vlasak¹²⁹, M. Vogel¹⁷⁹, P. Vokac¹²⁹, G. Volpi^{125a,125b}, M. Volpi⁹⁰, H. von der Schmitt¹⁰², E. von Toerne²³, V. Vorobel¹³⁰, K. Vorobev⁹⁹, M. Vos¹⁷¹, R. Voss³², J.H. Vosseveld⁷⁶, N. Vranjes¹⁴, M. Vranjes Milosavljevic¹⁴, V. Vrba¹²⁸, M. Vreeswijk¹⁰⁸, R. Vuillermet³², I. Vukotic³³, Z. Vykydal¹²⁹, P. Wagner²³, W. Wagner¹⁷⁹, H. Wahlberg⁷³, S. Wahrmund⁴⁶, J. Wakabayashi¹⁰⁴, J. Walder⁷⁴, R. Walker¹⁰¹, W. Walkowiak¹⁴⁴, V. Wallangen^{149a,149b}, C. Wang^{35b}, C. Wang^{140,87}, F. Wang¹⁷⁷, H. Wang¹⁶, H. Wang⁴², J. Wang⁴⁴, J. Wang¹⁵³, K. Wang⁸⁹, R. Wang⁶, S.M. Wang¹⁵⁴, T. Wang²³, T. Wang³⁷, W. Wang⁵⁹, C. Wanotayaroj¹¹⁷, A. Warburton⁸⁹, C.P. Ward³⁰, D.R. Wardrope⁸⁰, A. Washbrook⁴⁸, P.M. Watkins¹⁹, A.T. Watson¹⁹, M.F. Watson¹⁹, G. Watts¹³⁹, S. Watts⁸⁶, B.M. Waugh⁸⁰, S. Webb⁸⁵, M.S. Weber¹⁸, S.W. Weber¹⁷⁸, S.A. Weber³¹, J.S. Webster⁶, A.R. Weidberg¹²¹, B. Weinert⁶³, J. Weingarten⁵⁶, C. Weiser⁵⁰, H. Weits¹⁰⁸, P.S. Wells³², T. Wenaus²⁷, T. Wengler³², S. Wenig³², N. Wermes²³, M. Werner⁵⁰, M.D. Werner⁶⁶, P. Werner³², M. Wessels^{60a}, J. Wetter¹⁶⁶, K. Whalen¹¹⁷, N.L. Whallon¹³⁹, A.M. Wharton⁷⁴, A. White⁸, M.J. White¹, R. White^{34b}, D. Whiteson¹⁶⁷, F.J. Wickens¹³², W. Wiedenmann¹⁷⁷, M. Wielers¹³², C. Wiglesworth³⁸, L.A.M. Wiik-Fuchs²³, A. Wildauer¹⁰², F. Wilk⁸⁶, H.G. Wilkens³², H.H. Williams¹²³, S. Williams¹⁰⁸, C. Willis⁹², S. Willocq⁸⁸, J.A. Wilson¹⁹, I. Wingerter-Seez⁵, F. Winklmeier¹¹⁷, O.J. Winston¹⁵², B.T. Winter²³, M. Wittgen¹⁴⁶, J. Wittkowski¹⁰¹, T.M.H. Wolf¹⁰⁸, M.W. Wolter⁴¹, H. Wolters^{127a,127c}, S.D. Worm¹³², B.K. Wosiek⁴¹, J. Wotschack³², M.J. Woudstra⁸⁶, K.W. Wozniak⁴¹, M. Wu⁵⁷, M. Wu³³, S.L. Wu¹⁷⁷, X. Wu⁵¹, Y. Wu⁹¹, T.R. Wyatt⁸⁶, B.M. Wynne⁴⁸, S. Xella³⁸, D. Xu^{35a}, L. Xu²⁷, B. Yabsley¹⁵³, S. Yacoob^{148a}, D. Yamaguchi¹⁶⁰, Y. Yamaguchi¹¹⁹, A. Yamamoto⁶⁸, S. Yamamoto¹⁵⁸, T. Yamanaka¹⁵⁸, K. Yamauchi¹⁰⁴, Y. Yamazaki⁶⁹, Z. Yan²⁴, H. Yang¹⁴¹, H. Yang¹⁷⁷, Y. Yang¹⁵⁴, Z. Yang¹⁵, W-M. Yao¹⁶, Y.C. Yap⁸², Y. Yasu⁶⁸, E. Yatsenko⁵, K.H. Yau Wong²³, J. Ye⁴², S. Ye²⁷, I. Yeletsikh⁶⁷, E. Yildirim⁸⁵, K. Yorita¹⁷⁵, R. Yoshida⁶, K. Yoshihara¹²³, C. Young¹⁴⁶, C.J.S. Young³², S. Youssef²⁴, D.R. Yu¹⁶, J. Yu⁸, J.M. Yu⁹¹, J. Yu⁶⁶, L. Yuan⁶⁹, S.P.Y. Yuen²³, I. Yusuff^{30,au}, B. Zabinski⁴¹, R. Zaidan⁶⁵, A.M. Zaitsev^{131,af}, N. Zakharchuk⁴⁴, J. Zalieckas¹⁵, A. Zaman¹⁵¹, S. Zambito⁵⁸, L. Zanello^{133a,133b}, D. Zanzi⁹⁰, C. Zeitnitz¹⁷⁹, M. Zeman¹²⁹, A. Zemla^{40a}, J.C. Zeng¹⁷⁰, Q. Zeng¹⁴⁶, O. Zenin¹³¹, T. Ženiš^{147a}, D. Zerwas¹¹⁸, D. Zhang⁹¹, F. Zhang¹⁷⁷, G. Zhang^{59,ap}, H. Zhang^{35b}, J. Zhang⁶, L. Zhang⁵⁰, M. Zhang¹⁷⁰, R. Zhang²³, R. Zhang^{59,av}, X. Zhang¹⁴⁰, Z. Zhang¹¹⁸, X. Zhao⁴², Y. Zhao¹⁴⁰, Z. Zhao⁵⁹, A. Zhemchugov⁶⁷, J. Zhong¹²¹, B. Zhou⁹¹, C. Zhou¹⁷⁷, L. Zhou³⁷, L. Zhou⁴², M. Zhou¹⁵¹, N. Zhou^{35c}, C.G. Zhu¹⁴⁰, H. Zhu^{35a}, J. Zhu⁹¹, Y. Zhu⁵⁹, X. Zhuang^{35a}, K. Zhukov⁹⁷, A. Zibell¹⁷⁸, D. Zieminska⁶³, N.I. Zimine⁶⁷, C. Zimmermann⁸⁵, S. Zimmermann⁵⁰, Z. Zinonos⁵⁶, M. Zinser⁸⁵, M. Ziolkowski¹⁴⁴, L. Živković¹⁴, G. Zobernig¹⁷⁷, A. Zoccoli^{22a,22b}, M. zur Nedden¹⁷, L. Zwalinski³².

¹ Department of Physics, University of Adelaide, Adelaide, Australia

² Physics Department, SUNY Albany, Albany NY, United States of America

³ Department of Physics, University of Alberta, Edmonton AB, Canada

⁴ (a) Department of Physics, Ankara University, Ankara; (b) Istanbul Aydin University, Istanbul; (c)

Division of Physics, TOBB University of Economics and Technology, Ankara, Turkey

⁵ LAPP, CNRS/IN2P3 and Université Savoie Mont Blanc, Annecy-le-Vieux, France

⁶ High Energy Physics Division, Argonne National Laboratory, Argonne IL, United States of America

⁷ Department of Physics, University of Arizona, Tucson AZ, United States of America

⁸ Department of Physics, The University of Texas at Arlington, Arlington TX, United States of America

⁹ Physics Department, University of Athens, Athens, Greece

¹⁰ Physics Department, National Technical University of Athens, Zografou, Greece

¹¹ Department of Physics, The University of Texas at Austin, Austin TX, United States of America

¹² Institute of Physics, Azerbaijan Academy of Sciences, Baku, Azerbaijan

¹³ Institut de Física d'Altes Energies (IFAE), The Barcelona Institute of Science and Technology, Barcelona, Spain

¹⁴ Institute of Physics, University of Belgrade, Belgrade, Serbia

¹⁵ Department for Physics and Technology, University of Bergen, Bergen, Norway

¹⁶ Physics Division, Lawrence Berkeley National Laboratory and University of California, Berkeley CA, United States of America

¹⁷ Department of Physics, Humboldt University, Berlin, Germany

¹⁸ Albert Einstein Center for Fundamental Physics and Laboratory for High Energy Physics, University of Bern, Bern, Switzerland

¹⁹ School of Physics and Astronomy, University of Birmingham, Birmingham, United Kingdom

²⁰ ^(a) Department of Physics, Bogazici University, Istanbul; ^(b) Department of Physics Engineering, Gaziantep University, Gaziantep; ^(d) Istanbul Bilgi University, Faculty of Engineering and Natural Sciences, Istanbul, Turkey; ^(e) Bahcesehir University, Faculty of Engineering and Natural Sciences, Istanbul, Turkey, Turkey

²¹ Centro de Investigaciones, Universidad Antonio Narino, Bogota, Colombia

²² ^(a) INFN Sezione di Bologna; ^(b) Dipartimento di Fisica e Astronomia, Università di Bologna, Bologna, Italy

²³ Physikalisches Institut, University of Bonn, Bonn, Germany

²⁴ Department of Physics, Boston University, Boston MA, United States of America

²⁵ Department of Physics, Brandeis University, Waltham MA, United States of America

²⁶ ^(a) Universidade Federal do Rio De Janeiro COPPE/EE/IF, Rio de Janeiro; ^(b) Electrical Circuits Department, Federal University of Juiz de Fora (UFJF), Juiz de Fora; ^(c) Federal University of Sao Joao del Rei (UFSJ), Sao Joao del Rei; ^(d) Instituto de Fisica, Universidade de Sao Paulo, Sao Paulo, Brazil

²⁷ Physics Department, Brookhaven National Laboratory, Upton NY, United States of America

²⁸ ^(a) Transilvania University of Brasov, Brasov, Romania; ^(b) National Institute of Physics and Nuclear Engineering, Bucharest; ^(c) National Institute for Research and Development of Isotopic and Molecular Technologies, Physics Department, Cluj Napoca; ^(d) University Politehnica Bucharest, Bucharest; ^(e) West University in Timisoara, Timisoara, Romania

²⁹ Departamento de Física, Universidad de Buenos Aires, Buenos Aires, Argentina

³⁰ Cavendish Laboratory, University of Cambridge, Cambridge, United Kingdom

³¹ Department of Physics, Carleton University, Ottawa ON, Canada

³² CERN, Geneva, Switzerland

³³ Enrico Fermi Institute, University of Chicago, Chicago IL, United States of America

³⁴ ^(a) Departamento de Física, Pontificia Universidad Católica de Chile, Santiago; ^(b) Departamento de Física, Universidad Técnica Federico Santa María, Valparaíso, Chile

³⁵ ^(a) Institute of High Energy Physics, Chinese Academy of Sciences, Beijing; ^(b) Department of Physics, Nanjing University, Jiangsu; ^(c) Physics Department, Tsinghua University, Beijing 100084, China

- ³⁶ Laboratoire de Physique Corpusculaire, Clermont Université and Université Blaise Pascal and CNRS/IN2P3, Clermont-Ferrand, France
- ³⁷ Nevis Laboratory, Columbia University, Irvington NY, United States of America
- ³⁸ Niels Bohr Institute, University of Copenhagen, Kobenhavn, Denmark
- ³⁹ ^(a) INFN Gruppo Collegato di Cosenza, Laboratori Nazionali di Frascati; ^(b) Dipartimento di Fisica, Università della Calabria, Rende, Italy
- ⁴⁰ ^(a) AGH University of Science and Technology, Faculty of Physics and Applied Computer Science, Krakow; ^(b) Marian Smoluchowski Institute of Physics, Jagiellonian University, Krakow, Poland
- ⁴¹ Institute of Nuclear Physics Polish Academy of Sciences, Krakow, Poland
- ⁴² Physics Department, Southern Methodist University, Dallas TX, United States of America
- ⁴³ Physics Department, University of Texas at Dallas, Richardson TX, United States of America
- ⁴⁴ DESY, Hamburg and Zeuthen, Germany
- ⁴⁵ Lehrstuhl für Experimentelle Physik IV, Technische Universität Dortmund, Dortmund, Germany
- ⁴⁶ Institut für Kern- und Teilchenphysik, Technische Universität Dresden, Dresden, Germany
- ⁴⁷ Department of Physics, Duke University, Durham NC, United States of America
- ⁴⁸ SUPA - School of Physics and Astronomy, University of Edinburgh, Edinburgh, United Kingdom
- ⁴⁹ INFN Laboratori Nazionali di Frascati, Frascati, Italy
- ⁵⁰ Fakultät für Mathematik und Physik, Albert-Ludwigs-Universität, Freiburg, Germany
- ⁵¹ Section de Physique, Université de Genève, Geneva, Switzerland
- ⁵² ^(a) INFN Sezione di Genova; ^(b) Dipartimento di Fisica, Università di Genova, Genova, Italy
- ⁵³ ^(a) E. Andronikashvili Institute of Physics, Iv. Javakhishvili Tbilisi State University, Tbilisi; ^(b) High Energy Physics Institute, Tbilisi State University, Tbilisi, Georgia
- ⁵⁴ II Physikalisches Institut, Justus-Liebig-Universität Giessen, Giessen, Germany
- ⁵⁵ SUPA - School of Physics and Astronomy, University of Glasgow, Glasgow, United Kingdom
- ⁵⁶ II Physikalisches Institut, Georg-August-Universität, Göttingen, Germany
- ⁵⁷ Laboratoire de Physique Subatomique et de Cosmologie, Université Grenoble-Alpes, CNRS/IN2P3, Grenoble, France
- ⁵⁸ Laboratory for Particle Physics and Cosmology, Harvard University, Cambridge MA, United States of America
- ⁵⁹ Department of Modern Physics, University of Science and Technology of China, Anhui, China
- ⁶⁰ ^(a) Kirchhoff-Institut für Physik, Ruprecht-Karls-Universität Heidelberg, Heidelberg; ^(b) Physikalisches Institut, Ruprecht-Karls-Universität Heidelberg, Heidelberg; ^(c) ZITI Institut für technische Informatik, Ruprecht-Karls-Universität Heidelberg, Mannheim, Germany
- ⁶¹ Faculty of Applied Information Science, Hiroshima Institute of Technology, Hiroshima, Japan
- ⁶² ^(a) Department of Physics, The Chinese University of Hong Kong, Shatin, N.T., Hong Kong; ^(b) Department of Physics, The University of Hong Kong, Hong Kong; ^(c) Department of Physics, The Hong Kong University of Science and Technology, Clear Water Bay, Kowloon, Hong Kong, China
- ⁶³ Department of Physics, Indiana University, Bloomington IN, United States of America
- ⁶⁴ Institut für Astro- und Teilchenphysik, Leopold-Franzens-Universität, Innsbruck, Austria
- ⁶⁵ University of Iowa, Iowa City IA, United States of America
- ⁶⁶ Department of Physics and Astronomy, Iowa State University, Ames IA, United States of America
- ⁶⁷ Joint Institute for Nuclear Research, JINR Dubna, Dubna, Russia
- ⁶⁸ KEK, High Energy Accelerator Research Organization, Tsukuba, Japan
- ⁶⁹ Graduate School of Science, Kobe University, Kobe, Japan
- ⁷⁰ Faculty of Science, Kyoto University, Kyoto, Japan
- ⁷¹ Kyoto University of Education, Kyoto, Japan
- ⁷² Department of Physics, Kyushu University, Fukuoka, Japan

- ⁷³ Instituto de Física La Plata, Universidad Nacional de La Plata and CONICET, La Plata, Argentina
- ⁷⁴ Physics Department, Lancaster University, Lancaster, United Kingdom
- ⁷⁵ ^(a) INFN Sezione di Lecce; ^(b) Dipartimento di Matematica e Fisica, Università del Salento, Lecce, Italy
- ⁷⁶ Oliver Lodge Laboratory, University of Liverpool, Liverpool, United Kingdom
- ⁷⁷ Department of Physics, Jožef Stefan Institute and University of Ljubljana, Ljubljana, Slovenia
- ⁷⁸ School of Physics and Astronomy, Queen Mary University of London, London, United Kingdom
- ⁷⁹ Department of Physics, Royal Holloway University of London, Surrey, United Kingdom
- ⁸⁰ Department of Physics and Astronomy, University College London, London, United Kingdom
- ⁸¹ Louisiana Tech University, Ruston LA, United States of America
- ⁸² Laboratoire de Physique Nucléaire et de Hautes Energies, UPMC and Université Paris-Diderot and CNRS/IN2P3, Paris, France
- ⁸³ Fysiska institutionen, Lunds universitet, Lund, Sweden
- ⁸⁴ Departamento de Física Teórica C-15, Universidad Autónoma de Madrid, Madrid, Spain
- ⁸⁵ Institut für Physik, Universität Mainz, Mainz, Germany
- ⁸⁶ School of Physics and Astronomy, University of Manchester, Manchester, United Kingdom
- ⁸⁷ CPPM, Aix-Marseille Université and CNRS/IN2P3, Marseille, France
- ⁸⁸ Department of Physics, University of Massachusetts, Amherst MA, United States of America
- ⁸⁹ Department of Physics, McGill University, Montreal QC, Canada
- ⁹⁰ School of Physics, University of Melbourne, Victoria, Australia
- ⁹¹ Department of Physics, The University of Michigan, Ann Arbor MI, United States of America
- ⁹² Department of Physics and Astronomy, Michigan State University, East Lansing MI, United States of America
- ⁹³ ^(a) INFN Sezione di Milano; ^(b) Dipartimento di Fisica, Università di Milano, Milano, Italy
- ⁹⁴ B.I. Stepanov Institute of Physics, National Academy of Sciences of Belarus, Minsk, Republic of Belarus
- ⁹⁵ National Scientific and Educational Centre for Particle and High Energy Physics, Minsk, Republic of Belarus
- ⁹⁶ Group of Particle Physics, University of Montreal, Montreal QC, Canada
- ⁹⁷ P.N. Lebedev Physical Institute of the Russian Academy of Sciences, Moscow, Russia
- ⁹⁸ Institute for Theoretical and Experimental Physics (ITEP), Moscow, Russia
- ⁹⁹ National Research Nuclear University MEPhI, Moscow, Russia
- ¹⁰⁰ D.V. Skobeltsyn Institute of Nuclear Physics, M.V. Lomonosov Moscow State University, Moscow, Russia
- ¹⁰¹ Fakultät für Physik, Ludwig-Maximilians-Universität München, München, Germany
- ¹⁰² Max-Planck-Institut für Physik (Werner-Heisenberg-Institut), München, Germany
- ¹⁰³ Nagasaki Institute of Applied Science, Nagasaki, Japan
- ¹⁰⁴ Graduate School of Science and Kobayashi-Maskawa Institute, Nagoya University, Nagoya, Japan
- ¹⁰⁵ ^(a) INFN Sezione di Napoli; ^(b) Dipartimento di Fisica, Università di Napoli, Napoli, Italy
- ¹⁰⁶ Department of Physics and Astronomy, University of New Mexico, Albuquerque NM, United States of America
- ¹⁰⁷ Institute for Mathematics, Astrophysics and Particle Physics, Radboud University Nijmegen/Nikhef, Nijmegen, Netherlands
- ¹⁰⁸ Nikhef National Institute for Subatomic Physics and University of Amsterdam, Amsterdam, Netherlands
- ¹⁰⁹ Department of Physics, Northern Illinois University, DeKalb IL, United States of America
- ¹¹⁰ Budker Institute of Nuclear Physics, SB RAS, Novosibirsk, Russia

- ¹¹¹ Department of Physics, New York University, New York NY, United States of America
- ¹¹² Ohio State University, Columbus OH, United States of America
- ¹¹³ Faculty of Science, Okayama University, Okayama, Japan
- ¹¹⁴ Homer L. Dodge Department of Physics and Astronomy, University of Oklahoma, Norman OK, United States of America
- ¹¹⁵ Department of Physics, Oklahoma State University, Stillwater OK, United States of America
- ¹¹⁶ Palacký University, RCPTM, Olomouc, Czech Republic
- ¹¹⁷ Center for High Energy Physics, University of Oregon, Eugene OR, United States of America
- ¹¹⁸ LAL, Univ. Paris-Sud, CNRS/IN2P3, Université Paris-Saclay, Orsay, France
- ¹¹⁹ Graduate School of Science, Osaka University, Osaka, Japan
- ¹²⁰ Department of Physics, University of Oslo, Oslo, Norway
- ¹²¹ Department of Physics, Oxford University, Oxford, United Kingdom
- ¹²² ^(a) INFN Sezione di Pavia; ^(b) Dipartimento di Fisica, Università di Pavia, Pavia, Italy
- ¹²³ Department of Physics, University of Pennsylvania, Philadelphia PA, United States of America
- ¹²⁴ National Research Centre "Kurchatov Institute" B.P.Konstantinov Petersburg Nuclear Physics Institute, St. Petersburg, Russia
- ¹²⁵ ^(a) INFN Sezione di Pisa; ^(b) Dipartimento di Fisica E. Fermi, Università di Pisa, Pisa, Italy
- ¹²⁶ Department of Physics and Astronomy, University of Pittsburgh, Pittsburgh PA, United States of America
- ¹²⁷ ^(a) Laboratório de Instrumentação e Física Experimental de Partículas - LIP, Lisboa; ^(b) Faculdade de Ciências, Universidade de Lisboa, Lisboa; ^(c) Department of Physics, University of Coimbra, Coimbra; ^(d) Centro de Física Nuclear da Universidade de Lisboa, Lisboa; ^(e) Departamento de Física, Universidade do Minho, Braga; ^(f) Departamento de Física Teórica y del Cosmos and CAFPE, Universidad de Granada, Granada (Spain); ^(g) Dep Física and CEFITEC of Faculdade de Ciências e Tecnologia, Universidade Nova de Lisboa, Caparica, Portugal
- ¹²⁸ Institute of Physics, Academy of Sciences of the Czech Republic, Praha, Czech Republic
- ¹²⁹ Czech Technical University in Prague, Praha, Czech Republic
- ¹³⁰ Faculty of Mathematics and Physics, Charles University in Prague, Praha, Czech Republic
- ¹³¹ State Research Center Institute for High Energy Physics (Protvino), NRC KI, Russia
- ¹³² Particle Physics Department, Rutherford Appleton Laboratory, Didcot, United Kingdom
- ¹³³ ^(a) INFN Sezione di Roma; ^(b) Dipartimento di Fisica, Sapienza Università di Roma, Roma, Italy
- ¹³⁴ ^(a) INFN Sezione di Roma Tor Vergata; ^(b) Dipartimento di Fisica, Università di Roma Tor Vergata, Roma, Italy
- ¹³⁵ ^(a) INFN Sezione di Roma Tre; ^(b) Dipartimento di Matematica e Fisica, Università Roma Tre, Roma, Italy
- ¹³⁶ ^(a) Faculté des Sciences Ain Chock, Réseau Universitaire de Physique des Hautes Energies - Université Hassan II, Casablanca; ^(b) Centre National de l'Energie des Sciences Techniques Nucleaires, Rabat; ^(c) Faculté des Sciences Semlalia, Université Cadi Ayyad, LPHEA-Marrakech; ^(d) Faculté des Sciences, Université Mohamed Premier and LTPM, Oujda; ^(e) Faculté des sciences, Université Mohammed V, Rabat, Morocco
- ¹³⁷ DSM/IRFU (Institut de Recherches sur les Lois Fondamentales de l'Univers), CEA Saclay (Commissariat à l'Energie Atomique et aux Energies Alternatives), Gif-sur-Yvette, France
- ¹³⁸ Santa Cruz Institute for Particle Physics, University of California Santa Cruz, Santa Cruz CA, United States of America
- ¹³⁹ Department of Physics, University of Washington, Seattle WA, United States of America
- ¹⁴⁰ School of Physics, Shandong University, Shandong, China
- ¹⁴¹ Department of Physics and Astronomy, Shanghai Key Laboratory for Particle Physics and

Cosmology, Shanghai Jiao Tong University, Shanghai; (also affiliated with PKU-CHEP), China

¹⁴² Department of Physics and Astronomy, University of Sheffield, Sheffield, United Kingdom

¹⁴³ Department of Physics, Shinshu University, Nagano, Japan

¹⁴⁴ Fachbereich Physik, Universität Siegen, Siegen, Germany

¹⁴⁵ Department of Physics, Simon Fraser University, Burnaby BC, Canada

¹⁴⁶ SLAC National Accelerator Laboratory, Stanford CA, United States of America

¹⁴⁷ ^(a) Faculty of Mathematics, Physics & Informatics, Comenius University, Bratislava; ^(b) Department of Subnuclear Physics, Institute of Experimental Physics of the Slovak Academy of Sciences, Kosice, Slovak Republic

¹⁴⁸ ^(a) Department of Physics, University of Cape Town, Cape Town; ^(b) Department of Physics, University of Johannesburg, Johannesburg; ^(c) School of Physics, University of the Witwatersrand, Johannesburg, South Africa

¹⁴⁹ ^(a) Department of Physics, Stockholm University; ^(b) The Oskar Klein Centre, Stockholm, Sweden

¹⁵⁰ Physics Department, Royal Institute of Technology, Stockholm, Sweden

¹⁵¹ Departments of Physics & Astronomy and Chemistry, Stony Brook University, Stony Brook NY, United States of America

¹⁵² Department of Physics and Astronomy, University of Sussex, Brighton, United Kingdom

¹⁵³ School of Physics, University of Sydney, Sydney, Australia

¹⁵⁴ Institute of Physics, Academia Sinica, Taipei, Taiwan

¹⁵⁵ Department of Physics, Technion: Israel Institute of Technology, Haifa, Israel

¹⁵⁶ Raymond and Beverly Sackler School of Physics and Astronomy, Tel Aviv University, Tel Aviv, Israel

¹⁵⁷ Department of Physics, Aristotle University of Thessaloniki, Thessaloniki, Greece

¹⁵⁸ International Center for Elementary Particle Physics and Department of Physics, The University of Tokyo, Tokyo, Japan

¹⁵⁹ Graduate School of Science and Technology, Tokyo Metropolitan University, Tokyo, Japan

¹⁶⁰ Department of Physics, Tokyo Institute of Technology, Tokyo, Japan

¹⁶¹ Tomsk State University, Tomsk, Russia, Russia

¹⁶² Department of Physics, University of Toronto, Toronto ON, Canada

¹⁶³ ^(a) INFN-TIFPA; ^(b) University of Trento, Trento, Italy, Italy

¹⁶⁴ ^(a) TRIUMF, Vancouver BC; ^(b) Department of Physics and Astronomy, York University, Toronto ON, Canada

¹⁶⁵ Faculty of Pure and Applied Sciences, and Center for Integrated Research in Fundamental Science and Engineering, University of Tsukuba, Tsukuba, Japan

¹⁶⁶ Department of Physics and Astronomy, Tufts University, Medford MA, United States of America

¹⁶⁷ Department of Physics and Astronomy, University of California Irvine, Irvine CA, United States of America

¹⁶⁸ ^(a) INFN Gruppo Collegato di Udine, Sezione di Trieste, Udine; ^(b) ICTP, Trieste; ^(c) Dipartimento di Chimica, Fisica e Ambiente, Università di Udine, Udine, Italy

¹⁶⁹ Department of Physics and Astronomy, University of Uppsala, Uppsala, Sweden

¹⁷⁰ Department of Physics, University of Illinois, Urbana IL, United States of America

¹⁷¹ Instituto de Física Corpuscular (IFIC) and Departamento de Física Atómica, Molecular y Nuclear and Departamento de Ingeniería Electrónica and Instituto de Microelectrónica de Barcelona (IMB-CNM), University of Valencia and CSIC, Valencia, Spain

¹⁷² Department of Physics, University of British Columbia, Vancouver BC, Canada

¹⁷³ Department of Physics and Astronomy, University of Victoria, Victoria BC, Canada

¹⁷⁴ Department of Physics, University of Warwick, Coventry, United Kingdom

- ¹⁷⁵ Waseda University, Tokyo, Japan
- ¹⁷⁶ Department of Particle Physics, The Weizmann Institute of Science, Rehovot, Israel
- ¹⁷⁷ Department of Physics, University of Wisconsin, Madison WI, United States of America
- ¹⁷⁸ Fakultät für Physik und Astronomie, Julius-Maximilians-Universität, Würzburg, Germany
- ¹⁷⁹ Fakultät für Mathematik und Naturwissenschaften, Fachgruppe Physik, Bergische Universität Wuppertal, Wuppertal, Germany
- ¹⁸⁰ Department of Physics, Yale University, New Haven CT, United States of America
- ¹⁸¹ Yerevan Physics Institute, Yerevan, Armenia
- ¹⁸² Centre de Calcul de l'Institut National de Physique Nucléaire et de Physique des Particules (IN2P3), Villeurbanne, France
- ^a Also at Department of Physics, King's College London, London, United Kingdom
- ^b Also at Institute of Physics, Azerbaijan Academy of Sciences, Baku, Azerbaijan
- ^c Also at Novosibirsk State University, Novosibirsk, Russia
- ^d Also at TRIUMF, Vancouver BC, Canada
- ^e Also at Department of Physics & Astronomy, University of Louisville, Louisville, KY, United States of America
- ^f Also at Physics Department, An-Najah National University, Nablus, Palestine
- ^g Also at Department of Physics, California State University, Fresno CA, United States of America
- ^h Also at Department of Physics, University of Fribourg, Fribourg, Switzerland
- ⁱ Also at Departament de Física de la Universitat Autònoma de Barcelona, Barcelona, Spain
- ^j Also at Departamento de Física e Astronomia, Faculdade de Ciências, Universidade do Porto, Portugal
- ^k Also at Tomsk State University, Tomsk, Russia, Russia
- ^l Also at Università di Napoli Parthenope, Napoli, Italy
- ^m Also at Institute of Particle Physics (IPP), Canada
- ⁿ Also at National Institute of Physics and Nuclear Engineering, Bucharest, Romania
- ^o Also at Department of Physics, St. Petersburg State Polytechnical University, St. Petersburg, Russia
- ^p Also at Department of Physics, The University of Michigan, Ann Arbor MI, United States of America
- ^q Also at Centre for High Performance Computing, CSIR Campus, Rosebank, Cape Town, South Africa
- ^r Also at Louisiana Tech University, Ruston LA, United States of America
- ^s Also at Institutio Catalana de Recerca i Estudis Avancats, ICREA, Barcelona, Spain
- ^t Also at Graduate School of Science, Osaka University, Osaka, Japan
- ^u Also at Department of Physics, National Tsing Hua University, Taiwan
- ^v Also at Institute for Mathematics, Astrophysics and Particle Physics, Radboud University Nijmegen/Nikhef, Nijmegen, Netherlands
- ^w Also at Department of Physics, The University of Texas at Austin, Austin TX, United States of America
- ^x Also at CERN, Geneva, Switzerland
- ^y Also at Georgian Technical University (GTU), Tbilisi, Georgia
- ^z Also at Ochadai Academic Production, Ochanomizu University, Tokyo, Japan
- ^{aa} Also at Manhattan College, New York NY, United States of America
- ^{ab} Associated at Durham University, IPPP, Durham, United Kingdom, United Kingdom
- ^{ac} Also at Academia Sinica Grid Computing, Institute of Physics, Academia Sinica, Taipei, Taiwan
- ^{ad} Also at School of Physics, Shandong University, Shandong, China
- ^{ae} Also at Department of Physics, California State University, Sacramento CA, United States of America
- ^{af} Also at Moscow Institute of Physics and Technology State University, Dolgoprudny, Russia
- ^{ag} Also at Section de Physique, Université de Genève, Geneva, Switzerland
- ^{ah} Also at Eotvos Lorand University, Budapest, Hungary

- ^{ai} Also at Departments of Physics & Astronomy and Chemistry, Stony Brook University, Stony Brook NY, United States of America
- ^{aj} Also at International School for Advanced Studies (SISSA), Trieste, Italy
- ^{ak} Also at Department of Physics and Astronomy, University of South Carolina, Columbia SC, United States of America
- ^{al} Also at Institut de Física d'Altes Energies (IFAE), The Barcelona Institute of Science and Technology, Barcelona, Spain
- ^{am} Also at School of Physics and Engineering, Sun Yat-sen University, Guangzhou, China
- ^{an} Also at Institute for Nuclear Research and Nuclear Energy (INRNE) of the Bulgarian Academy of Sciences, Sofia, Bulgaria
- ^{ao} Also at Faculty of Physics, M.V.Lomonosov Moscow State University, Moscow, Russia
- ^{ap} Also at Institute of Physics, Academia Sinica, Taipei, Taiwan
- ^{aq} Also at National Research Nuclear University MEPhI, Moscow, Russia
- ^{ar} Also at Department of Physics, Stanford University, Stanford CA, United States of America
- ^{as} Also at Institute for Particle and Nuclear Physics, Wigner Research Centre for Physics, Budapest, Hungary
- ^{at} Also at Flensburg University of Applied Sciences, Flensburg, Germany
- ^{au} Also at University of Malaya, Department of Physics, Kuala Lumpur, Malaysia
- ^{av} Also at CPPM, Aix-Marseille Université and CNRS/IN2P3, Marseille, France
- * Deceased